VTT Technical Research Centre of Finland

Validation of the FINIX fuel behavior code version 0.13.9

Loukusa, Henri

Published: 25/10/2013

Document Version
Publisher's final version

RESEARCH REPORT

VTT-R-06565-13

Validation of the FINIX fuel behavior code version 0.13.9

Authors: Henri Loukusa

Confidentiality: Public

Report's title Validation of the FINIX fuel behavior code version 0.13.9	
Customer, contact person, address VYR	**Order reference** 25/2013SAF
Project name Polttoaineen laaja-alainen mallinnus	**Project number/Short name** 77462 1.3.1/PALAMA
Author(s) Henri Loukusa	**Pages** 78
Keywords fuel behaviour modelling, FINIX, validation	**Report identification code** VTT-R-06565-13

Summary

The FINIX fuel performance code has been developed at VTT to be coupled to existing thermal-hydraulics, reactor dynamics or neutronics codes used at VTT. In this report, the FINIX model is validated against experimental data from the OECD/NEA International Fuel Performance Experiments database. Transient scenarios used in the FRAPTRAN-1.4 integral assessment are used to compare transient performance of FINIX against the results calculated by FRAPTRAN. FRAPTRAN is a computer code for transient analysis of fuel rods developed at the Pacific Northwest National Laboratory in the US.

The comparisons to experimental data offer the best insight into how the FINIX model reflects real-world situations. When comparing the results calculated by FINIX to those calculated by another code, the assumptions and simplifications in the other code must be taken into account. Therefore during the validation process some investigation is done into FRAPTRAN as to clarify the manner in which FRAPTRAN calculates its results.

According to the validation results, FINIX calculates very similar results compared to FRAPTRAN. Some differences arise due to, for example, FINIX's lack of plastic clad deformation models and rod failure criteria. However, despite these differences, the temperature distributions match very closely. When compared to experimental steady state irradiation data, the error between computed and experimental centreline temperature increases with burnup. This can be explained by the lack of models for some burnup-dependent phenomena. Some open questions remain concerning the mechanical model in FINIX.

Confidentiality	Public

Espoo, 25.10.2013

Written by	**Reviewed by**	**Accepted by**
Henri Loukusa, Research Trainee	Timo Ikonen, Research Scientist	Timo Vanttola, Technology Manager

VTT's contact address

P.O. Box 1000, Tietotie 3, 02044 VTT, Espoo

Distribution (customer and VTT)

SAFIR2014/TR3
VTT Archive

Contents

1 Introduction

In this report, the FINIX fuel performance code, which has been developed at VTT, was validated against experimental data and another fuel performance code in public usage. This report considers the version 0.13.9 of FINIX, which has been modified from the first version 0.13.1. The results in this validation report have been calculated using an intermediate version between versions 0.13.1 and 0.13.9. Appropriate modifications have been made to the newest version 0.13.9, so this validation report applies to this newest version.

Fuel performance codes are used to assess fuel performance for design and safety purposes. A fuel performance code must calculate accurately the thermal, mechanical and physical processes taking place in a fuel rod during operation. There are multiple fuel performance codes in public use, such as FRAPTRAN [1] and FRAPCON [2], developed at the Pacific Northwest National Laboratory (PNNL) in the US, and others that are developed privately. The FINIX fuel performance code has been developed to be coupled to existing thermal-hydraulics, reactor dynamics or neutronics codes used at VTT. The complexity of the FINIX model is between a full fuel performance code and a simple thermal element to improve its performance and to expedite its development [3]. FINIX is best suited to the analysis of transients, but steady-state calculations can also be made.

FRAPTRAN-1.4 [1] is the latest version of FRAPTRAN, which is a single-rod code for transient analysis. It is similar to FINIX in its purpose, and uses many of the same correlations also being used in FINIX. FRAPTRAN-1.4 has also been validated thoroughly [4], so it was chosen as a target for comparison of FINIX-calculated results. It has to be noted that while FRAPTRAN is thoroughly validated to calculate realistic results and is thoroughly documented, there are open questions concerning some assumptions made in the actual calculations made by FRAPTRAN. Many of these may be simple, others more complex, but many of these may only be evident when comparing a similarly fashioned code and the results calculated by it to results calculated by FRAPTRAN. Some of these questions were asked and answered during this validation process, while others were left unanswered and must be investigated in the future.

FRAPCON-3.4 [2] is the latest version of FRAPCON, which in turn is a single-rod code for the steady-state analysis of fuel rods. FRAPCON can calculate accurately many burnup-related phenomena, and it is used to calculate some burnup-related parameters to initialize FRAPTRAN and FINIX when rods with non-zero burnup are modeled. There are many correlations that are the same in FRAPCON and FRAPTRAN, some that are different and some correlations that are not used in FRAPTRAN are used in FINIX, because many of the correlations used by FRAPCON are more detailed than those used by FRAPTRAN. For example, the correlations from both codes for the fuel rod pellet-cladding gap heat transfer coefficient can be used in FINIX, and their effects on the results were investigated during the validation process.

In the FRAPTRAN-1.4 integral assessment [4] FRAPTRAN was tested with several power transient test cases. These cases were based on experimental tests done at the CABRI, NSRR and BIGR reactors. FRAPTRAN was validated with reactivity-initiated-accident (RIA) and loss-of-coolant-accident (LOCA) cases. In a RIA event, the power in the rod peaks rapidly, in the order of a few or a few tens of milliseconds and then returns to zero. This kind of behavior could be seen in an actual reactor during a RIA caused by, for example, control rods being ejected from the reactor. The fuel rod behaviour during a RIA can be almost completely modelled with a model with only thermal, mechanical and physical modeling of the fuel rod itself, if some boundary conditions are

known. These boundary conditions can be the cladding outer surface temperature or the coolant temperature, in which case the heat transfer coefficient between the cladding outer surface and the coolant must be known. In a LOCA accident the coolant is promptly removed from the reactor, and the fuel rods heat up since heat transfer from the rod to the coolant has been prevented. The LOCA accident type is more dependent on the coolant model, as many thermal-hydraulic phenomena are present during a LOCA event. As the FINIX internal coolant model is primitive, LOCA calculations should be carried out with FINIX coupled into a thermal-hydraulics code, and only RIA scenarios were considered in this validation report.

The results calculated by FINIX were also compared to experimental data from the OECD/NEA International Fuel Performance Experiment (IFPE) Database. The data in this database has been collected from various fuel performance experiments done at the many research reactors in the world. The experimental data used in this validation are steady-state data from periods of years of continuous operation. As the current version of FINIX lacks some models for burnup-dependent phenomena, it was expected that FINIX would calculate accurate results only when the burnup is low. The assumption was supported by the validation data. The comparisons to experimental data offer the best insight into how the FINIX model reflects real-world situations. When comparing the results calculated by FINIX to those calculated by another code, the assumptions and simplifications in the other code must be taken into account. Therefore during the validation process some investigation was done into FRAPTRAN and FRAPCON as to clarify the manner in which these codes calculate their results.

2 Data

2.1 Transient scenarios

The scenarios from the integral assessment of FRAPTRAN-1.4 [4] that were used in the validation of FINIX-0.13.9 are listed in table 1. The scenarios are based on experimental data from various research reactors (CABRI, NSRR and BIGR). In the CABRI reactor, sodium coolant is used, whereas in the NSRR and BIGR tests, the rods reside in sealed water capsules.

Because plastic strain and other phenomena related to the failure of a rod are not yet modeled in FINIX, the failed rod cases can be considered thoroughly only up to the point where rod failure happens. Therefore it is reasonable to divide the scenarios into two groups on the basis of rod failure, which is known from the experimental data. However, as we are comparing the codes against each other, it was decided to use the rod burst information calculated by FRAPTRAN, which is mostly in agreement with the experimental data. FRAPTRAN also calculates the moment of rod burst, without which it would be impossible to say anything about the point until which FRAPTRAN and FINIX calculate results similarly. For each transient scenario, the moments of rod burst are listed in table 2.

Several notes on some of the test rods can be made from table 2, and they are also mentioned in the notes for individual scenarios in section 5. In most of the cases the power pulses are of small pulse width, under 10 ms. Only the CABRI REP-Na4 and REP-Na8 scenarios have pulse widths closer to 100 ms. The rod-average burnup is in the range of 40-70 GMd/MtU, with the exception of the scenario NSRR TS-5 where the burnup is only 26.6 GWd/MtU. In all but the VVER rod cases the

Table 1. *Details of some RIA scenarios used in FRAPTRAN-1.4 integral assessment.*

Base irradiation	Transient reactor	Rod	Rod type	Rod-average burnup (GWd/MtU)	Rod failure	Pulse width (ms)	Ref.
Gravelines-5	CABRI	Na-1	PWR 17x17	64	Yes	9.5	[6]
Gravelines-5	CABRI	Na-3	PWR 17x17	53.8	No	9.5	[6]
Gravelines-5	CABRI	Na-4	PWR 17x17	62	No	76.4	[6]
Gravelines-5	CABRI	Na-8	PWR 17x17	60	Yes	75	[6]
Fukushima-Daiichi 3	NSRR	FK-1	BWR 10x10	45.3	No	4.5	[7]
Ohi-1	NSRR	HBO-1	PWR 17x17	50.4	Yes	4.4	[8]
Ohi-1	NSRR	HBO-5	PWR 17x17	44	Yes	4.4	[8]
Ohi-1	NSRR	HBO-6	PWR 17x17	49	No	4.4	[8]
Tsuruga-1	NSRR	TS-5	BWR 7x7	26.6	No	4.6	[9]
Vandellos-2	NSRR	VA-1	PWR 17x17	71	Yes	4.4	[10, 11]
Vandellos-2	NSRR	VA-3	PWR 17x17	72	Yes	4.4	[10, 11]
Kolskaya	BIGR	RT-4	VVER-440	60.1	No	3	[12, 13]
Kolskaya	BIGR	RT-8	VVER-440	60	Yes	3	[12, 13]
Novovoronezhskaya	BIGR	RT-10	VVER-1000	46.9	No	3	[12, 13]
Novovoronezhskaya	BIGR	RT-12	VVER-1000	47.3	Yes	3	[12, 13]

cladding is Zircalloy-4. The VVER rods use Zr-1%Nb-type cladding. In one case, NSRR HBO-1, FRAPTRAN was not able to predict rod bursting, even though the rod had burst in the experiment.

2.2 Experimental data

Data from the Halden BWR test reactor experiments IFA-429 and IFA-432 were used in the assessment. IFA-429 data is based on one rod that has been cut to smaller test rods. IFA-432 data is based on test rods made from several different fuel rods. Coolant temperature and linear power data is available for most of the experiments, but fuel centerline temperature data is available only for five test rods of the IFA-432 experiment, and one rod of the IFA-429 experiment.

Full fuel centerline temperature histories are available only for IFA-432 experiment rods 2, 3 and 5 and IFA-429 experiment rod BC. To generate the fuel centerline temperature histories for IFA-432 rods 1 and 6 an estimation was made, which is explained in [5]. For IFA-432 experiment rod 6 the temperature history is incomplete because of a failed thermocouple. This was taken into account in the analysis, and the data after thermocouple failure was not used.

Table 2. *Moment of rod burst for scenarios with experimentally failed and unfailed rods according to FRAPTRAN.*

Failed rods		Unfailed rods	
Rod	Moment of rod burst as calculated by FRAPTRAN (ms)	Rod	Moment of rod burst as calculated by from FRAPTRAN (ms)
Na-1	79	Na-3	no rod burst
Na-8	524	Na-4	no rod burst
HBO-1	no rod burst	FK-1	no rod burst
HBO-5	211	HBO-6	no rod burst
VA-1	9	TS-5	no rod burst
VA-3	10	RT-4	no rod burst
RT-8	24	RT-10	no rod burst
RT-12	53		

3 Modifications to FINIX-0.13.1

Some modifications to FINIX were done during the validation process to remove erroneous code and to improve the model. When calculating the test scenarios with FINIX it was found that the gap heat transfer coefficient is underestimated by two orders of magnitude in case CABRI REP-Na4, which was one of the first scenarios run. The underestimation accounts for erroneous results in all the temperature calculations of the rod, and the scenario was investigated in detail to find out the cause for this discrepancy.

Two reasons for this were found: underestimation of the conduction heat transfer coefficient and underestimation of the contact heat transfer coefficient. According to the FRAPTRAN models, these two terms account for almost 99 % of the gap heat transfer coefficient in open and closed gap scenarios. Whereas in test scenarios of the FINIX-0.13.1 report the gas gap was open during the whole transient, in the test scenarios from the FRAPTRAN-1.4 integral assessment the gas gap closed in all cases. Therefore the calculation of the contact heat transfer coefficient was not tested until now.

The largest constituent of the heat transfer coefficient is the conduction heat transfer coefficient. The effective gap width has the largest effect on the conduction heat transfer coefficient. It was found that the effective gap width correlation was represented erroneously in the FINIX-0.13.1 report and was changed to the correct one, and the conduction heat transfer coefficient calculated by FINIX was thus more similar to that claculated by FRAPTRAN. The incorrectness was only evident when the gap contact pressure was above zero, so it could not be seen in the TMI-1 test case because no contact with the pellet and the cladding happened in this scenario.

In some cases the contact heat transfer coefficient may have a magnitude that is 10-30 % of the total heat transfer coefficient, so the effect of the contact heat transfer coefficient is notable, although smaller than the effect of the conduction fraction. Most of the contact heat transfer coefficient's dependency of temperature can be traced to the temperature dependency of Meyer's hardness [14]. With further investigation, a discrepancy in the correlation for Meyer's hardness of Zircalloy between the Materials Property Handbook [15] and the actual FRAPTRAN code was

found. Correcting this resulted also in a more reasonable contact heat transfer coefficient. The correlation present in FRAPTRAN code was confirmed to be the one based on data from [14]. Another bug in cladding thermal diametral strain correlation for gap temperatures of over 1073 K was found, which caused the calculation to halt in cases where gap temperature rose above this value, and the iteration procedure was also improved [3] to achieve smoother calculation of the transient scenarios used in this validation report.

4 Simulation methodology

In this chapter the methodology used with the simulations done for the validation are discussed. Details about the assumptions made and the data input methods are given. The simulations were done using an intermediate FINIX version between 0.13.1 and 0.13.9, which corresponds to the FINIX version 0.13.9. The changes made to FINIX mentioned in the previous section 3 were implemented in FINIX version 0.13.9. FINIX was compiled using Microsoft Visual Studio 2010 Professional and the data was processed with MATLAB R2012b.

Input parameters

Most parameters for FINIX could be found in FRAPTRAN input files. Some parameters, for example initial coolant pressure and temperature, were found from literature. In the CABRI tests, the coolant pressure is reported to be 0.5 MPa and the coolant temperature 280 °C [6]. The coolant used in the CABRI tests was sodium, so the coolant model in FINIX could not be used, since it is based on water. Because of rapid heat transfer between the cladding and the sodium coolant, the coolant temperatures are assumed equal with the cladding outer surface temperature, as is done in FRAPTRAN. In the NSRR tests the fuel rod resides in a closed capsule, which is filled with stagnant water at ambient temperature and atmospheric pressure [16], except for case VA-3, where the water temperature is 280 °C. In the NSRR tests, the coolant temperature data input into FRAPTRAN is actually the cladding surface temperature, which in FINIX can be directly input as the cladding surface temperature boundary condition. In FRAPTRAN this is achieved by using a very high cladding-to-coolant heat transfer coefficient and using the cladding surface temperatures as coolant temperaturs in the FRAPTRAN input. The BIGR test conditions were similar to those of the NSRR tests [12], but the boundary condition temperature data are coolant temperatures. A low cladding-to-coolant heat transfer coefficient is used in FRAPTRAN to model the stagnant water, and the same was done in FINIX.

Some assumptions were made because of dissimilar input methods in the two performance codes: If the fill gas was said to consist in part of air, it was assumed in FINIX to consist of nitrogen. Since FRAPTRAN uses a thickness of the oxide layer parameter and FINIX uses one of oxygen content in the cladding, an oxygen content of 0.0012 was assumed for all runs.

Input methods from scenario database

To efficiently calculate different scenarios repetitively, the switching from scenario to scenario was made very simple. All the transient scenario data was collected into a separate function finix_db_fetch_data(), which could be called providing a scenario identifier, and the function would return the linear power history, the coolant temperature history and the axial power distribution. The power and coolant temperature histories were based on three-dimensional arrays to

accommodate differing amounts of axial zones for each.

The steady-state scenario data were also collected in a different function, finix_db_fetch_ss_data(). A different function was used because of the data for the steady-state scenarios are represented differently in the IFPE database and in a larger amount of time steps, so it first had to be translated to the same form that is used in the transient cases. Time interval data was converted into cumulative time and the histories input to a three-dimensional array that can be operated on with the same functions as the transient data.

To allocate memory for the history information, an initialization function finix_db_initialize_database() was used. In this function, the amount of power history and coolant temperature history zones and time steps are given, as well as the number of elevations in the axial power distribution. For the division of the scenario to time steps with different time interval for calculation the function finix_db_timestep_division() was used. This resulted in that all the data for each scenario was situated in a function that was addressed with the variable rodtype. The same host code could now be run with different scenarios by only altering the rodtype variable.

Often the coolant temperature or the linear power data is given at a few axial zones. The axial power factor accounts for the axial variation of linear power in most cases, but in this study for example the IFA-432 experiment data gives the linear power at three points along the axis and no axial power factor is given, only a mention that the axial power distribution is linear and increasing from bottom to top of the rod [5]. In that case, no axial power factor is needed, since a similar solution for the input of this data was used as with the coolant temperature histories: the given linear power is assumed to occur at an arbitrary location (in the cases used here, the thermocouple locations from where the coolant temperature data was from, since the linear power data was calculated for these locations) and then linear power is linearly interpolated for every axial node elevation from a separate array. In the code, it is assumed that if the linear power history is given at more than one location on the rod, no axial power factor is used. For example, in the IFA-432 experiment rods the linear power is given at three points along the rod and this is sufficient to calculate the axial linear power distribution with the assumptions mentioned above.

Because the axial nodalization of the scenario and the amount of zones in the used data are often very different, a method of calculation for the coolant temperature and the linear power at various axial locations was developed. The coolant temperature and the linear power calculation are similar. For each time step, the function finix_db_set_T_bconds() is called in which an axial coolant temperature array is filled with values from the corresponding coolant temperature values at all zones. For purposes of calculation, the rod bottom and top ends that are beyond the data zone center elevation are assumed to have the same temperature as the lowest and the highest axial zone centers, respectively. In the axial coolant temperature array, the temperatures are assigned to arbitrarily chosen locations that might best represent the actual situation. Two solutions are convenient: temperatures can be set to be at axial elevations corresponding to each zone's central elevations or, as was the case in the IFPE data, at the actual thermocouple locations. From this array the coolant temperature is interpolated for every axial node centerline elevation and saved as the boundary condition for this node.

This is in contrast to how axial zones in coolant temperature history are handled in FRAPTRAN. In FRAPTRAN the coolant temperature is set to the corresponding zones as is, e.g. no interpolation is done. However, it is more realistic if the data, be it coolant temperature or linear power, is interpolated between data zone center elevations.

Output methods

All the simulation results were plotted from the topmost axial node in all cases. This applies also to the appendices, where results for each scenario are presented in detail. In most of the cases the axial variation in the linear power is small, which means that there is little variation in the results over the axial nodes. In the CABRI sodium loop tests there is also variation in the coolant temperature boundary condition, which results in larger differences in the results over the axial nodes.

The gap thickness from FINIX is extracted as the difference between pellet outermost and cladding innermost radial nodes. It is defined in the coding that they cannot be closer to one another than the sum of the pellet and cladding roughnesses, as it is in FRAPTRAN. However, the structural gap thickness value output from FRAPTRAN can be zero. Therefore the sum of pellet and cladding roughnesses was substracted from the FINIX-calculated values to make them comparable to the results calculated by FRAPTRAN. The sum of the pellet and cladding roughnesses is 2.5 μm for most of the scenarios, but in the case IFA-429 rod BC the sum is 2 μm and for the IFA-432 experiment rods 2.8 μm.

5 Transient modeling performance

5.1 Classification of scenarios

The scenarios were divided into groups so that similarly behaved simulations formed a single group. Because of the limiting fact that no plastic deformation is yet modeled in FINIX, the rods were divided into those with plastic deformation (discussed in section 5.2) and those without (discussed in section 5.3). Plastic deformation was taken to occur when the structural gap as calculated by FRAPTRAN first closes and then begins to widen again, which is indicative of cladding ballooning. These groups were further divided into those rods that had been reported as burst by FRAPTRAN. FRAPTRAN calculations differ from the regular routine and so from FINIX after the rod has been reported as burst, since no similar routine is yet implemented in FINIX. Rods are divided into groups as follows:

- Unfailed rods with plastic deformation: CABRI REP-Na3, NSRR HBO-1, HBO-6, TS-5 and FK-1, BIGR RT-4 and RT-10
- Failed rods with plastic deformation: NSRR HBO-5, VA-1 and VA-3, BIGR RT-8 and RT-12
- Unfailed rods with little plastic deformation: CABRI REP-Na4
- Failed rods with little plastic deformation: CABRI REP-Na1 and REP-Na8

5.2 Rods with plastic deformation

5.2.1 General results

Two cases illustrate the rods with plastic deformation: CABRI REP-Na3 illustrates an unfailed rod with some plastic deformation taking place and NSRR HBO-5 illustrates a failed rod with some plastic deformation taking place. The other cases from each group behave similarly to these two, and these cases are representative of their respective groups. The VVER rods are included in this group. Their cladding material is different and this has some effects that are discussed in section 5.5.

No rod burst

In the REP-Na3 scenario plastic deformation can be seen as the structural gap thickness (figure 1) begins to rise shortly after being closed. This implies that some cladding ballooning may occur. Since only elastic strain is modeled in FINIX, the value calculated by FINIX for structural gap thickness stays zero even after FRAPTRAN calculates non-zero values for the gap thickness.

The heat transfer coefficient as seen from figure 3 is overestimated by FINIX by an order of magnitude towards the end of the scenario. This happens because the gap stays closed in the absence of cladding ballooning in the FINIX model. The effective gap width (figure 2) has the largest effect on the conduction heat transfer coefficient, which in turn is the largest constituent of the total gap heat transfer coefficient. After the structural gap begins to widen, also the effective gap width widens and the conduction heat transfer begins to decrease.

In the REP-Na3 scenario there is also a small effect from the contact heat transfer coefficient in the end of the scenario, which can be traced back to the contact pressure between the fuel and the cladding. The contact pressure results vary between FINIX and FRAPTRAN, most likely because of the absence of the plastic strain model. In FINIX, the contact pressure rises as the gap closes, but also stays high, which by FRAPTRAN calculation would not happen. According to FRAPTRAN, the contact pressure peaks during a small time step and then decreases back to zero. This can also be explained by cladding ballooning, where the gap opens up again after being closed for a finite time.

The internal gas pressure (figure 4) of the rod is calculated to be higher in FINIX than in FRAPTRAN. This can also be explained by cladding ballooning in the later stages of the scenario, as the rod internal volume gets higher with ballooning. As ballooning is not modeled in FINIX, the internal volume is lower during the scenario and so the pressure is higher. The volume of the gas that resides in the plenum affects the internal pressure greatly. Since in FINIX the heat capacity of the gas is assumed to be zero, the plenum heats more rapidly than in FRAPTRAN, where the heat capacity of the fill gas is nonzero. There may also be other differences in the plenum temperature models in the two codes that were not investigated during the validation. As can be seen from figure 7, the plenum temperature is therefore higher as calculated by FINIX, and because of this the gas pressure is also higher in FINIX.

As for the internal pressure discrepancy in the beginning of the scenario, where no heating of the fill gas has occurred, the cause is for the most part a difference in the internal volume of the rod. In the case REP-Na3, the internal volume of the rod in the beginning calculated by FINIX is 7.3 % lower than that calculated by FRAPTRAN and the internal pressure is 10.4 % higher in FINIX. The internal volume of the rod consists of the gap volume and the plenum volume. FINIX calculates a 23 % higher gap volume, but its effect on the total rod internal volume is small, since the gap volume accounts for 8.8 % of the total rod volume in FINIX and 6.6 % in FRAPTRAN. However, the plenum volume, that accounts for the rest of the total rod internal volume, is 9.5 % smaller according to FINIX. This means that most of the pressure difference can be traced to the difference in the plenum volume. FRAPTRAN also calculates an open porosity fraction that is added to the internal volume of the rod that the fill gas can occupy, and this is not done in FINIX. However, the open porosity fraction calculated by FRAPTRAN accounts only a small fraction of the discrepancy.

The temperatures calculated by the two codes for the fuel and cladding are very similar. Few differences can be found, which can be explained by the different heat transfer coefficients. The fuel centerline and surface temperatures are presented in figure 5 and the cladding inner and outer surface temperatures in figure 6. As can be seen, the fuel centerline temperature is lower in FINIX, which is a result of the higher heat transfer coefficient. The fuel surface temperature is also somewhat lower and the the cladding inner surface temperature somewhat higher for the same reason. The cladding outer surface temperatures are the same for both codes, since it is used as a boundary condition.

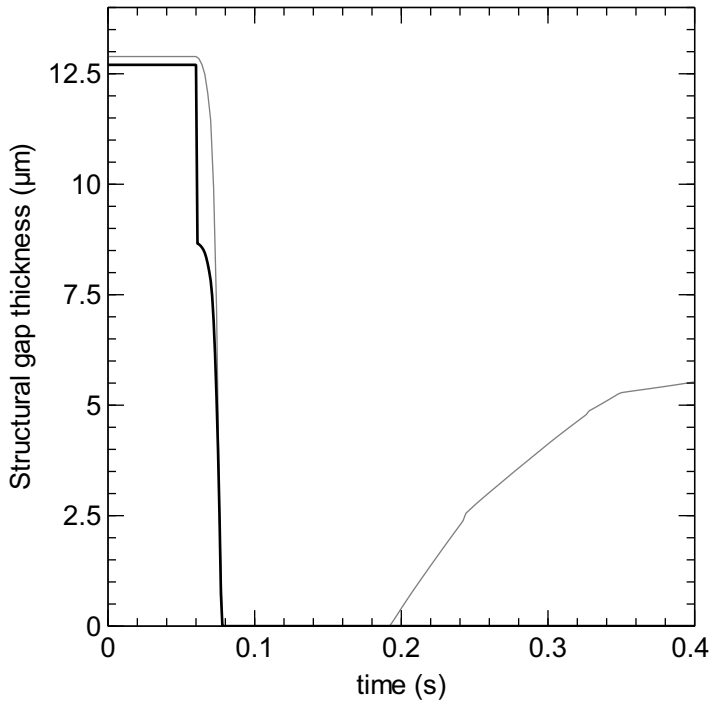

Figure 1. *Structural gap thickness in CABRI REP-Na3 as calculated by FINIX (solid black line) and FRAPTRAN (solid grey line).*

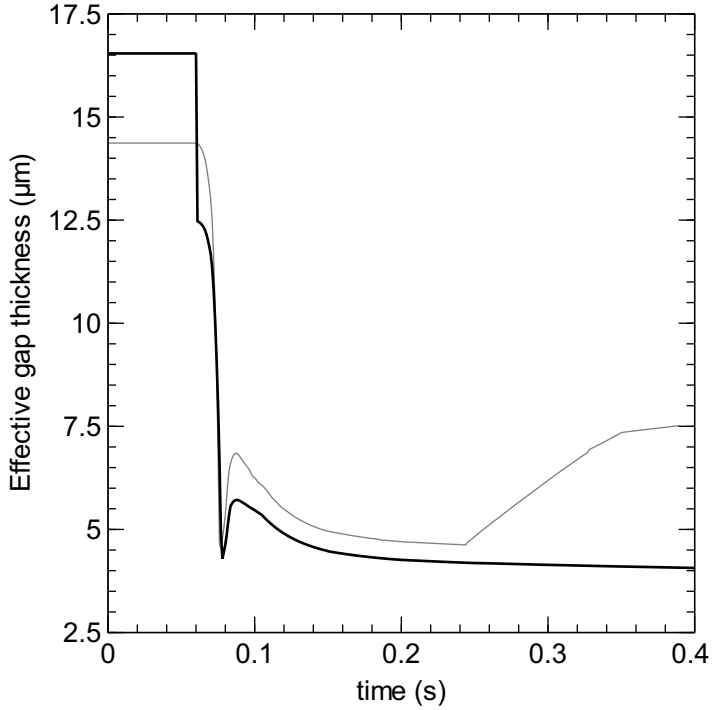

Figure 2. *Effective gap thickness in CABRI REP-Na3 as calculated by FINIX (solid black line) and FRAPTRAN (solid grey line).*

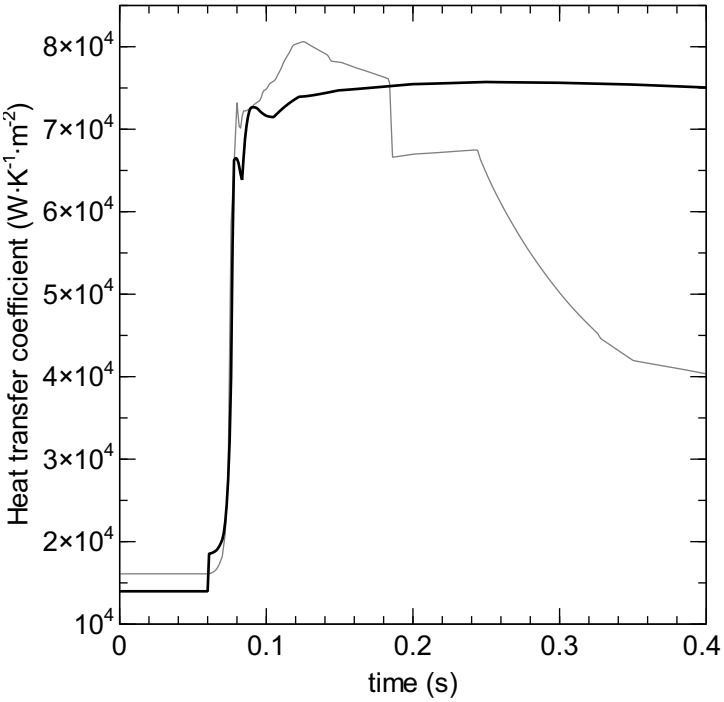

Figure 3. *Gap heat transfer coefficient in CABRI REP-Na3 as calculated by FINIX (solid black line) and FRAPTRAN (solid grey line).*

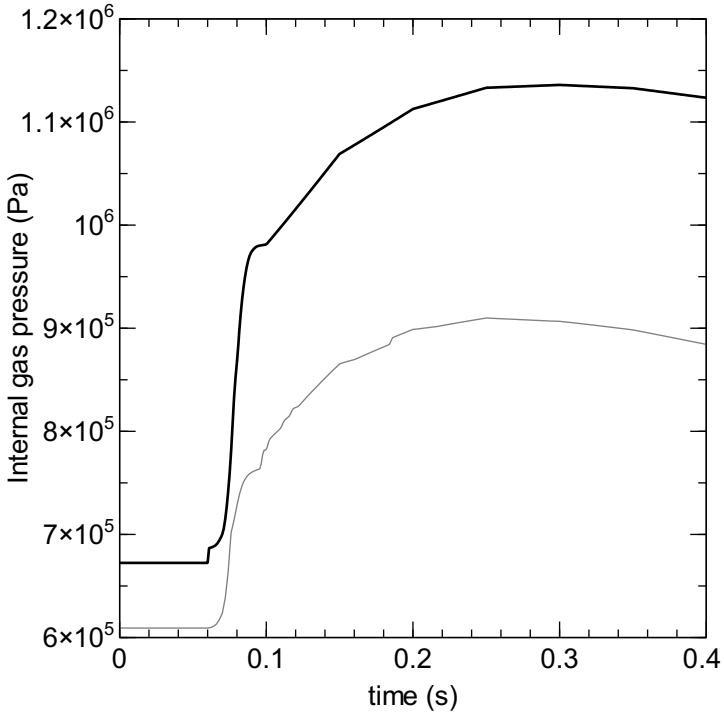

Figure 4. *Internal gas pressure in CABRI REP-Na3 as calculated by FINIX (solid black line) and FRAPTRAN (solid grey line).*

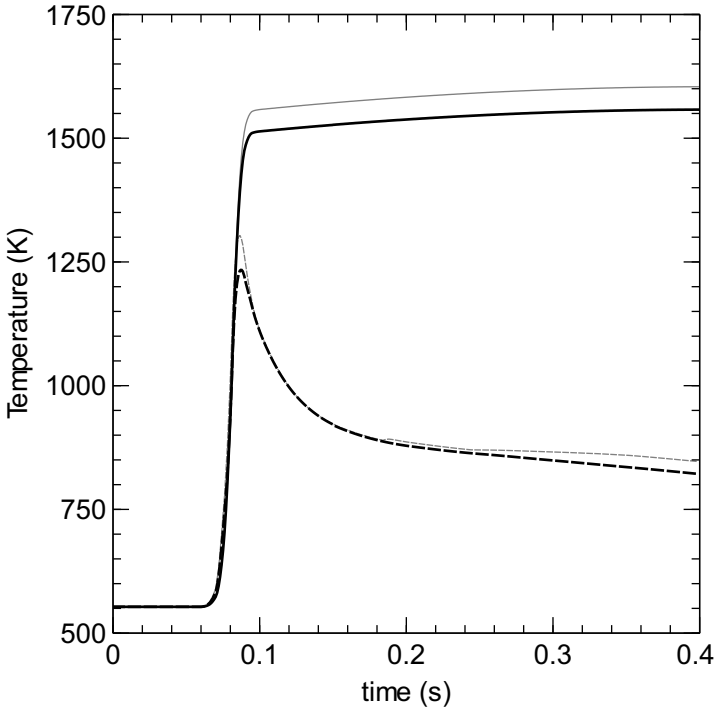

Figure 5. *Fuel centerline (solid lines) and fuel surface (dashed lines) temperatures in CABRI REP-Na3 as calculated by FINIX (black lines) and FRAPTRAN (grey lines).*

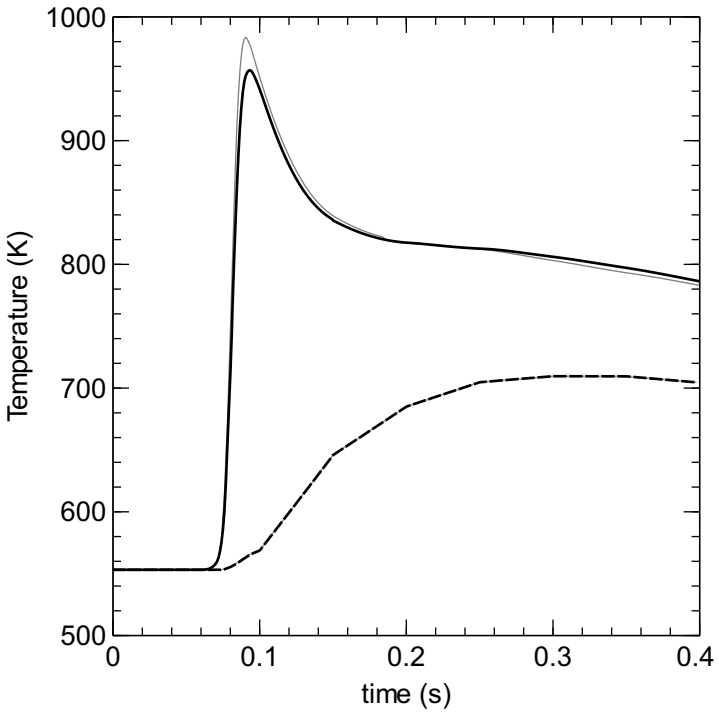

Figure 6. *Cladding inner surface (solid lines) and outer surface (dashed lines) temperatures in CABRI REP-Na3 as calculated by FINIX (black lines) and FRAPTRAN (grey lines).*

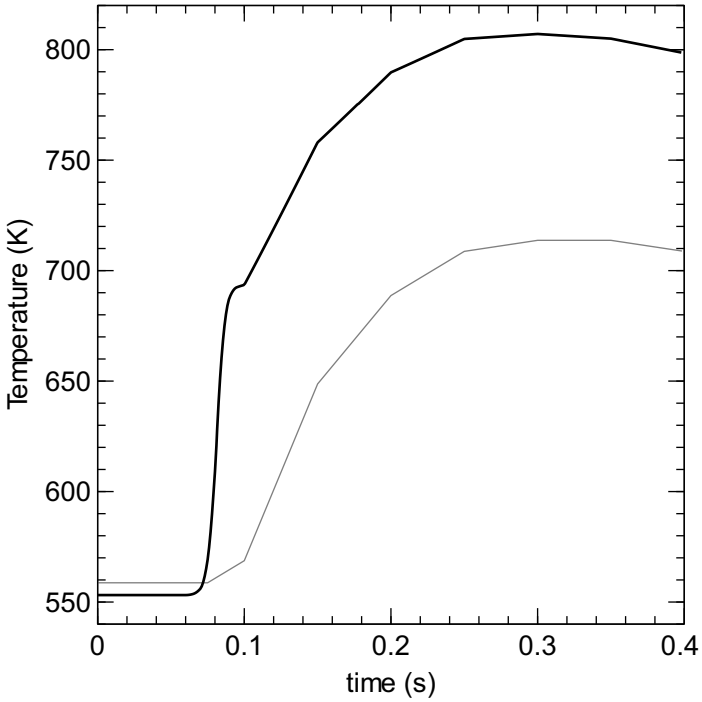

Figure 7. *Plenum temperature in CABRI REP-Na3 as calculated by FINIX (solid black line) and FRAPTRAN (solid grey line).*

Rod failure

The NSRR HBO-5 case behaves very similarly compared to the CABRI REP-Na3 scenario. The structural gap thickness is shown in figure 8 and the rod burst is marked with a circle on the x-axis. The rod bursts immediately after contact with the pellet and the cladding. FINIX calculates a somewhat smaller initial structural gap width but, as can be seen from figure 9 the effective gap widths are very similar. After the rod burst the effective gap thickness has different values in FINIX and FRAPTRAN, which results in different heat transfer coefficients. Cladding ballooning as seen in figure 8 can be assumed to be the main reason for this.

The heat transfer coefficient from FINIX is higher as can be seen in figure 10, which is a result of the smaller effective gap thickness. This is the reason for the somewhat lower fuel temperatures in figure 13 and higher peak cladding inner surface temperature in figure 12.

The internal gas pressure behaviour according to FRAPTRAN as seen in figure 11, where the internal gas pressure is set to the coolant pressure and stays at this value after rod burst, is caused by the FRAPTRAN rod burst criterion. In FINIX, the rod burst is not yet modelled and the pressure is therefore calculated in a different manner.

The contact pressure in HBO-5 in underestimated by several orders of magnitude. In this case the contact pressure appears as a narrow peak, returning to zero as cladding ballooning begins. FINIX calculates the contact pressure as being a very low value, but the behavior is similar to the unfailed rod scenarios: a peak value is achieved and then contact pressure slowly decreases having a value other than zero at the end of the scenario. Most likely the contact pressure dissipates along with heat flowing out of the rod and the fuel pellet slowly decreasing in volume.

The value of the structural gap width differs when calculated by FINIX and FRAPTRAN, as can be seen from figure 8. Similar behavior can aslo be seen in cases CABRI REP-Na1 (figure 21) and REP-Na4 (figure 14). The cause of this discrepancy is still unknown. It must be noted, that even though the value in the beginning is different, the change during the power ramp occurs very similarly in all cases. When the structural gap width is calculated by FINIX to be higher than that calculated by FRAPTRAN, the internal volume of the rod is greater in FINIX than in FRAPTRAN. The open porosity fraction (discussed in section 5.2.1) is taken into account in the internal volume calculated by FRAPTRAN, but not in that calculated by FINIX, so the gap thickness has a greater effect in the internal volume (and therefore internal pressure) of the rod than the open porosity fraction.

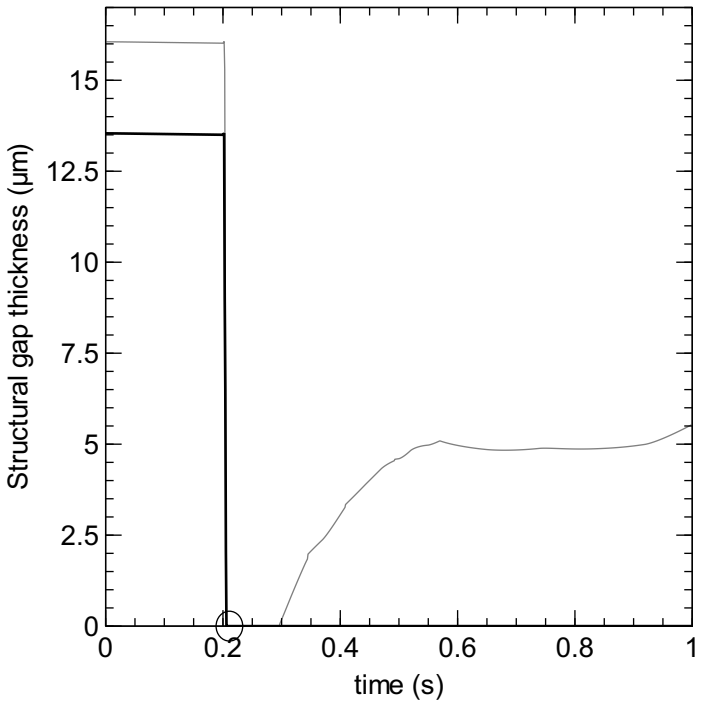

Figure 8. *Structural gap thickness in NSRR HBO-5 as calculated by FINIX (solid black line) and FRAPTRAN (solid grey line). Circle on x-axis marks rod burst.*

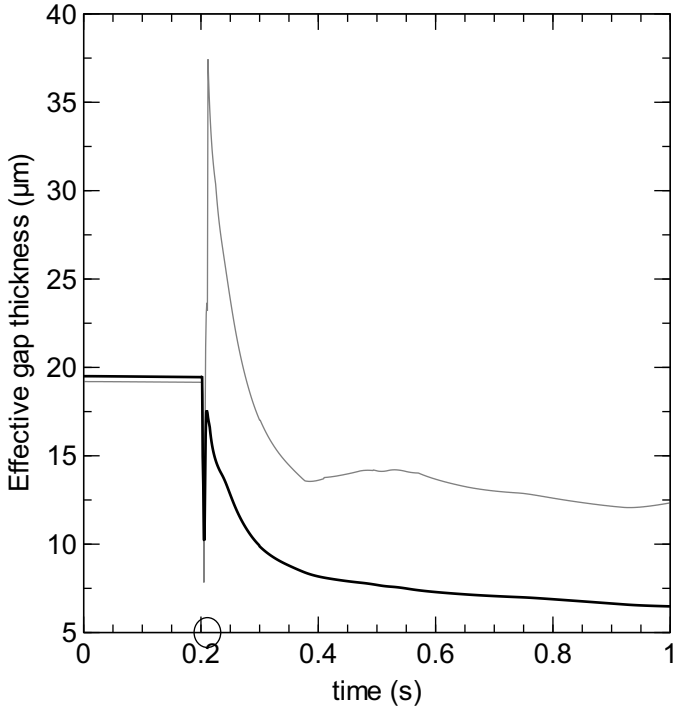

Figure 9. *Effective gap thickness in NSRR HBO-5 as calculated by FINIX (solid black line) and FRAPTRAN (solid grey line). Circle as before.*

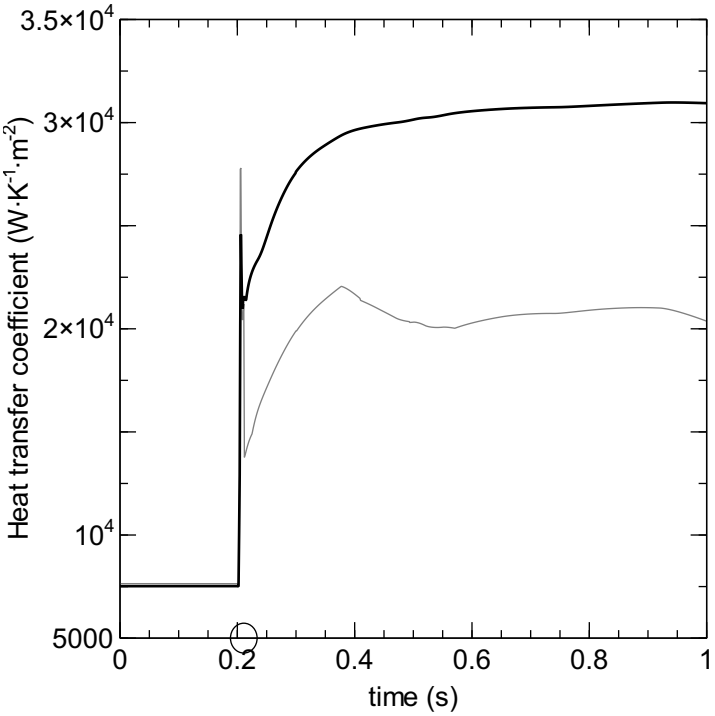

Figure 10. *Gap heat transfer coefficient in NSRR HBO-5 as calculated by FINIX (solid black line) and FRAPTRAN (solid grey line). Circle as before.*

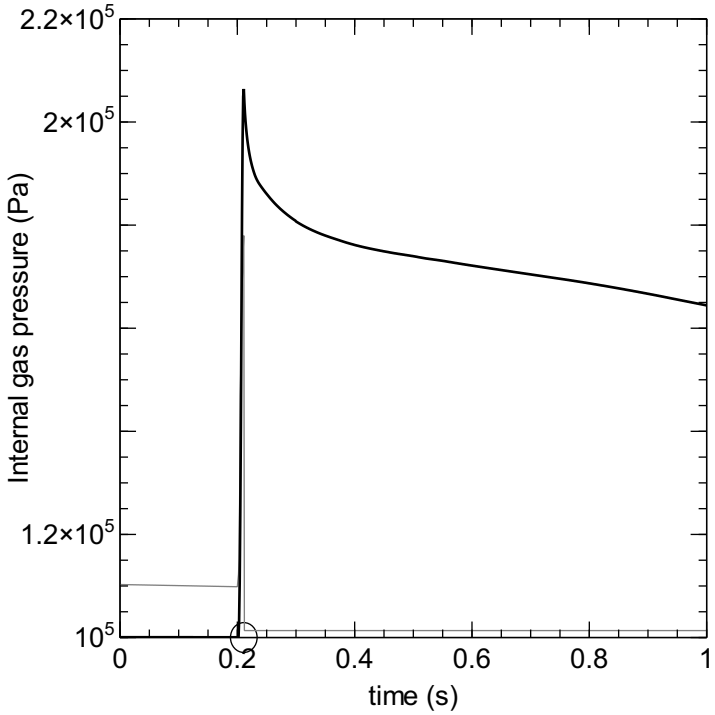

Figure 11. *Internal gas pressure in NSRR HBO-5 as calculated by FINIX (solid black line) and FRAPTRAN (solid grey line). Circle as before.*

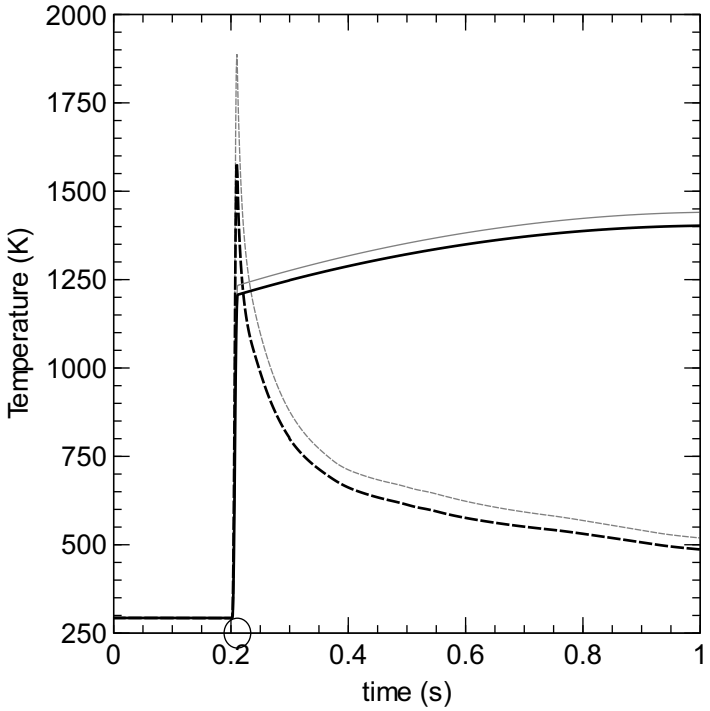

Figure 12. *Fuel centerline (solid lines) and fuel surface (dashed lines) temperatures in NSRR HBO-5 as calculated by FINIX (black lines) and FRAPTRAN (grey lines). Circle as before.*

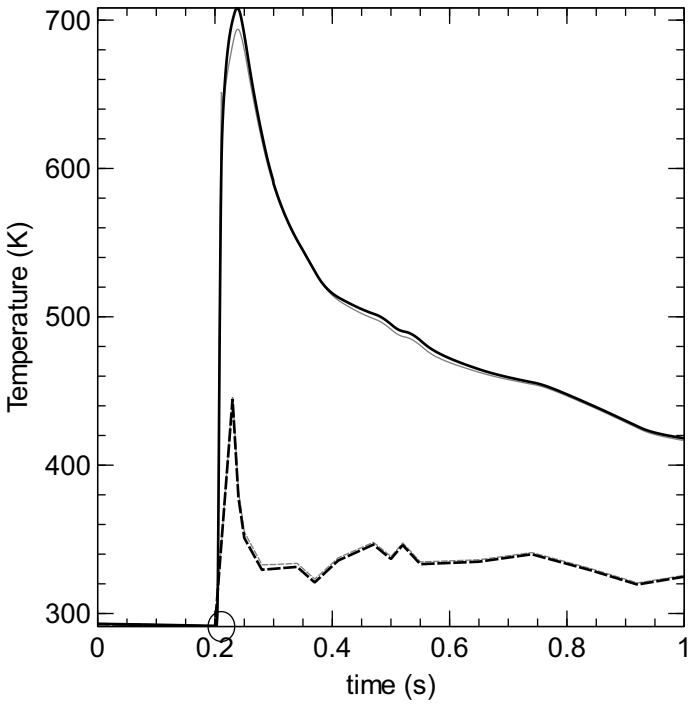

Figure 13. *Cladding inner surface (solid lines) and outer surface (dashed lines) temperatures in NSRR HBO-5 as calculated by FINIX (black lines) and FRAPTRAN (grey lines). Circle as before.*

5.2.2 Notes on individual scenarios

CABRI REP-Na3: Detailed description in section 5.2.1.

NSRR FK-1: Unfailed rod with cladding ballooning. Oscillation in contact pressure calculation and cladding hoop strain calculation, detailed discussion in section 5.6. Mostly behaves similarly to REP-Na3.

NSRR HBO-1: This scenario is different from all the rest of the transient scenarios in that it had failed experimentally, but FRAPTRAN did not report the rod as burst. Oscillation in contact pressure calculation, detailed discussion in section 5.6. Mostly behaves similarly to REP-Na3.

NSRR HBO-5: Detailed description in section 5.2.1.

NSRR HBO-6: Unfailed rod with cladding ballooning. Oscillation in contact pressure calculation, detailed discussion in section 5.6. Mostly behaves similarly to REP-Na3.

NSRR TS-5: Unfailed rod with cladding ballooning. Contact pressure behavior similar with REP-Na3, which has the same effects as described in section 5.2.1. Lowest burnup of the scenarios, 26.6 GWd/MtU, whereas the other scenarios have rods with burnup over 40 GWd/MtU.

NSRR VA-1: Burst rod with cladding ballooning, so FINIX calculates the heat transfer coefficient very high compared to FRAPTRAN. Contact pressure is high, and contact heat transfer has a high proportion of the total heat transfer coefficient. Otherwise similar to HBO-5.

NSRR VA-3: Similar to the VA-1 scenario. Experimentally different in that this is a so-called hot capsule test where the stagnant water in the test capsule at the beginning of the test was not at room temperature but at 280 °C.

BIGR RT-4: VVER rod. A jump in the cladding hoop strain, possible problem with the mechanical solution.

BIGR RT-8: Similar to RT-4, but higher power and no problems in the mechanical solution. Very high contact heat transfer coefficient in FRAPTRAN because of a different Meyer's hardness correlation.

BIGR RT-10: Similar to RT-4, but higher power and no problems in the mechanical solution.

BIGR RT-12: Similar to RT-8.

5.3 Rods with little plastic deformation

5.3.1 General results

Two cases illustrate the rods with little plastic deformation: CABRI REP-Na4 illustrates an unfailed rod with some plastic deformation taking place being the only rod in this category and CABRI REP-Na1 illustrates a failed rod with little plastic deformation taking place. The only other failed rod with little plastic deformation is the REP-Na8.

No rod burst

Generally, the CABRI REP-Na4 scenario behaves as the previous scenarios with plastic deformation. The difference to the scenarios with plastic deformation can be seen from figure 14, where both codes calculate the structural gap thickness to zero for REP-Na4 from the closing of the gap to the end of the calculation. Both codes calculate very similar results: the heat transfer coefficient is very similar (figure 16) and even the pellet-cladding contact pressures are very closely matched (figure 20).

The main difference is in the calculation of the internal gas pressure (figure 17), which is higher in FINIX. The causes for the different results for the rod internal pressure are explained in section 5.2.1. Also the contact pressure is higher in FINIX, which can be explained by the lack of plastic deformation in FINIX. Even though the gap stays closed, no plastic deformation can occur in FINIX to relieve the contact pressure partially.

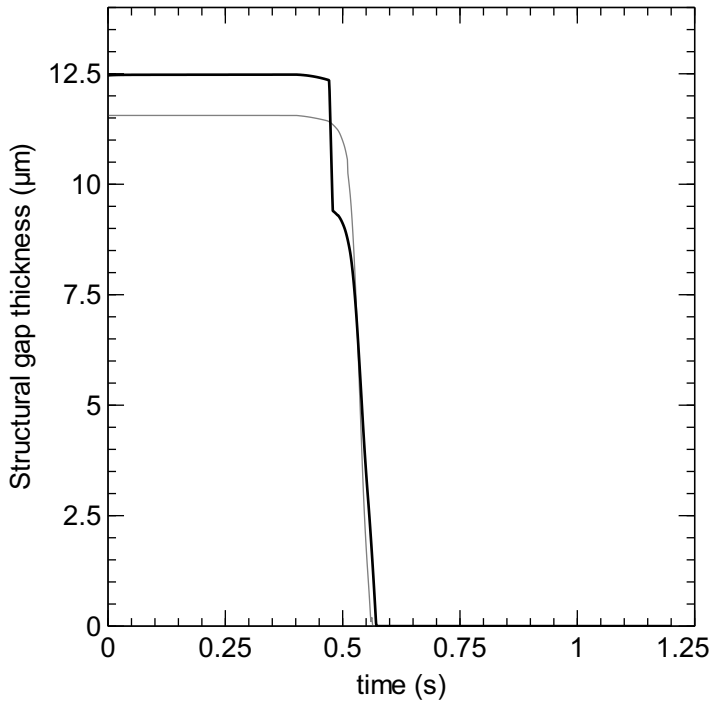

Figure 14. *Structural gap thickness in CABRI REP-Na4 as calculated by FINIX (solid black line) and FRAPTRAN (solid grey line).*

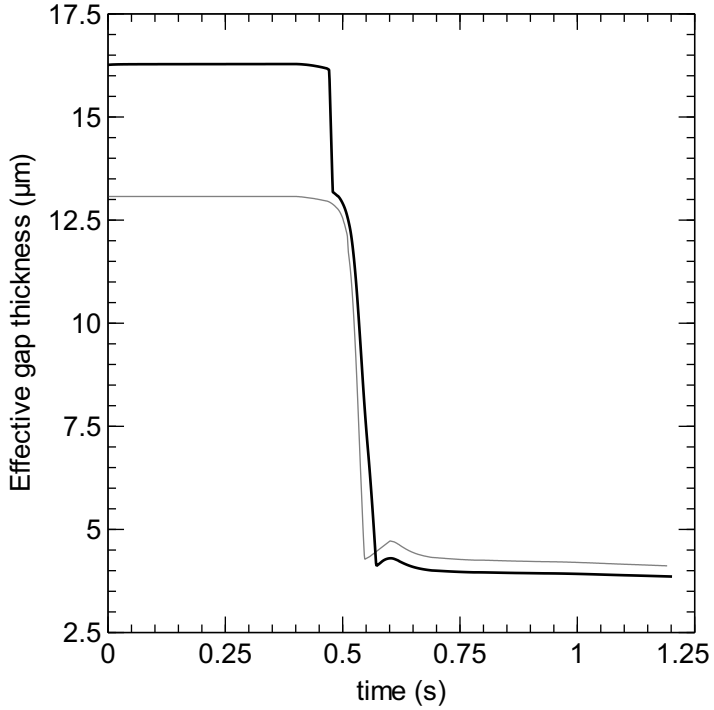

Figure 15. *Effective gap thickness in CABRI REP-Na4 as calculated by FINIX (solid black line) and FRAPTRAN (solid grey line).*

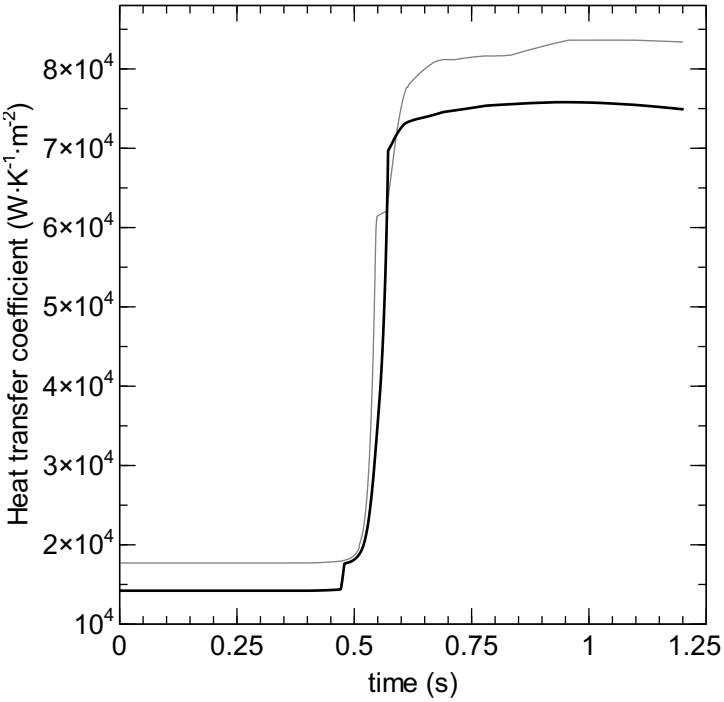

Figure 16. *Gap heat transfer coefficient in CABRI REP-Na4 as calculated by FINIX (solid black line) and FRAPTRAN (solid grey line).*

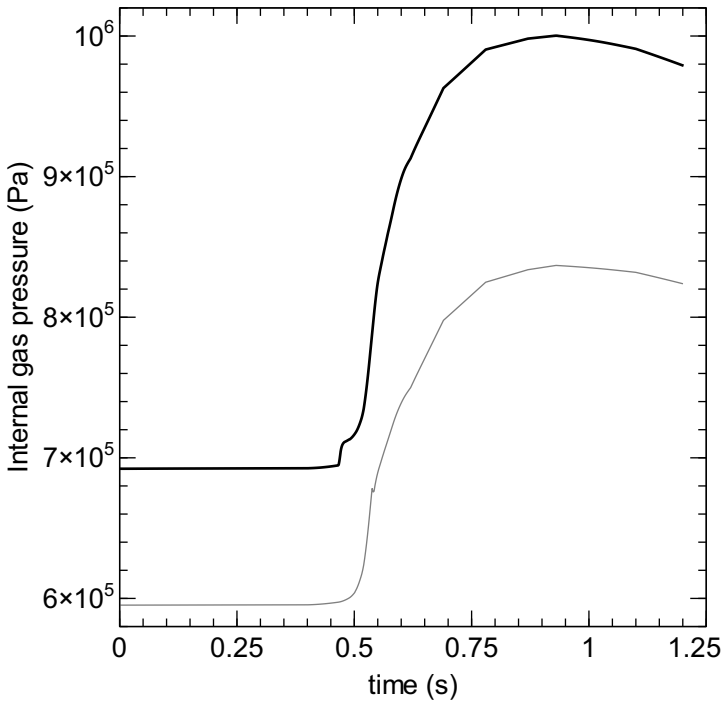

Figure 17. *Internal gas pressure in CABRI REP-Na4 as calculated by FINIX (solid black line) and FRAPTRAN (solid grey line).*

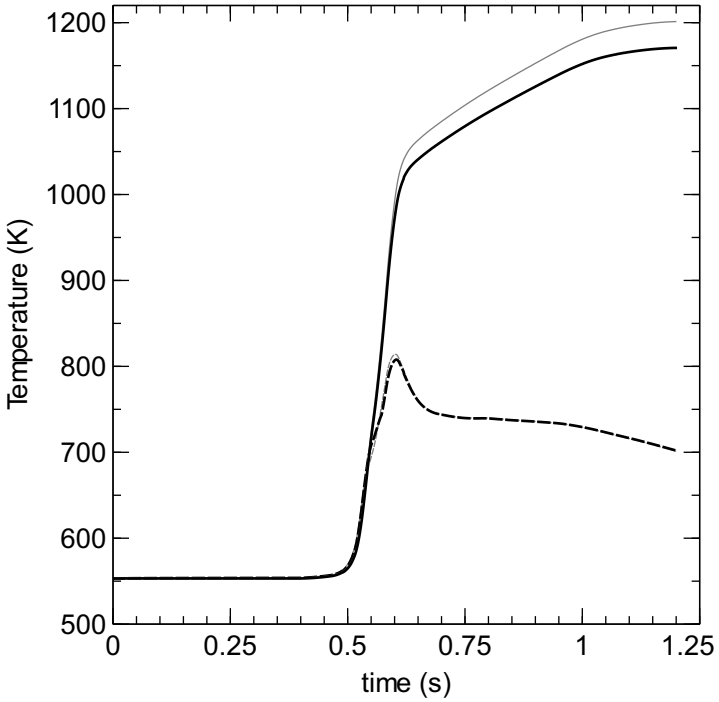

Figure 18. *Fuel centerline (solid lines) and fuel surface (dashed lines) temperatures in CABRI REP-Na4 as calculated by FINIX (black lines) and FRAPTRAN (grey lines).*

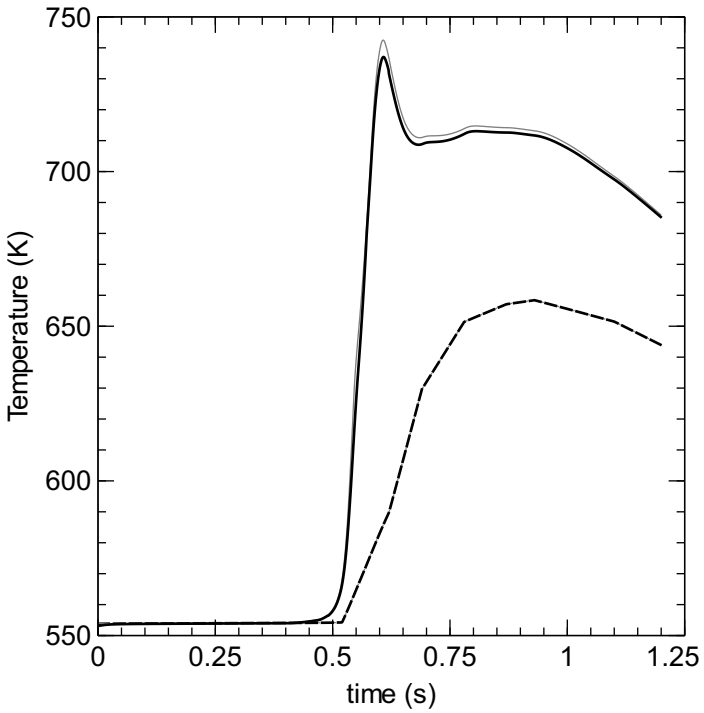

Figure 19. *Cladding inner surface (solid lines) and outer surface (dashed lines) temperatures in CABRI REP-Na4 as calculated by FINIX (black lines) and FRAPTRAN (grey lines).*

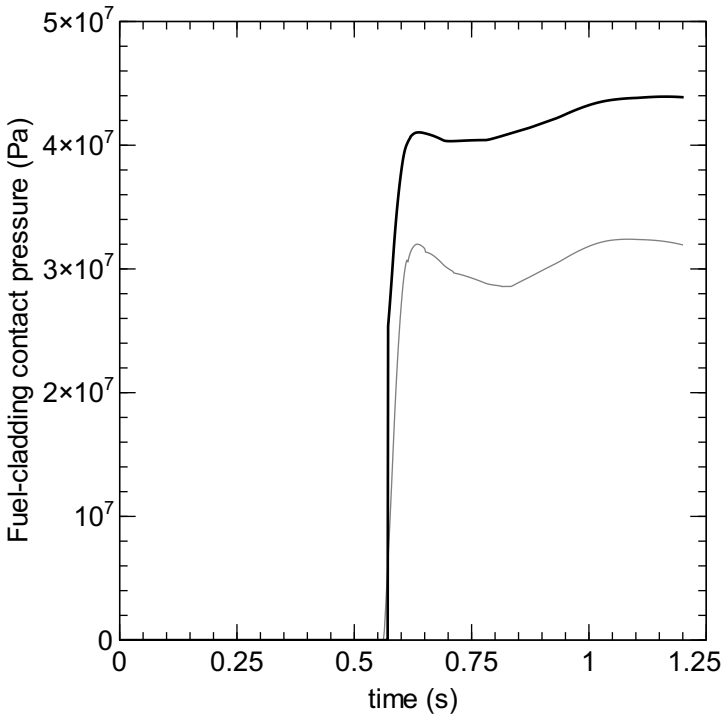

Figure 20. *Pellet-cladding contact pressure in CABRI REP-Na4 as calculated by FINIX (black lines) and FRAPTRAN (grey lines).*

Failed rod

In the scenario REP-Na1 there is more plastic deformation than in REP-Na4, which can be seen from the pellet-cladding contact pressure (figure 27): as with the scenarios with more plastic deformation, the contact pressure peaks and then returns to zero as calculated by FRAPTRAN. FINIX-calculated contact pressure behavior is then similar to the cases in section 5.2.1, where contact pressure only slowly decreases.

Gap heat transfer coefficient (figure 23) and the fuel (figure 25) and cladding (figure 26) temperatures are very closely matched. In this case, the gas pressure (figure 24) is also calculated to similar values, but it must be brought to mind that this rod has burst and the pressure set to coolant pressure in FRAPTRAN.

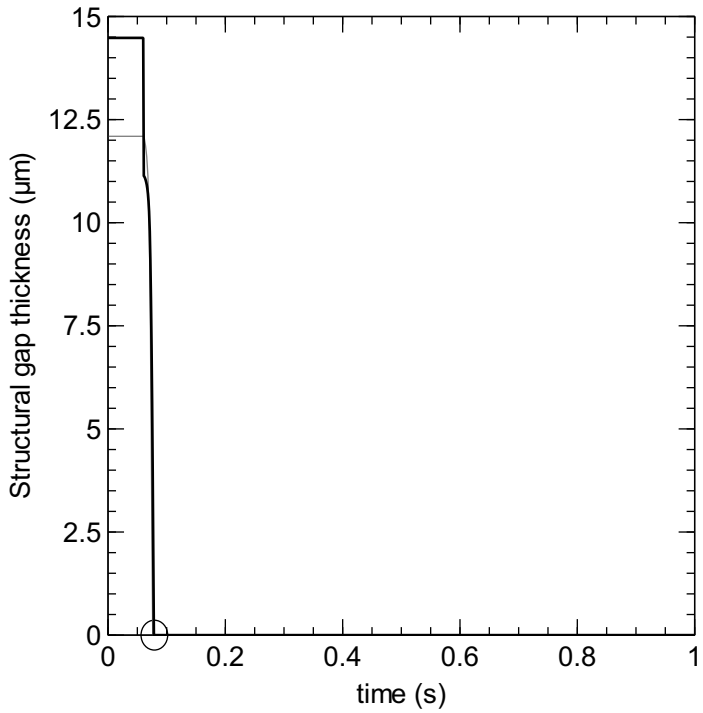

Figure 21. *Structural gap thickness in CABRI REP-Na1 as calculated by FINIX (solid black line) and FRAPTRAN (solid grey line). Circle on x-axis marks rod burst.*

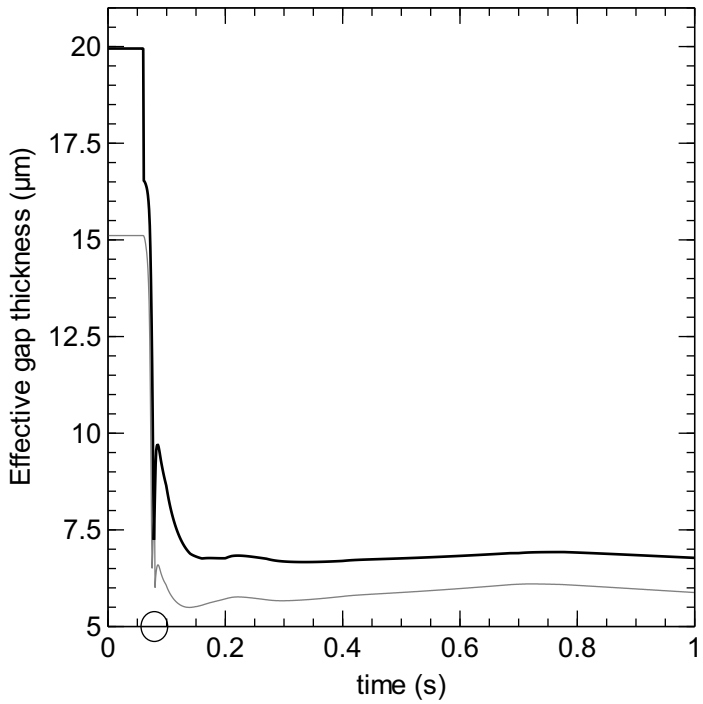

Figure 22. *Effective gap thickness in CABRI REP-Na1 as calculated by FINIX (solid black line) and FRAPTRAN (solid grey line). Circle as before.*

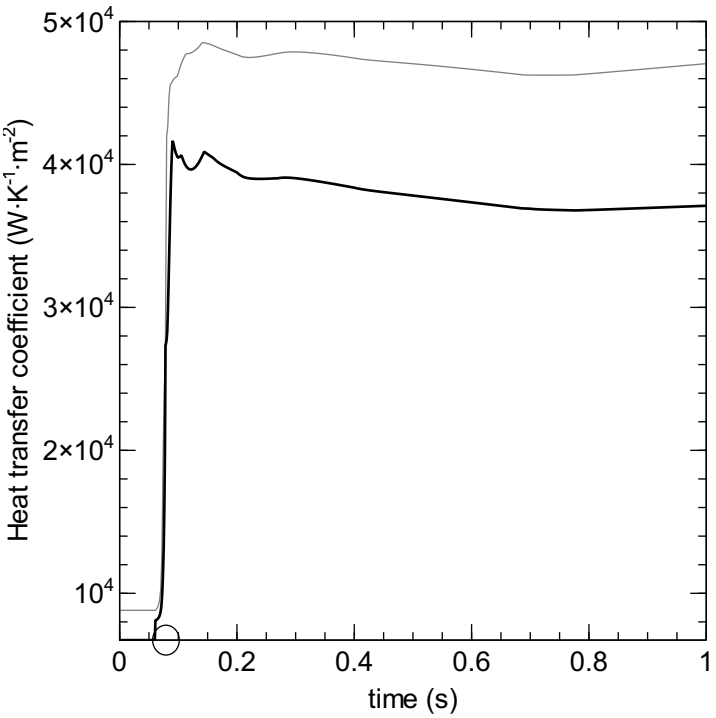

Figure 23. *Gap heat transfer coefficient in CABRI REP-Na1 as calculated by FINIX (solid black line) and FRAPTRAN (solid grey line). Circle as before.*

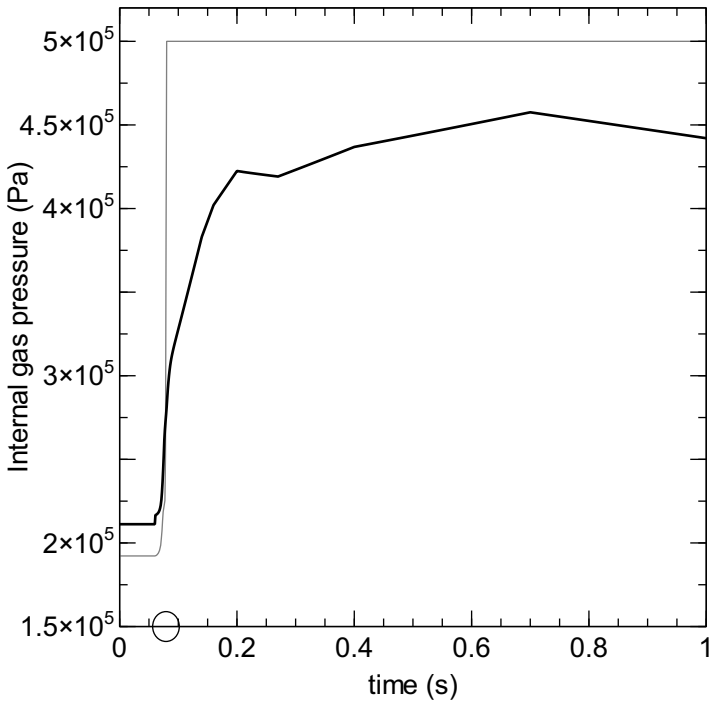

Figure 24. *Internal gas pressure in CABRI REP-Na1 as calculated by FINIX (solid black line) and FRAPTRAN (solid grey line). Circle as before.*

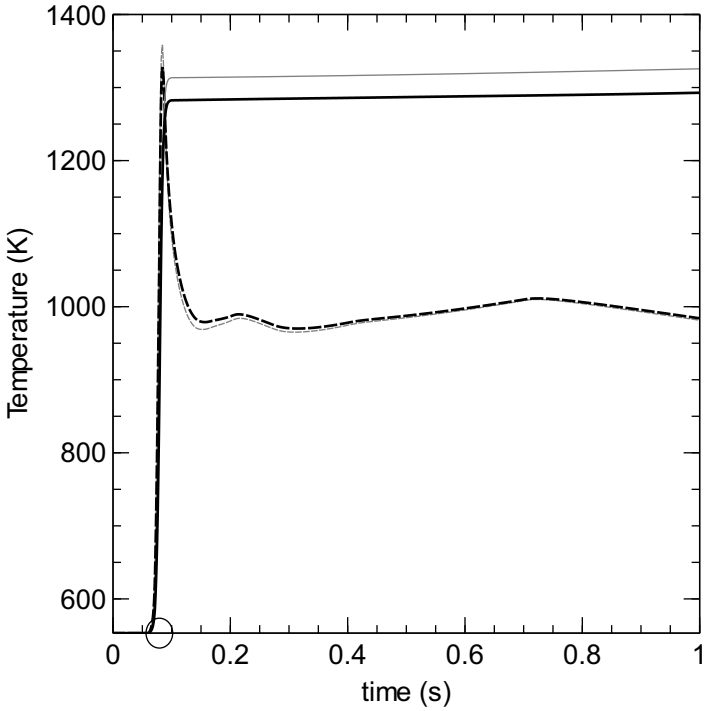

Figure 25. *Fuel centerline (solid lines) and fuel surface (dashed lines) temperatures in CABRI REP-Na1 as calculated by FINIX (black lines) and FRAPTRAN (grey lines). Circle as before.*

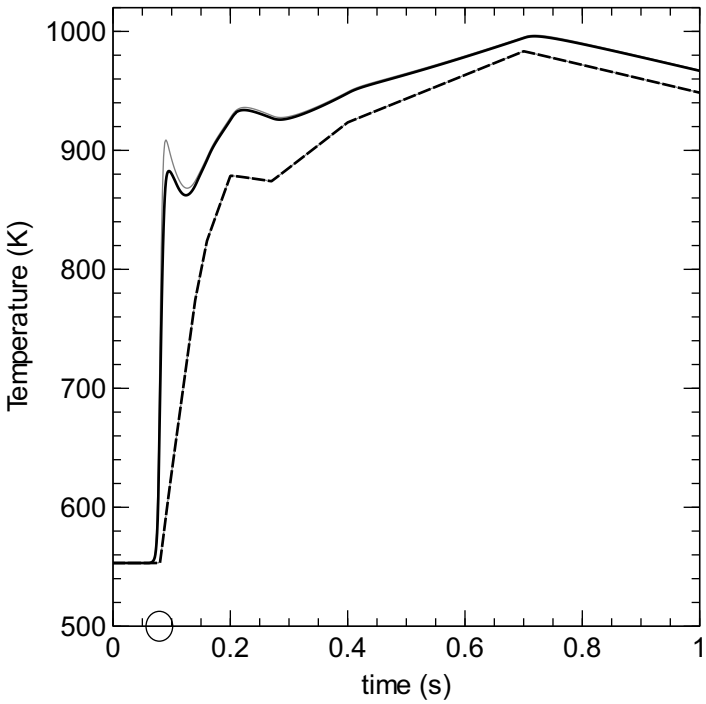

Figure 26. *Cladding inner surface (solid lines) and outer surface (dashed lines) temperatures in CABRI REP-Na1 as calculated by FINIX (black lines) and FRAPTRAN (grey lines). Circle as before.*

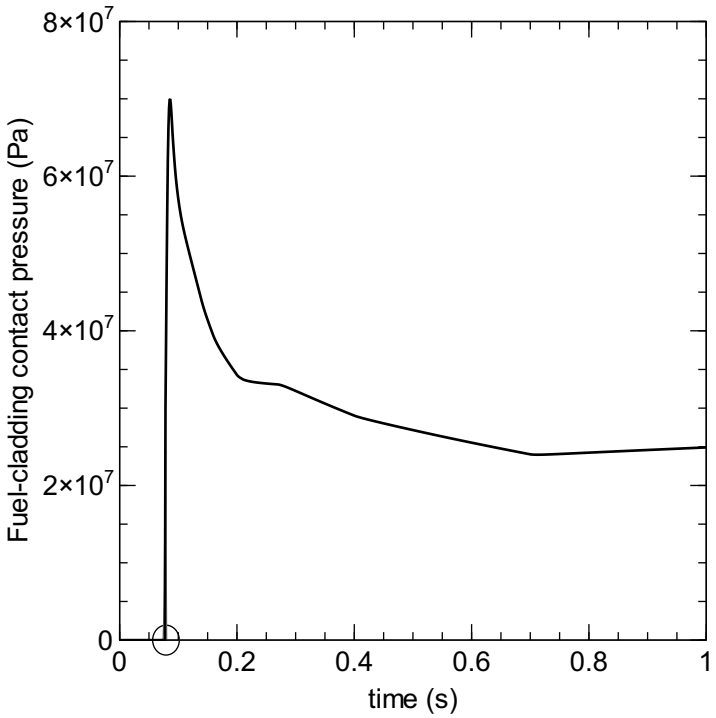

Figure 27. *Pellet-cladding contact pressure in CABRI REP-Na1 as calculated by FINIX (black lines) and FRAPTRAN (not visible because of difference in magnitude).*

5.3.2 Notes on individual scenarios

CABRI REP-Na1: Detailed description in section 5.3.1.

CABRI REP-Na4: Detailed description in section 5.3.1. Large power pulse width, 76.4 ms.

CABRI REP-Na8: Similar to the REP-Na1, but the power pulse width is large, 75 ms (9.5 ms for REP-Na1).

5.4 Relocation model

Before the corrections made to FINIX the FINIX and FRAPTRAN models differed in their calculation of the heat transfer coefficient and so the parameters affecting the calculation of its values were of interest. Effective gap width is directly related to the heat transfer coefficient, and the main factor influencing the effective gap width was found to be the soft relocation that diminishes the effective gap width excessively when using the FRAPTRAN correlation for its calculation. The relocation models and their influence on the results were investigated further from FRAPTRAN code and some test runs with FINIX. Only calculations done by using the FRACAS-I model were investigated from the code, since no model corresponding to FRACAS-II (the FRAPTRAN FEM model) is present in FINIX.

Two cases are possible for the relocation calculation: either the relocation strain is calculated from the relocation parameter calculated by FRAPCON in the restart file, or the relocation is calculated

by internal correlations. In the transient scenarios used in this study the relocation strain is always taken from a restart file. It must then be known what actually is printed out in the FRAPCON-made restart file, and how the FRAPTRAN and FRAPCON relocation models differ.

In FINIX, the relocation read in from the restart file is put into variables for hard relocation strain and soft relocation strain after dividing with cold state pellet radius, treating the number in the restart file as being half of the total relocation. The number actually put into the restart file by FRAPCON is half of the amount of total relocation as calculated by FRAPCON. There is another parameter in the restart file for fuel displacement due to swelling and densification, which includes only these effects, not relocation, so it is safe to say that relocation is not counted twice if the effect of both of these variables are added up in FINIX.

FRAPTRAN also reads in the relocation from the FRAPCON-made restart file. This amount, defined as hard relocation in FINIX, is defined as permanent relocation in FRAPTRAN and FRAPCON. FRAPTRAN divides this relocation evenly over all the radial nodes, so that the relocation is then contained in the radial node locations. Thermal relocation is not covered in FRAPTRAN in the calculation of the heat transfer coefficient. The gap thickness used in the heat transfer coefficient calculation is simply the gap thickness calculated from the radial node positions, and so includes the permanent (hard) relocation.

In the FINIX version 0.13.1 there are no correlations for relocation of the pellet. FRAPTRAN uses a simple correlation where relocation has a value of 30 % of gap thickness if burnup is zero, and 45 % of gap thickness otherwise. FINIX-0.13.9, however, uses the FRAPCON correlation for pellet relocation, which is burnup-dependent and more accurate. With the TMI-1 test case it was tested how the what model would best match the FRAPTRAN model with respect to the handling of relocation. Best agreement with the FRAPTRAN model was found when soft and hard relocation were set in FINIX at 30 % of gap width, when structural gap width is of concern. If the FRAPTRAN relocation correlation is used and gap width in the effective gap width correlation set to the structural gap width (ignoring soft relocation), the effective gap width is calculated by FINIX to be very close to the value calculated by FRAPTRAN itself. The values calculated with different correlations for the case CABRI REP-Na4 can be seen in figure 28. As is evident from the figure, the FRAPTRAN correlation which uses a structural gap width taking into account the soft relocation calculates a minimal effective gap width for the whole scenario. From this it can be concluded, as before, that FRAPTRAN ignores the soft relocation effect in calculating the effective gap width for gap heat conductance.

It was also found that FRAPCON checks whether there is contact with the pellet and cladding in the calculation of relocation for the pellet. If there is contact with the cladding, no relocation is added. A similar check is not performed in FINIX, but it might be useful to modify FINIX in this way in the future.

5.5 Gap heat conductance

FRAPCON and FRAPTRAN correlations

The gap heat conductance correlation used by FRAPCON-3.4 and FRAPTRAN-1.4 are different. FRAPTRAN does not take into account the contact pressure in the effective gap width correlation, whereas FRAPCON does. It was also tested what FRAPTRAN assumes to be the gap width from

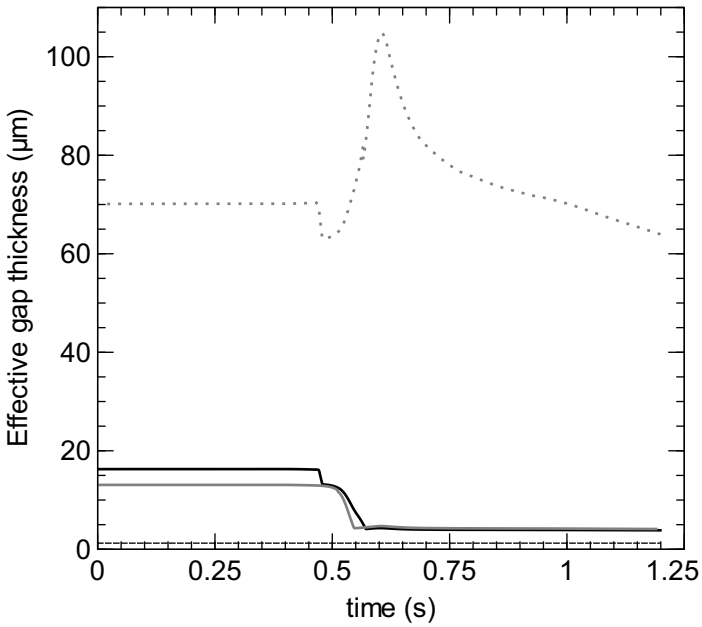

Figure 28. *Effective gap width calculated by FRAPTRAN (thick solid grey line) and FINIX with different correlations for the CABRI REP-Na4 scenario: FRAPCON (grey dotted line), FRAPTRAN with relocation (grey dashed line) and FRAPTRAN without relocation (thick black line).*

which it calculates the effective gap width, and it was found that FRAPTRAN ignores the soft or non-permanent relocation in this respect, as was discussed in section 5.4. The correlations tested are as follows:

(1) $d_{eff} = e^{-0.00125 P_{contact}}(\rho_f + \rho_c) + 1.8(g_f + g_c) - b + d$

(2) $d_{eff} = 0.024688(g_f + g_c) + d$

Correlation (1) is the FRAPCON correlation andd correlation (2) the FRAPTRAN correlation, and in them $P_{contact}$ is the contact pressure, ρ_i the cladding and fuel roughnesses, $g_f + g_c$ the sum of the temperature jump distances and d the gap width. In the FRAPTRAN correlation, if $d = r_{ci} - r_{fo}$ is used, the soft relocation is ignored (recommended) and if $d = r_{ci} - r_{fo} - x_{reloc}$ is used, soft relocation is taken into account. Here r_{ci} is the cladding inner radius, r_{fo} the pellet outer radius and x_{reloc} the soft relocation in units of length.

In the transient cases, the FRAPCON correlation often calculates very large effective gap widths, as can be seen from figure 28. If soft relocation is taken into account in the FRAPTRAN correlation, the effective gap width is very low for the whole time interval. The FRAPTRAN correlation with no soft relocation taken into account calculates the effective gap width in FINIX in a very similar manner compared to the values calculated by FRAPTRAN itself, so this method of calculation is recommended for future use.

Meyer's hardness for VVER cladding

Meyer's hardness has the greatest effect on the contact heat transfer coefficient. Even though the VVER cladding is different in composition than Zircalloy-4, for which the Meyer's hardness correlations used in FINIX are based, it was found that similar results are calculated compared

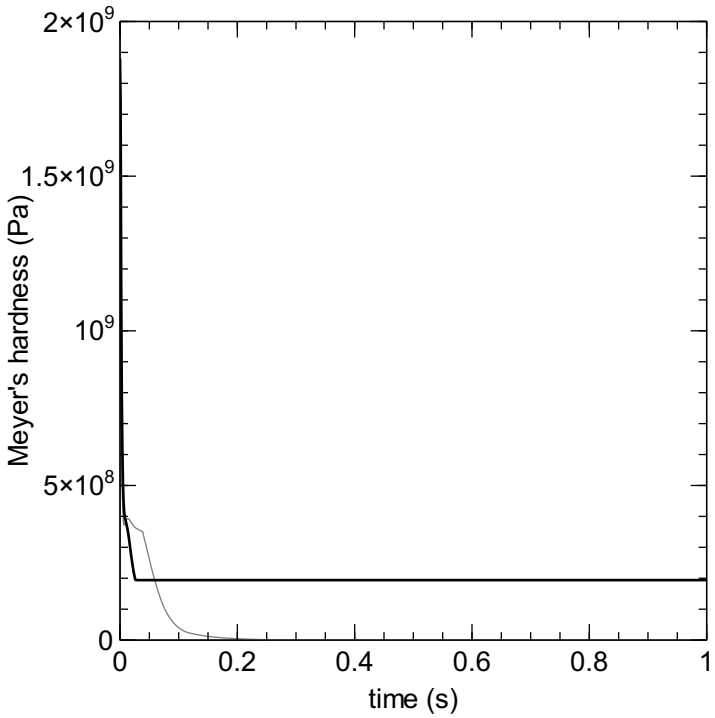

Figure 29. *Meyer's hardness for scenario BIGR RT-4 as calculated by FINIX (black lines) with the Zircalloy Meyer's hardness correlation with lower limit of 194 MPa and FRAPTRAN (grey lines) with the Zr-1%Nb correlation with a lower limit of 0.1 MPa.*

to FRAPTRAN with the Zircalloy-4 correlation. In FRAPTRAN, there is a Meyer's hardness correlation for M5^{TM}-type cladding. The M5^{TM}cladding and the VVER claddings are both made of a zirconium alloy with 1

It was found that also the lower limit for Meyer's hardness of the Zr-1%Nb cladding is set to a different value for this cladding than for Zircalloy: for Zircalloy the lower limit is 194 MPa but for Zr-1%Nb alloy it is set to 0.1 MPa. The 194 MPa limit has been selected because this is the Meyer's hardness at the highest temperature data point in the data on which the correlation is based on, whereas the 0.1 MPa limit is the minimum Meyer's hardness for Zircalloy [15]. When the calculation of low Meyer's hardness values is allowed, very high relative contact pressures are calculated which results in very high contact heat transfer coefficients as they are directly proportional. The effect on Meyer's hardness of these different correlations and their different lower limits are illustrated in figure 29.

5.6 Mechanical calculations

There are some issues with the mechanical calculation from scenarios NSRR HBO-1 and FK-1. The contact pressure oscillates in both of these cases, and in FK-1 the cladding hoop strain is seen to behave in a step-like fashion towards the end of the scenario. Another matter is the value of the cladding hoop strain in the beginning of the scenario, which is different from that output by FRAPTRAN.

In figure 30 the cladding hoop strain in the scenario NSRR HBO-1 is shown. As can be seen, the hoop strain from FINIX has negative values in the beginning. This happens because of the plastic cladding hoop strain, which is read in from the FRAPCON-made restart file, is negative. In FINIX, the plastic strain is added into the total hoop strain after the restart file is read and it is the largest component of the total hoop strain in the beginning. In FRAPTRAN, however, another kind of calculation is done to take into account the FRAPCON-calculated plastic strain. The cladding effective plastic strain is read in from the restart file and used to calculate the next values for plastic strain in the plastic strain calculation, but the plastic strain at the beginning of the scenario is assumed to be zero. In effect, the effective plastic strain parameter is used to remember the strain history, but the actual plastic strains are ignored. In absence of a better way to deal with plastic strain, it was thought that the addition of the FRAPCON-calculated plastic strain is the best and most realistic way to deal with the plastic strain present in the rod in the beginning, even though the strain values calculated in this manner by FINIX differ from those calculated by FRAPTRAN.

The pellet-cladding contact pressure seems to oscillate as can be seen from figures 31 and 33. The cause of the contact pressure oscillation is still unresolved and must be investigated in the future. As for the "oscillation" of the cladding hoop strain, the cause was identified to be the switching between models. The cladding hoop strain jumps between two calculation methods resulting in jumping of the hoop strain value in the case of scenario NSRR FK-1, as is evident from figure 32, and also in the case BIGR RT-4. When the contact pressure is below the internal gas pressure, the mechanical model assumes weak contact and iterates the cladding outer diameter by Newton-Raphson iteration from a different equation. At the moment when contact pressure rises over the internal gas pressure of the rod, the mechanical model assumes strong contact between the pellet and the cladding and solves the cladding outer diameter explicitly. At this point, the cladding hoop strain jumps to a higher value. When the contact pressure again drops below the rod internal gas pressure, the cladding hoop strain is lowered instantaneously to the magnitude it had before strong contact between the pellet and the cladding.

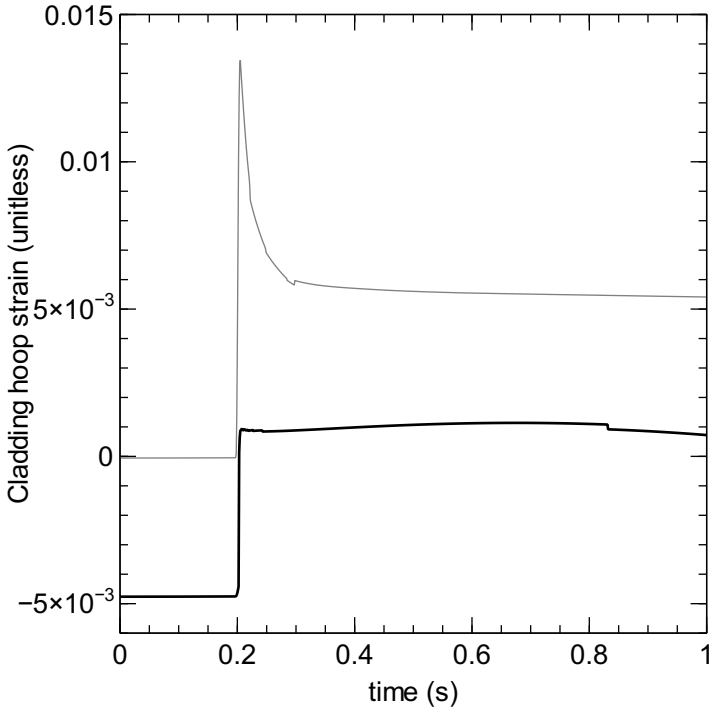

Figure 30. *Cladding hoop strain in the NSRR HBO-1 scenario as calculated by FINIX (black lines) and FRAPTRAN (grey lines).*

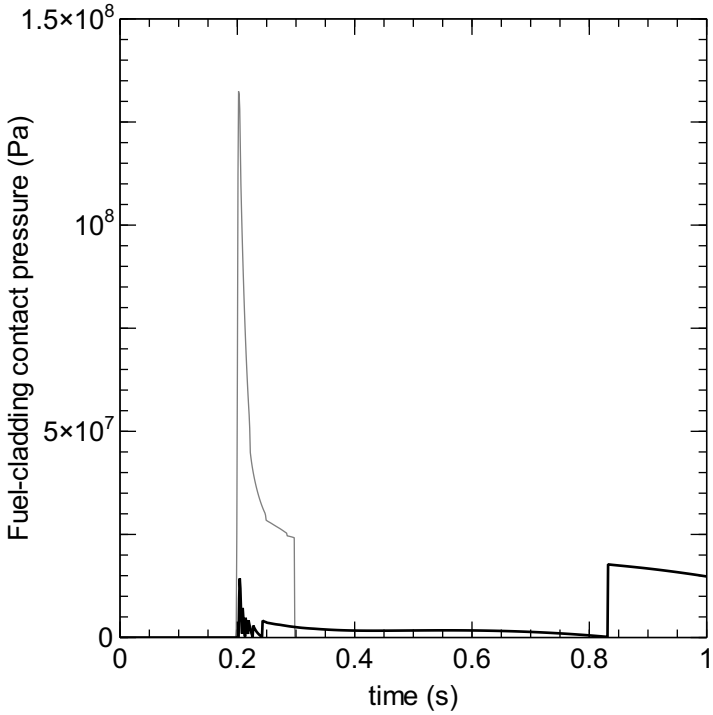

Figure 31. *Pellet-cladding contact pressure in the NSRR HBO-1 scenario as calculated by FINIX (black lines) and FRAPTRAN (grey lines).*

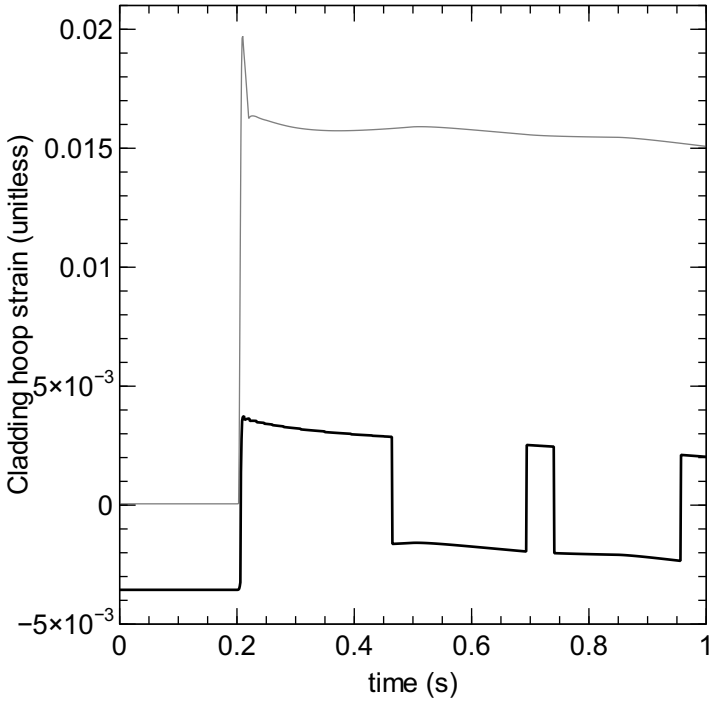

Figure 32. *Cladding hoop strain in the NSRR FK-1 scenario as calculated by FINIX (black lines) and FRAPTRAN (grey lines).*

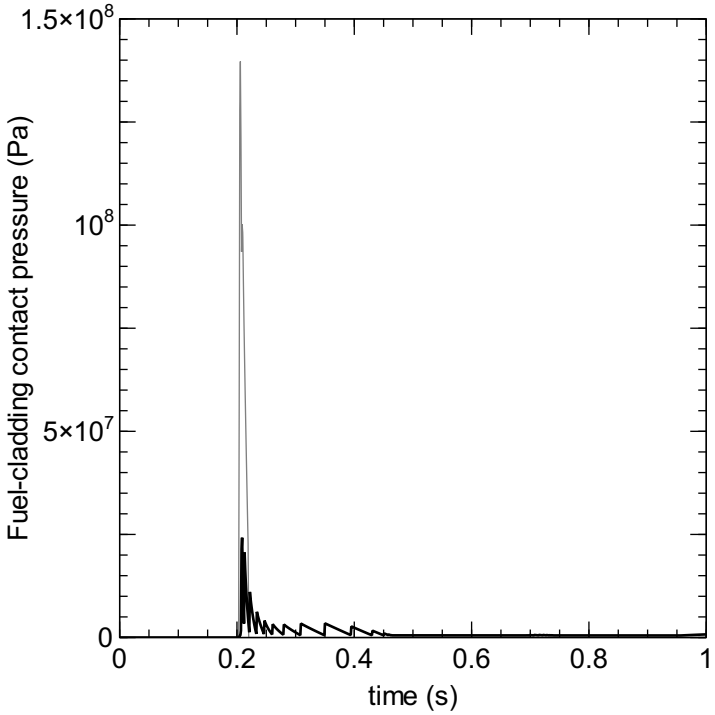

Figure 33. *Pellet-cladding contact pressure in the NSRR FK-1 scenario as calculated by FINIX (black lines) and FRAPTRAN (grey lines).*

5.7 Summary

The transient scenarios are mostly calculated by FINIX very similarly compared to FRAPTRAN. The cases with the least plastic deformation happening are calculated most similarly. In twelve of the 15 scenarios used in this validation report much plastic deformation is taking place, so at this point of the development of FINIX the lack of a plastic deformation model affects the results largely.

There are differences in the gas pressure results calculated by FINIX and FRAPTRAN. Some of the difference can be explained by the different plenum temperature models in the two codes, and some with the lack of a model for the open porosity fraction. It was found, that most of the difference in the pressure results in the beginning of a scenario could be traced to a difference in the plenum volume. The other differences are in the strain calculation, which are discussed in section 5.6. Although no plastic strain is yet modelled in the code, also the cases with more plastic deformation taking place were calculated by both codes in a very similar fashion. The differences in these cases could be accounted by the absence of a plastic deformation model.

Some problems with the mechanical calculations were still present at the end of the validation, as was explained in section 5.6. These problems must be resolved in the future.

6 Steady-state modeling performance

The steady-state modeling performance of FINIX was tested with a scenario involving a rod from the experiment IFA-429 and five scenarios involving rods from the experiment IFA-432. The steady-state modeling performance was assessed with a "cumulative average error" parameter, which was defined as the square root of the squared error averaged from the beginning of the scenario to the current time step.

The comparisons to experimental data can be thought to afford information about how the FINIX-calculated results reflect reality. Since the data are actual experimental values, the FINIX fuel performance model should be developed so that it would calculate results with the best agreement with experimental data. Here we used this data to evaluate gap conductance correlations.

6.1 IFA-429

Only one rod, rod BC, had fuel centerline temperature data from the rods in experiment IFA-429.

From figure 34 it can be seen that there is only on average a 50 K error in the fuel centerline temperature calculated by FINIX. The FRAPCON and FRAPTRAN (without soft relocation) correlations calculate the best results at burnups less than 20 MWd/kgUO2, but after this the FRAPTRAN correlation with relocation has the lowest cumulative average error. It must be noted that the differences in the average error for all of the correlations are very small, so it is impossible to say from this data which of these would best represent reality.

In figure 35 the fuel centerline temperature data from the IFPE database are compared to the fuel centerline temperatures calculated by FINIX with different gap heat conductance correlations. Also from this comparison it can be seen that the differences in this case between the different correlations are very small.

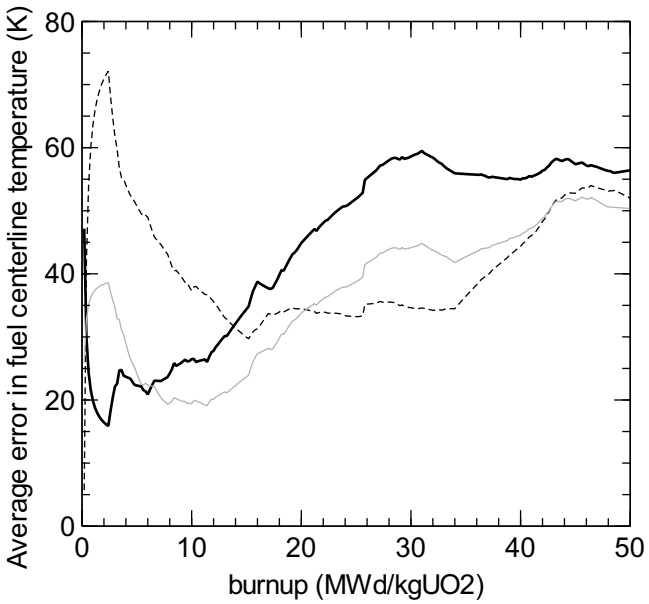

Figure 34. *Average cumulative error between FINIX-calculated value and IFA-429 experiment rod BC data. Gray solid line is the value calculated by the FRAPCON correlation, black dashed line by the FRAPTRAN correlation taking into account the soft relocation and thick black solid line by the FRAPTRAN correlation ignoring the soft relocation (recommended).*

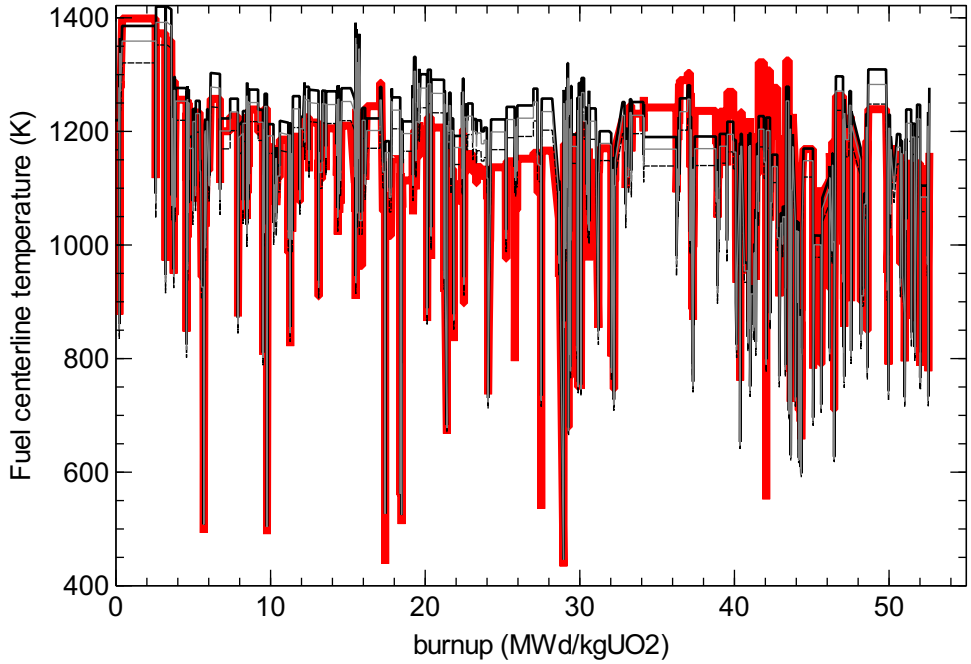

Figure 35. *Fuel centerline temperature as a function of time for IFA-429 experiment rod BC as calculated by FINIX with different gap heat conductance correlations (FRAPCON: gray solid line, FRAPTRAN with relocation: black dashed line, FRAPTRAN without relocation: black thick line (recommended)) compared to IFPE experimental data (thick red line).*

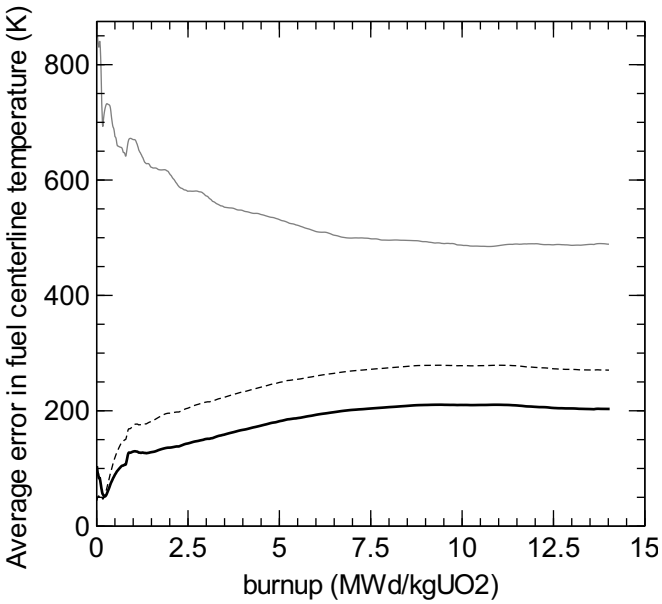

Figure 36. *Average cumulative error between FINIX-calculated value and IFA-432 experiment data. Gray solid line is the value calculated by the FRAPCON correlation, black dashed line by the FRAPTRAN correlation taking into account the soft relocation and black solid line by the FRAPTRAN correlation ignoring the soft relocation.*

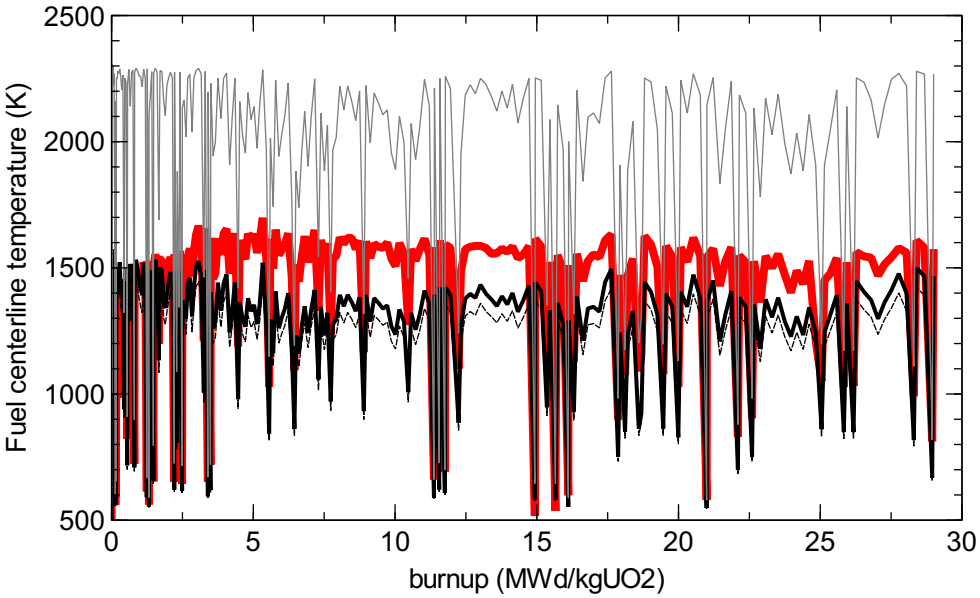

Figure 37. *Fuel centerline temperature as a function of time for IFA-432 experiment rod 1 as calculated by FINIX with different gap heat conductance correlations (FRAPCON: gray solid line, FRAPTRAN with relocation: black dashed line, FRAPTRAN without relocation: black thick line (recommended)) compared to IFPE experimental data (thick red line).*

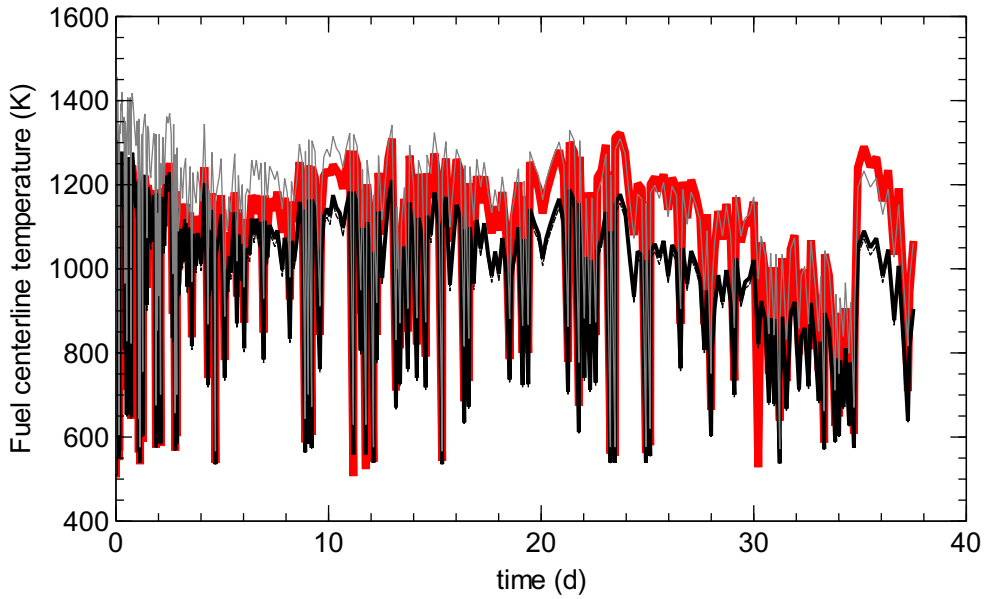

Figure 38. *Fuel centerline temperature as a function of time for IFA-432 experiment rod 3 as calculated by FINIX with different gap heat conductance correlations (FRAPCON: gray solid line, FRAPTRAN with relocation: black dashed line, FRAPTRAN without relocation: black thick line (recommended)) compared to IFPE experimental data (thick red line).*

6.2 IFA-432

Five rods, numbered 1, 2, 3, 5 and 6 had fuel centerline temperature data available. No time-dependent burnup data is available for the IFA-432 experiment, only a final burnup value. Therefore the burnup value by FINIX was used in calculation of figure 36, but this value was normalized so that the end-of-life burnup was equal to the experimental burnup. For rod 6, the temperature data is not available for the latter part of the experiment because of thermocouple failure, so the data for rod 6 was only used until the thermocouple fails at a burnup of 14.5 MWd/kgUO2.

The minimum error in figure 36 is at burnup 0.26 MWd/kgUO2. After this, the error rises sharply. The reason for the underestimation of the fuel centerline temperature by FINIX can be thought to be a result from the lack of some models pertaining to burnup-dependent effects such as fuel densification and swelling. As the fuel pellet swells with increasing burnup, the heat conductivity of the pellet decreases and the temperatures in the fuel are higher. However, the fuel also densifies by irradiation, which has the opposite effect on heat conductivity. It is impossible to say which of these effects dominates in the IFA-432 cases without further calculation by future FINIX versions.

In figures 37 and 38 the fuel centerline temperatures calculated by all three correlations are compared to the experimental data. In figure 37 IFA-432 rod 1 fuel centerline temperatures are presented and in figure 38 the data is for IFA-432 rod 3. As is evident from the figures, the results for the two rods are very different for the FRAPCON correlation: for rod 1 the temperatures calculated by FINIX are very high compared to the experimental data but for rod 3 all the correlations calculate more similar results. The other rods from experiment IFA-432 follow the rod 1 pattern, and it was found that rod 3 was the only one of these rods where FINIX calculated contact pressures greater than zero. This doesn't explain the fact that the results calculated for IFA-429 rod

BC were even closer to the experimental values, since with IFA-429 rod BC no pellet-cladding contact occured according to FINIX.

As for the two different FRAPTRAN gap heat conductance correlations, based on this data it is impossible to say which would be better suited to calculate realistic results.

6.3 Summary

To find out a burnup limit before which FINIX calculates realistic results, the experimental data was divided into three zones according to the cumulative average error described in the beginning of section . The zones were determined for each experimental case, and then the average of the limits was used for all in comparing the data. First burnup zone occurred under 3.38 MWd/kgUO2, where the error was low. The second zone was between 3.38 and 10.65 MWd/kgUO2, and at this burnup interval the error began to rise. The third zone was at over 10.65 MWd/kgUO2, where the error was noticeably larger than at lower burnups, but remained stable.

The comparisons to experimental data are summarized in figure 39. In the figure, the values calculated by FINIX of the fuel centerline temperature are plotted against the experimental values. IFA-429 rod BC and the rods from IFA-432 are used, but the data for IFA-432 rod 6 is ignored because of the incompleteness of the data. The blue line is the diagonal, and it can be seen that the values plotted as red circles which are those from data at burnup below 3.38 MWd/kgUO2 position themselves mostly along the diagonal. The green crosses, from data at burnup between 3.38 and 10.65 MWd/kgUO2, and yellow circles, from data at burnup over 10.65 MWd/kgUO2, indicate that at burnups over 10.65 MWd/kgUO2 FINIX calculates the fuel centerline temperatures lower than the experimental values. There is some dispersion in the values, which is in part a consequence of setting the same burnup limit values for all the rods for the limits of the three regions from which the data were plotted and because the different areas of burnup appeared at different burnup values for different rods.

The limits described here and the data associated with them imply that during the first burnup interval from 0 to 3.38 MWd/kgUO2, FINIX calculates most realistic values in steady-state scenarios. The cumulative average error at this burnup level is approximately 100 K. At the third burnup level, over 10.65 MWd/kgUO2, where the error is largest, the error is approximately 150 K.

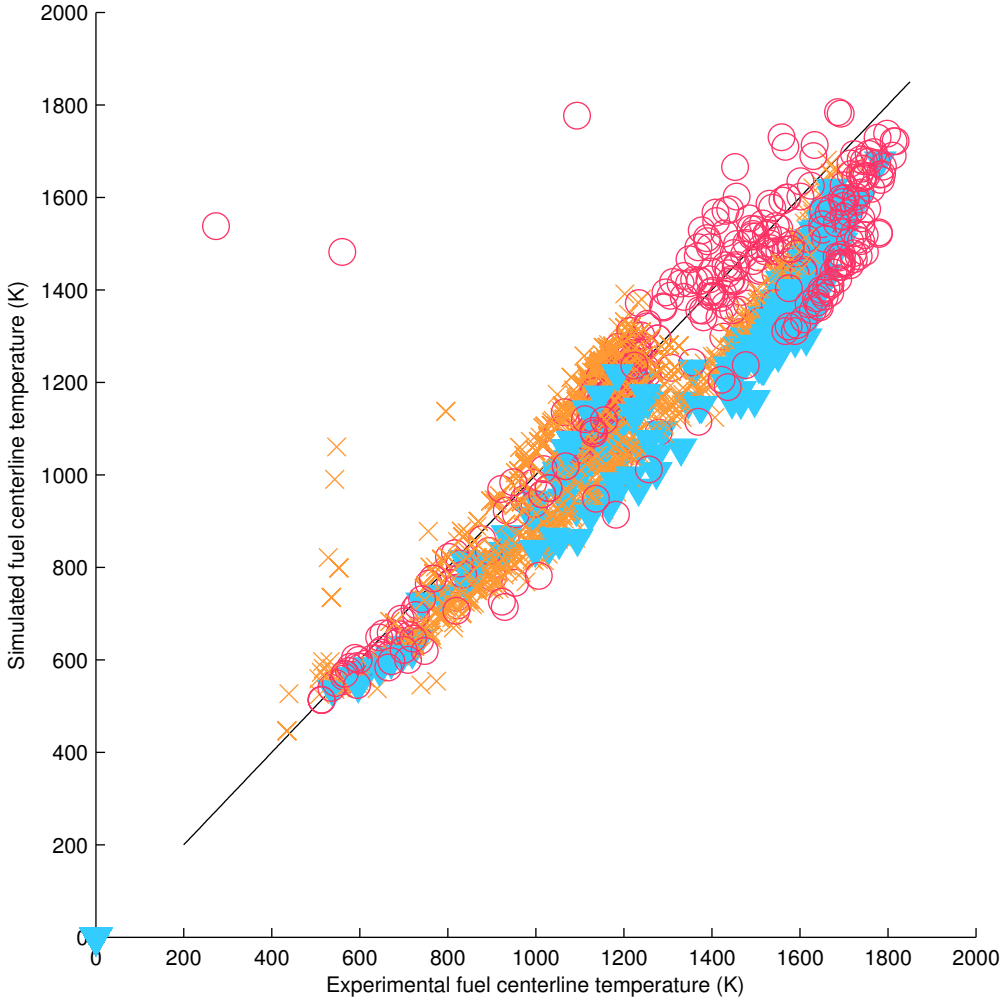

Figure 39. *Fuel centerline temperature calculated by FINIX plotted against the experimental fuel centerline temperature. Values plotted for several sections of burnup: red circles for low burnup and low error (under 3.38 MWd/kgUO2), blue filled triangles for medium burnup and increasing error (over 3.38 but under 10.65 MWd/kgUO2) and orange crosses for high burnup and stable but large error (over 10.65 MWd/kgUO2).*

7 Conclusions

The FINIX fuel performance code for multiphysics applications was validated with transient and steady-state scenarios. The FINIX version used in the validation was comparable to the version 0.13.9. The transient scenarios used in the validation of FINIX were from the integral assessment of FRAPTRAN-1.4, which is an established fuel performance code for transient analysis. The scenarios were based on experimental data, but the data the comparison was made with was calculated by FRAPTRAN and must be considered affected by the simplifications and assumptions made in FRAPTRAN. With the comparison against another code it was easy to investigate the

effects of various variables on intermediate results in the models. It is helpful to compare intermediate results calculated by the two codes to gain knowledge about how different phenomena are modelled in these codes. The interrelated nature of variables within the models make them very complex, and the piece-by-piece unraveling of their calculation methods is educational at the least.

FINIX was also compared to experimental data from the IFPE database from two experiments, IFA-429 and IFA-432. Fuel centerline temperatures from these experiments in six rods were compared to those calculated by FINIX. The experimental data comparisons can be thought to convey information about how the FINIX model reflects reality. At this time, only steady-state scenarios were compared with experimental data.

7.1 Results

It was found that in transient cases with little or no plastic deformation, FINIX calculates very similar results compared to FRAPTRAN. This is in accordance with the fact that FINIX has no plastic deformation model in itself, and can only accurately calculate elastic deformations. With those cases with plastic deformation the results have to be considered with caution after the plastic deformation dominates. The differences in the results calculated by FRAPTRAN and FINIX after this point can be explained by the lack of the plastic deformation model. FRAPTRAN also calculates results differently after it has determined that the rod has burst, for example setting the internal pressure to equal the coolant pressure. Therefore the results calculated by FINIX and FRAPTRAN are not fully comparable after the rod has burst, since no similar model is applied in FINIX. This being said, the rod temperature results agree very well even after the rod has burst.

An open question at the beginning was the choice of a gap heat transfer coefficient correlation, since FRAPTRAN and FRAPCON use different ones. In these correlations it was also not clear what the parameters used in them actually are, but concerning the effect of relocation it was found that in FRAPTRAN the soft or non-permanent relocation is ignored completely. From the data in sections 5.5 and 6.2 it was concluded that the FRAPTRAN gap conductance correlation with soft relocation not taken into account calculates results similarly both compared to those results calculated by FRAPTRAN but also when compared to experimental data. It was also found that the FRAPCON effective gap width correlation calculates very high values for the gap heat conduction coefficient calculation, so if used, the FRAPCON correlation must be used with caution.

When comparing the FINIX-calculated fuel centerline temperatures to experimental data, it was found that there is a clear difference in the gap heat conductance correlations. In the case of most of the IFA-432 rods, it was found that the FRAPCON correlation calculates very high fuel centerline temperatures. The difference between the other correlations, FRAPTRAN with and without relocation taken into account, were minimal. It can therefore be said that the FRAPCON correlation is not recommended to be used, even though in some cases, such as the IFA-429 rod BC, the results calculated by it are realistic. At higher burnups, some burnup-dependent effects that are not yet implemented in FINIX can be thought to be the cause of the differences of the results calculated by FINIX.

The results can be summarized as follows:

1. Transient scenarios with little plastic deformation are calculated very similarly compared to

FRAPTRAN.

2. Transient scenarios with some plastic deformation are calculated very similarly compared to FRAPTRAN in the nonfailed rod cases and also in the failed rod cases up to the point where rod failure happens. After rod failure, good agreement in the temperature results is still achieved.

3. At low burnup, steady-state calculation calculates very realistic fuel centerline temperatures. Some burnup-dependent phenomena are not implemented and this affects the steady-state calculation results at higher burnup.

4. The FRAPTRAN gap heat transfer coefficient correlation with soft relocation ignored was found to calculate most similar results compared **both** to experimental data and FRAPTRAN results.

5. Soft relocation is treated differently in FINIX with the FRAPCON gap heat conductance correlation than in FRAPTRAN in that in FRAPTRAN it is ignored.

7.2 Open questions and future work

Some open questions remained at the end of the validation that could not be resolved at the present. These questions must be answered in the near future before further development of FINIX. First of the open questions concern the oscillation seen in the contact pressure in some scenarios. The cause for this oscillation is yet to be determined. Regarding the jumping behavior seen in some cases with the cladding hoop strain, the cause was found to be the strong and weak contact models where the cladding outer diameter is calculated in two ways according to the ratio of contact pressure to rod internal gas pressure. A solution for this problem is yet to be found.

Another open question relating to the starting values for the strains calculated by FINIX is the handling of plastic strains calculated by FRAPCON in FRAPTRAN. In FINIX the plastic strain calculated by FRAPCON is directly added to the total strain at the beginning of the calculation, whereas in FRAPTRAN the handling of the plastic strain is at this point unclear.

There are a number of recommendations formulated on the basis of this validation report for the targets of future work. A few of these require larger effort: the development of a plastic deformation model, development of models to account for phenomena occurring in high-burnup fuel and solving the problems with the mechanical calculations present in FINIX.

The remaining recommendations are minor compared to those mentioned, but nevertheless important, and are as follows:

1. A check for pellet-cladding contact in the pellet relocation calculation should be implemented in the future.

2. The manner in which FRAPTRAN utilizes the plastic strain calculated by FRAPCON should be investigated (involving the as-of-yet undeveloped plastic deformation model in FINIX).

3. Material property correlations for different cladding materials should be implemented.

4. Heat capacity of the fill gas should be calculated more accurately.

5. Plenum volume calculation should be investigated for errors that affect the rod internal pressure results.

References

[1] K. J. Geelhood, W. G. Luscher, C. E. Beyer, and J. M. Cuta. FRAPTRAN 1.4: A computer code for the transient analysis of oxide fuel rods. Technical Report NUREG/CR-7023, US NRC, 2011.

[2] K. J. Geelhood, W. G. Luscher, and C. E. Beyer. FRAPCON-3.4: A computer code for the calculation of steady-state thermal-mechanical behavior of oxide fuel rods for high burnup. Technical Report NUREG/CR-7022, US NRC, 2011.

[3] T. Ikonen. FINIX - fuel behavior model and interface for multiphysics applications - code documentation for version 0.13.9. Technical Report VTT-R-06563-13, VTT, 2013.

[4] K. J. Geelhood, W. G. Luscher, and C. E. Beyer. FRAPTRAN 1.4: Integral assessment. Technical Report NUREG/CR-7023, US NRC Pacific Northwest National Laboratory, 2011.

[5] D. D. Lanning and E. R. Bradley. Final irradiation and postirradiation data from the NRC/PNL instrumented assembly IFA-432. Technical Report HPR-329/7, US NRC Pacific Northwest National Laboratory, 1986.

[6] J. Papin, B. Cazalis, J. M. Frizonnet, E. Federici, and F. Lemoine. Synthesis of CABRI-RIA tests interpretation. 2003.

[7] T. Nakamura, M. Yoshinaga, M. Takahashi, K. Okonogi, and K. Ishijima. Boiling water reactor fuel behavior under reactivity-initiated-accident conditions at burnup of 41 to 45 GWd/tonne U. *Nuclear Technology*, 129:141–151, 2000.

[8] T. Fuketa, H. Sasajima, and T. Sugiyama. Behavior of high-burnup PWR fuels with low-tin zircaloy-4 cladding under reactivity-initiated-accident conditions. *Nuclear Technology*, 133:50–62, 2001.

[9] T. Nakamura, M. Yoshinaga, M. M. Sobajima, K. Ishijima, and T. Fujishiro. Boiling water reactor fuel behavior at burnup of 26 GWd/tonne U under reactivity-initiated-accident conditions. *Nuclear Technology*, 108:45–59, 1994.

[10] V. Georgenthum. Influence of test conditions on the PCMI behaviour during RIA based CIP0-1, VA-1 and VA-3 tests. 2009.

[11] T. Sugiyama. PCMI failure of high burnup fuel under high temperature RIA conditions. 2009.

[12] L. Yegorova, K. Lioutov, N. Jouravkova, O. Nechaeva, A. Salatov, V. Smirnov, A. Goryachev, V. Ustinenko, and I. Smirnov. Experimental study of narrow pulse effects on the behavior of high burnup fuel rods with Zr-1%Nb cladding and UO2 fuel (VVER type) under reactivity-initiated accident conditions: test conditions and results. Technical Report NUREG/IA-0213, Vol. 2, Nuclear Safety Institute of Russian Research Center Kurchatov Institute, 2005.

[13] L. Yegorova, K. Lioutov, N. Jouravkova, O. Nechaeva, A. Salatov, V. Smirnov, A. Goryachev, V. Ustinenko, and I. Smirnov. Experimental study of narrow pulse effects on the behavior of high burnup fuel rods with Zr-1%Nb cladding and UO2 fuel (VVER type) under reactivity-

initiated accident conditions: test conditions and results. Technical Report NUREG/IA-0213, Vol. 1, Nuclear Safety Institute of Russian Research Center Kurchatov Institute, 2005.

[14] L. E. Herranz and A. Tigeras. Solid-solid conductance in nuclear fuel: an assessment of it in-code models performance. *Progress in Nuclear Energy*, 52:435–441, 2010.

[15] K. J. Geelhood and W. G. Luscher. Material property correlations: Comparisons between FRAPCON-3.4, FRAPTRAN-1.4 and MATPRO. Technical Report NUREG/CR-7024, US NRC, 2011.

[16] T. Nakamura, M. Yoshinaga, M. M. Sobajima, T. Fujishiro, O. Horiki, T. Yamahara, Y. Ichihashi, and T. Kikuchi. Experimental data report for test TS-1 - reactivity initiated accident test in NSRR with pre-irradiated BWR fuel rod. Technical Report JAERI-M 91-217, JAERI, 1992.

A Appendices

A.1 Appendix 1: Simulation results for all scenarios

In this appendix all simulation results for all scenarios are plotted. For the transient scenarios, the values for the following variables are presented as a function of time: Pellet-cladding structural gap thickness, gap heat transfer coefficient, internal gas pressure, cladding hoop strain, fuel centerline and surface temperatures, cladding inner and outer surface temperatures, conduction heat transfer coefficient, radiative heat transfer coefficient, contact heat transfer coefficient, gas heat capacity, pellet-cladding gap effective width (used in gap heat transfer coefficient calculation), Meyer's hardness, relative contact pressure and contact pressure.

CABRI Na1 scenario, star marks rod burst

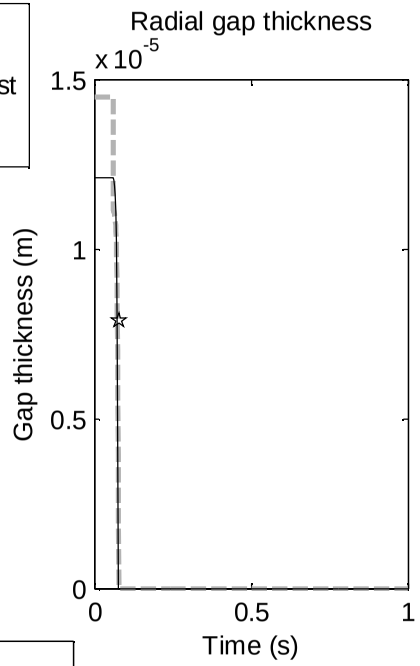

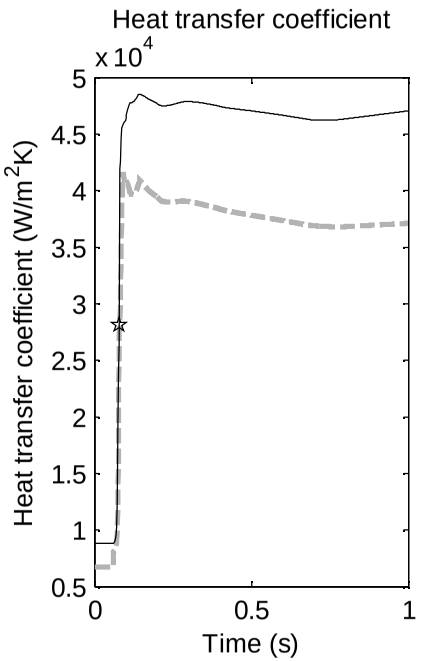

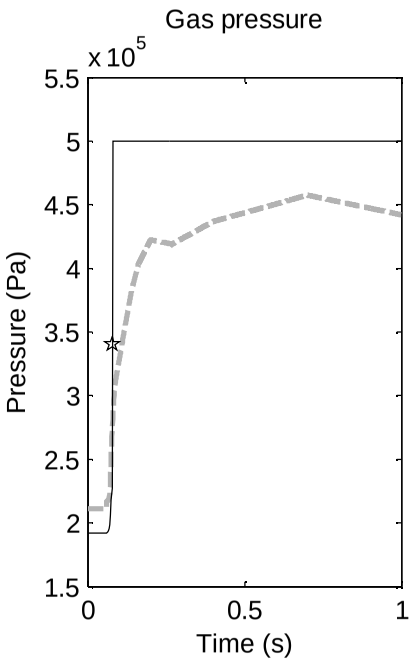

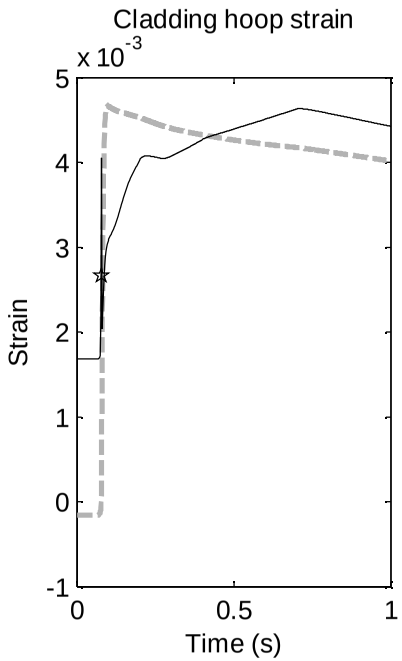

FINIX
FRAPTRAN

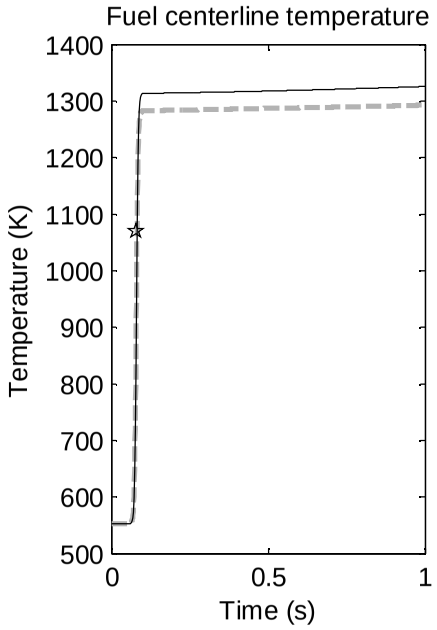

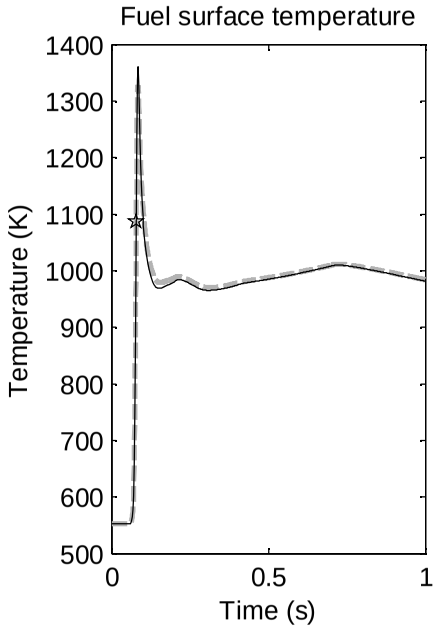

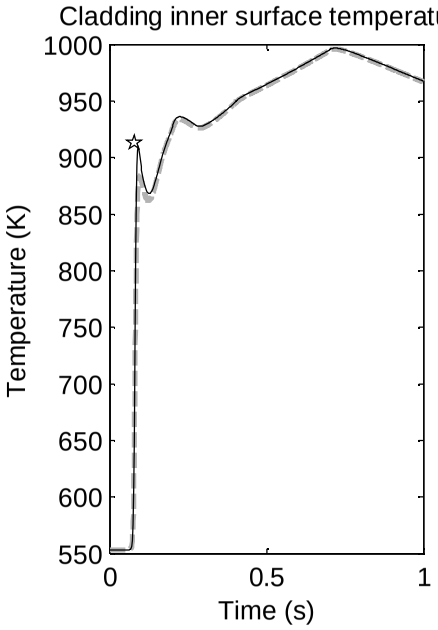

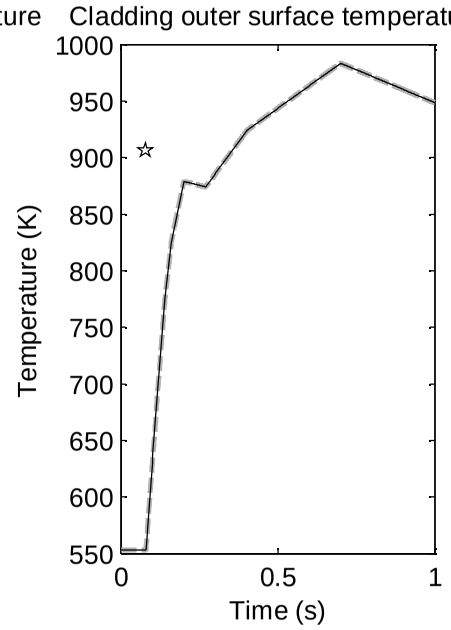

CABRI
Na1
scenario,
star
marks
rod
burst

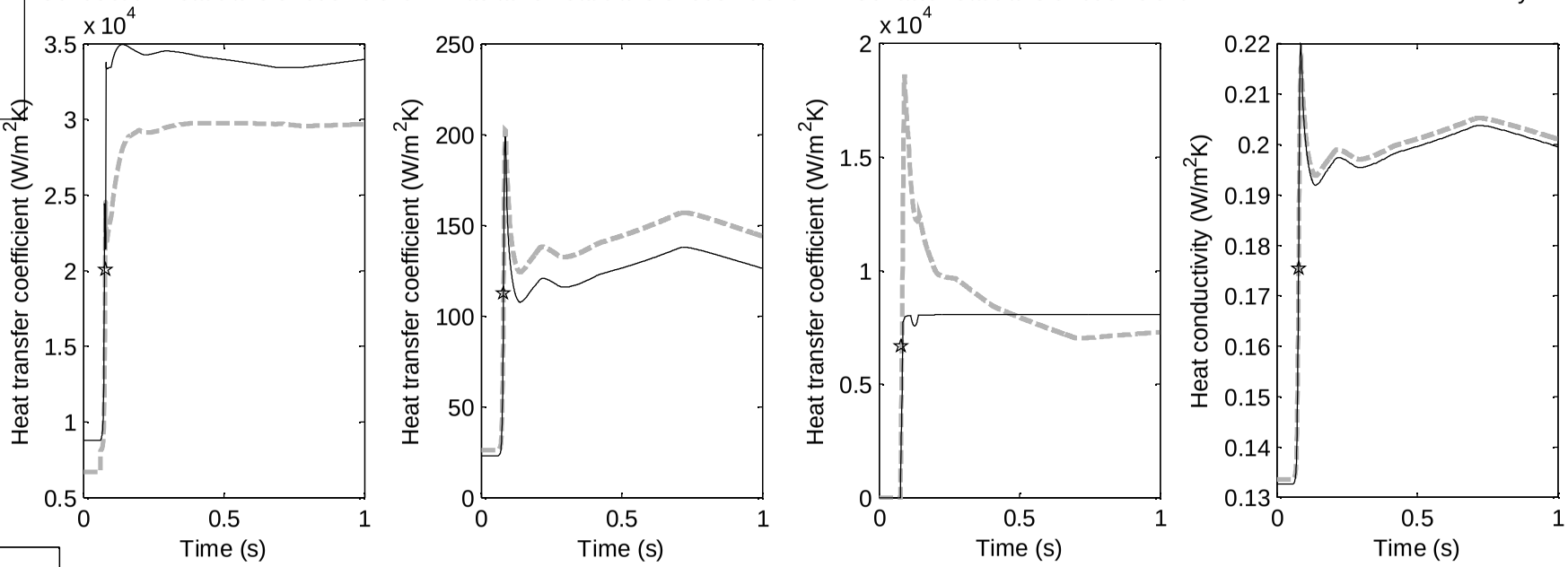

FINIX
FRAPTRAN

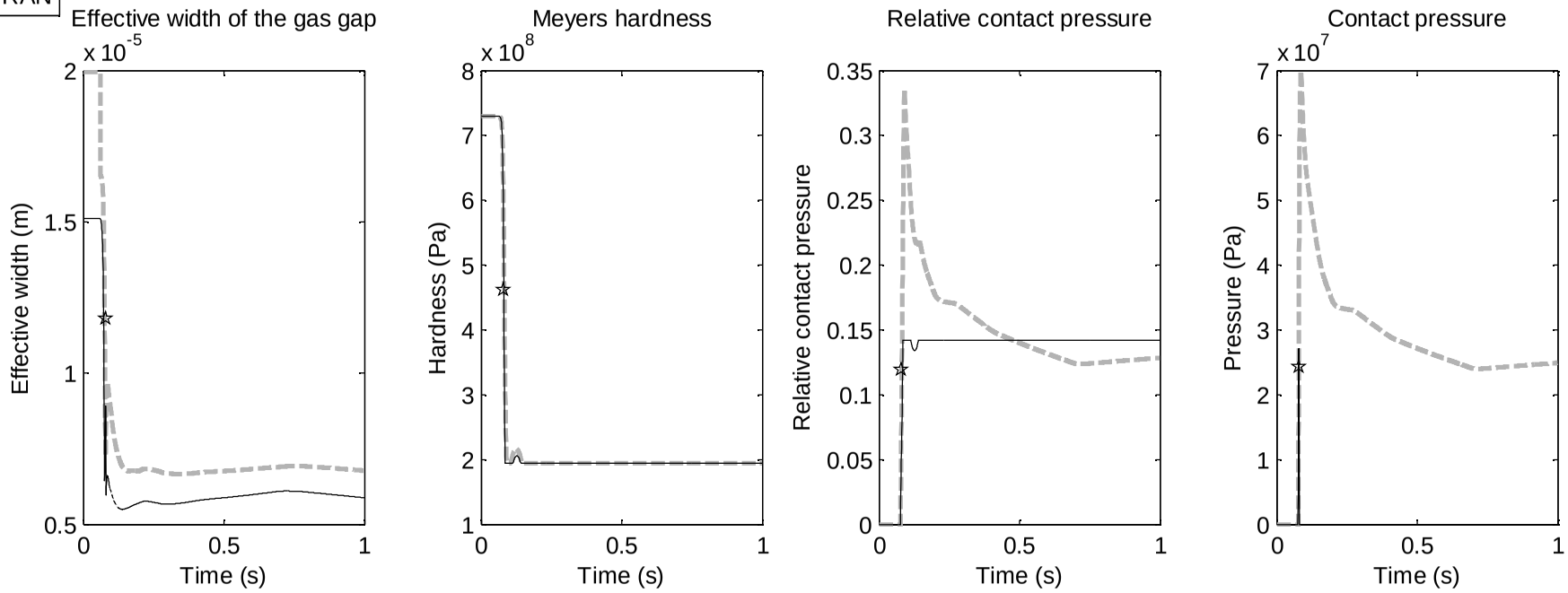

CABRI Na3 scenario

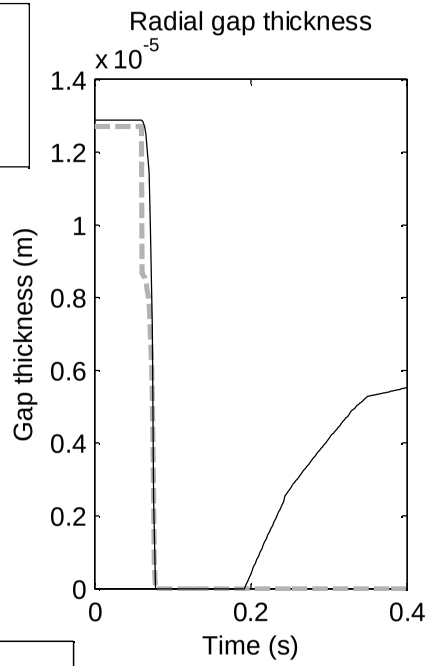

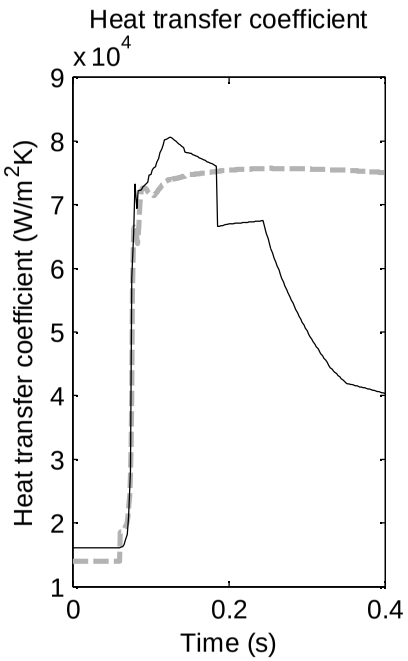

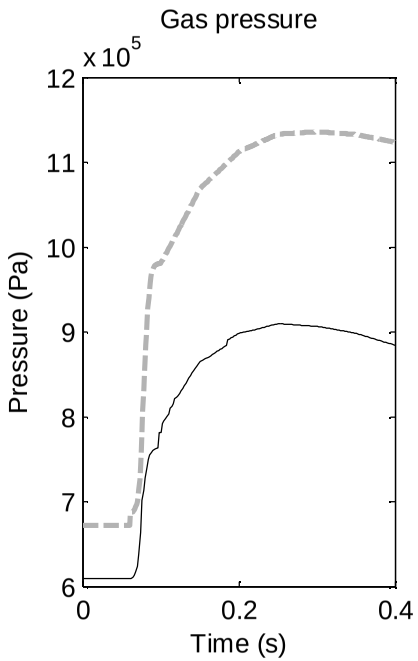

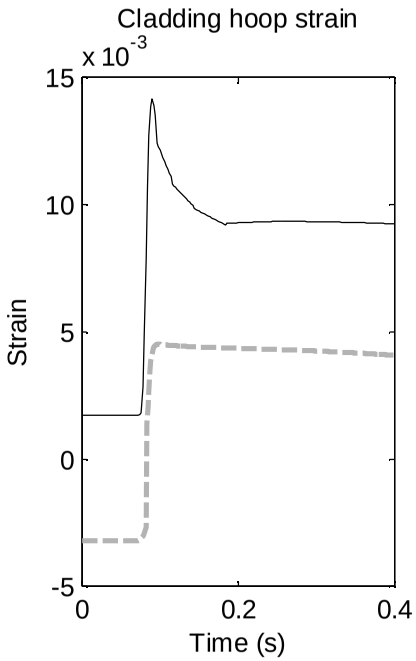

FINIX
FRAPTRAN

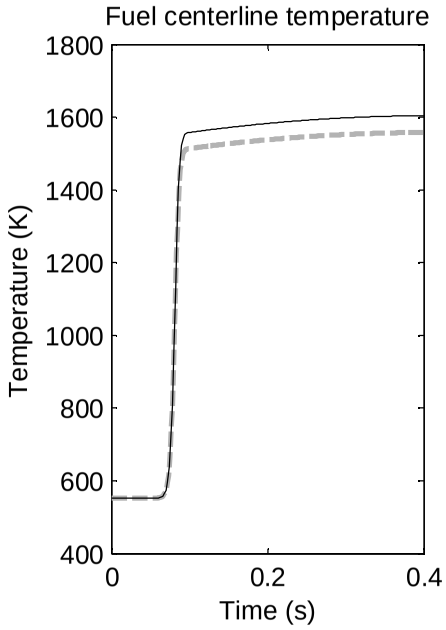

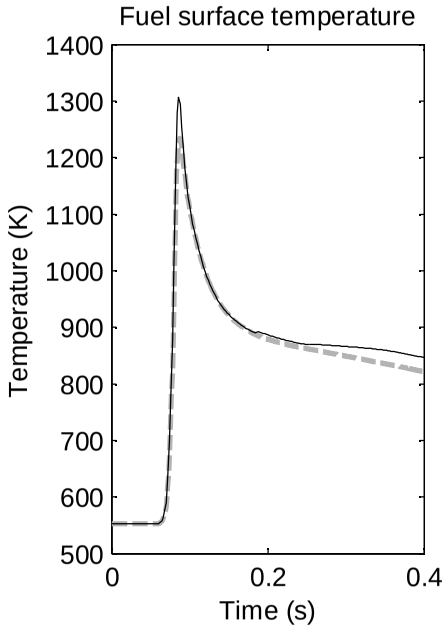

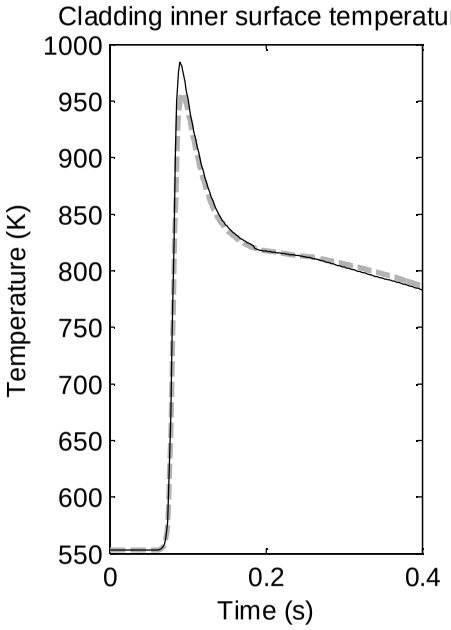

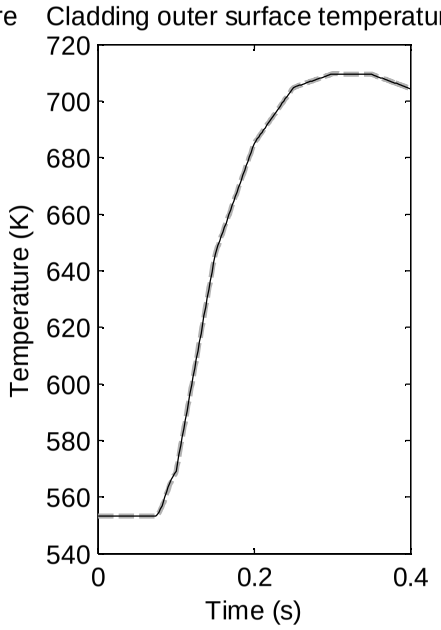

CABRI Na3 scenario

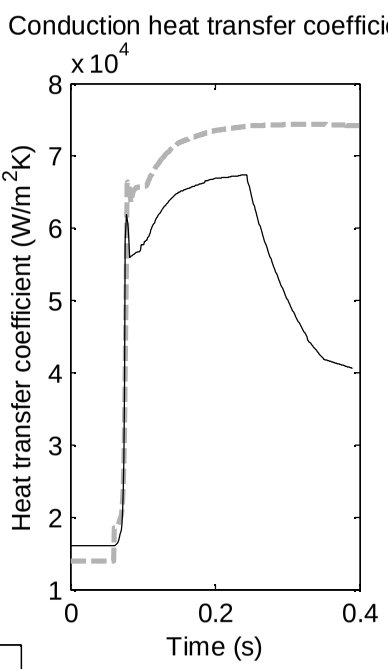

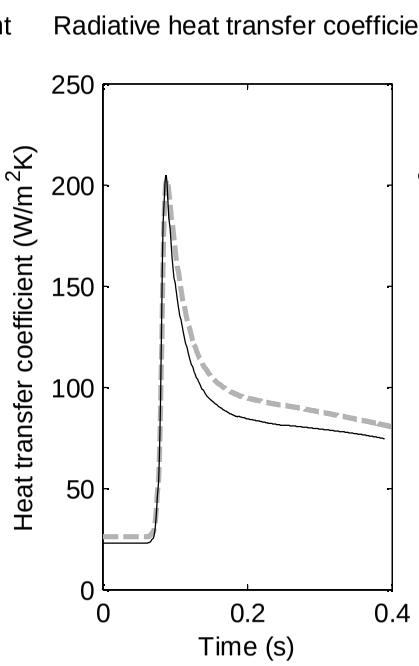

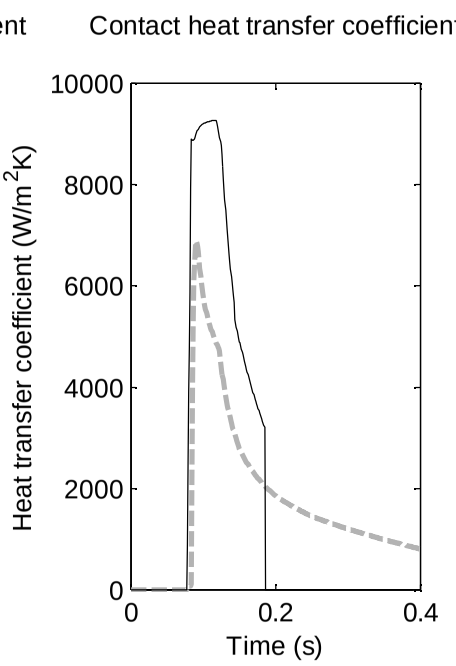

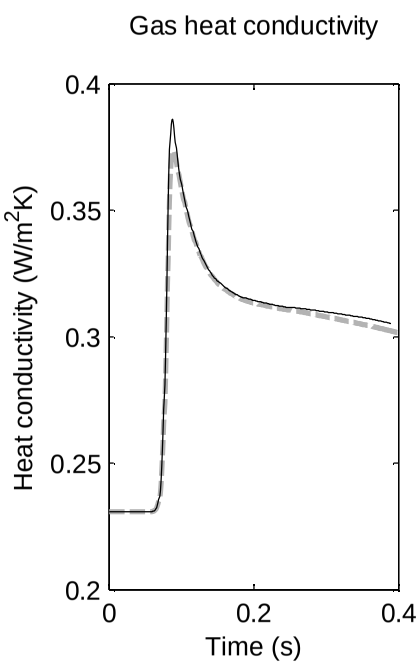

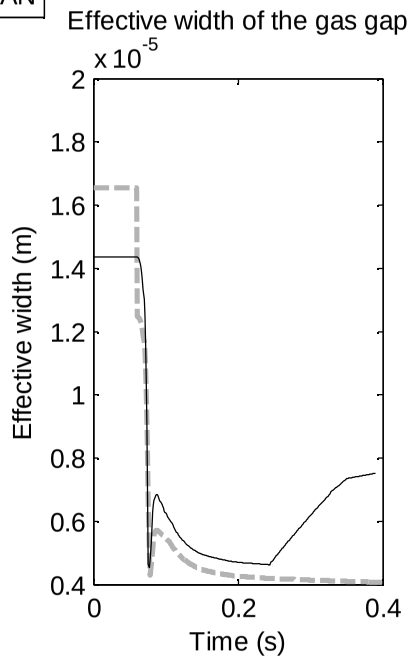

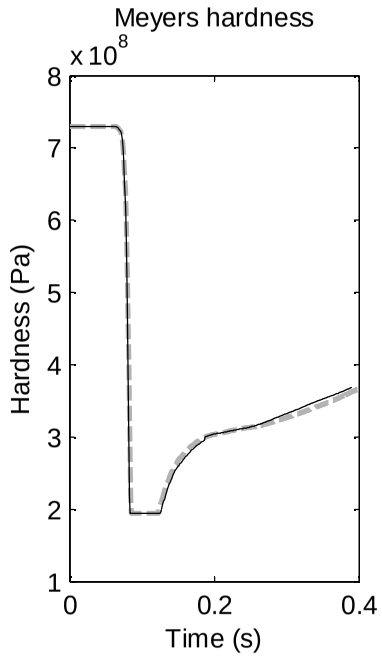

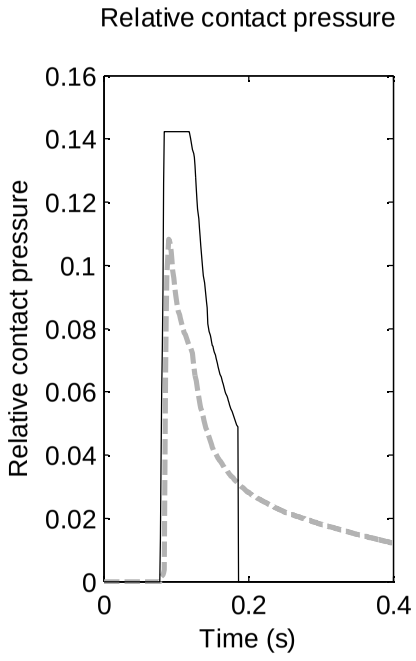

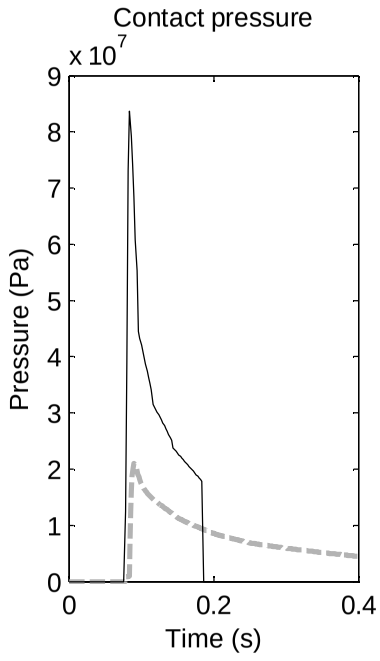

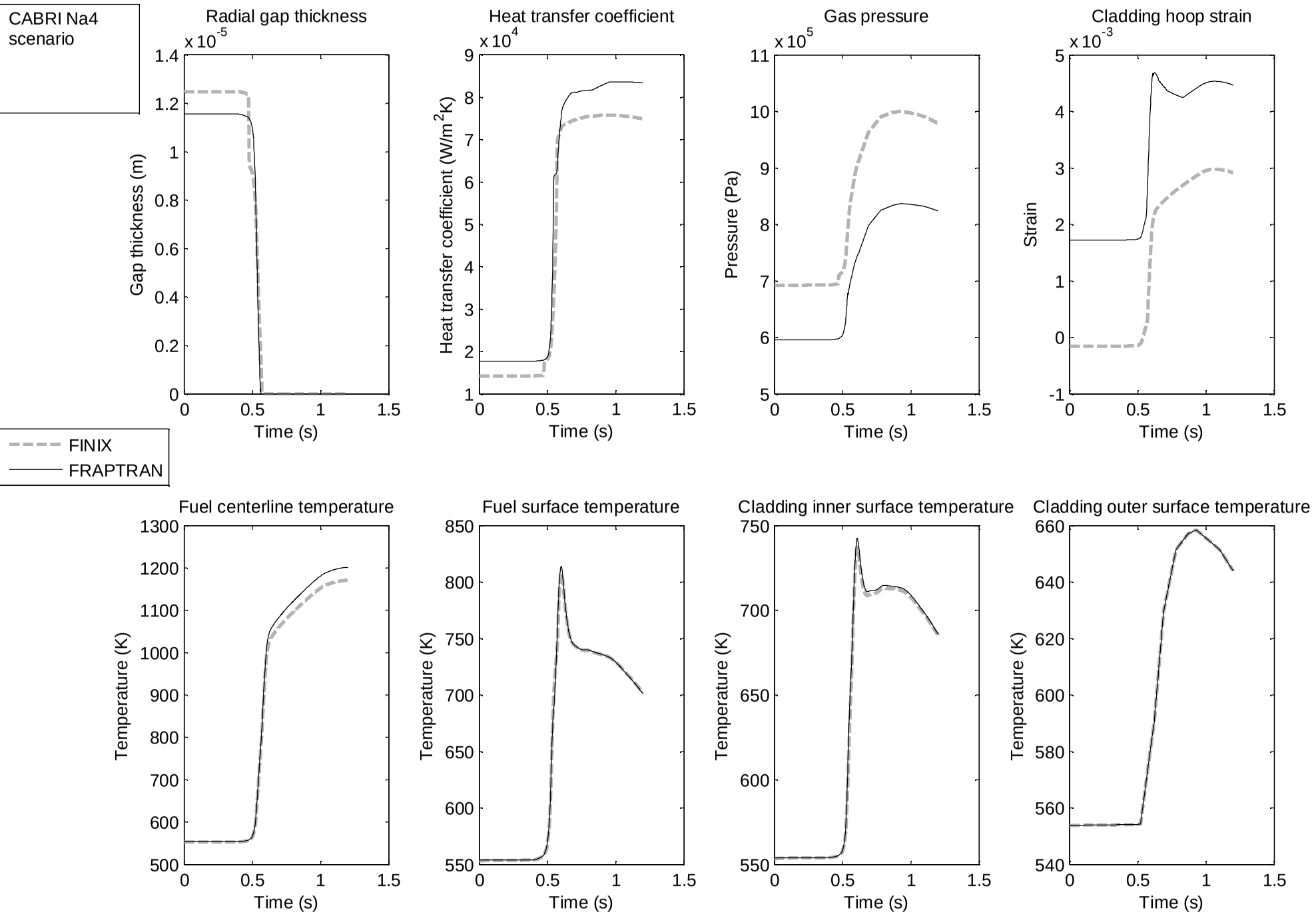
CABRI Na4 scenario
Radial gap thickness
x 10^-5
Gap thickness (m)
Time (s)
Heat transfer coefficient
x 10^4
Heat transfer coefficient (W/m^2K)
Time (s)
Gas pressure
x 10^5
Pressure (Pa)
Time (s)
Cladding hoop strain
x 10^-3
Strain
Time (s)
FINIX
FRAPTRAN
Fuel centerline temperature
Temperature (K)
Time (s)
Fuel surface temperature
Temperature (K)
Time (s)
Cladding inner surface temperature
Temperature (K)
Time (s)
Cladding outer surface temperature
Temperature (K)
Time (s)

CABRI
Na4
scenario

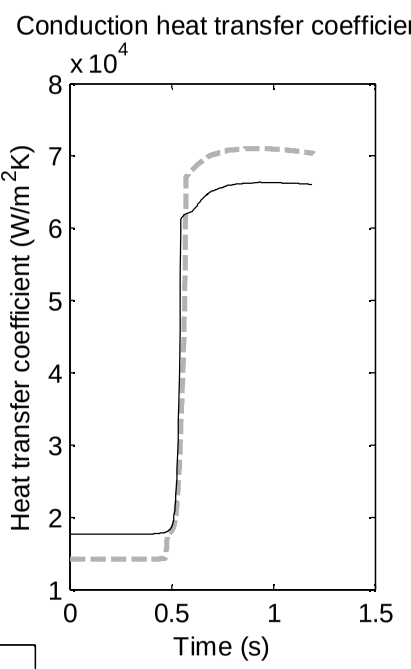

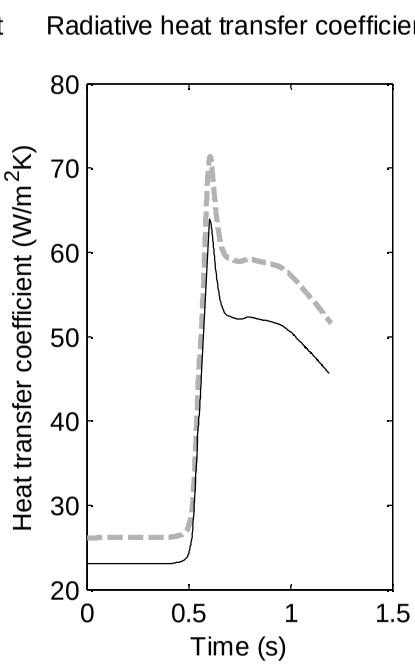

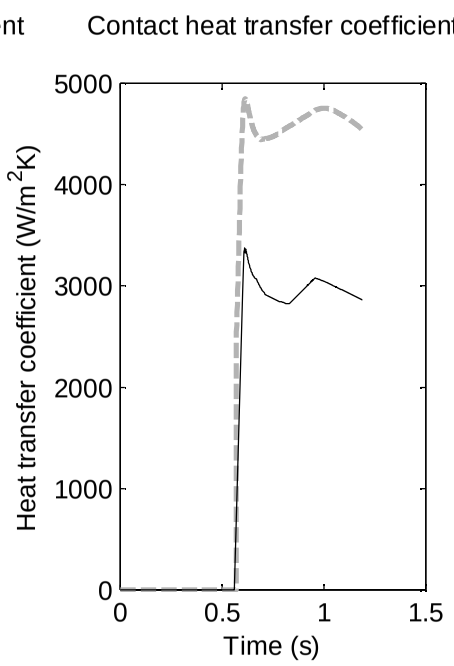

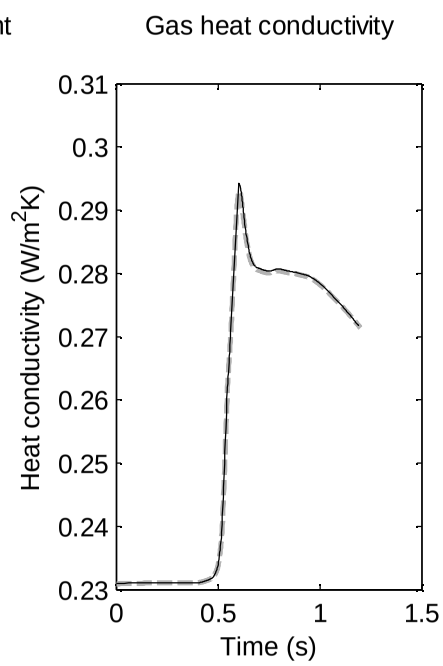

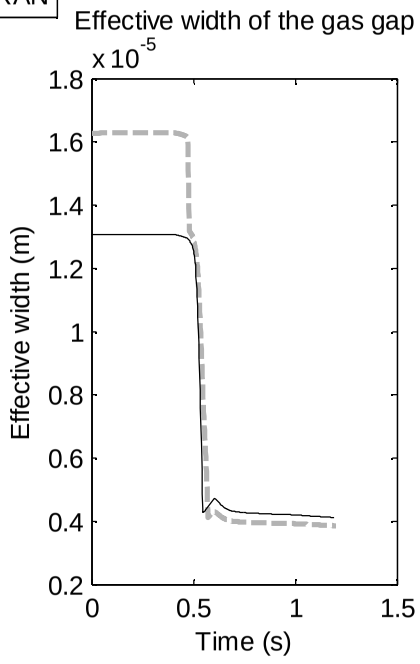

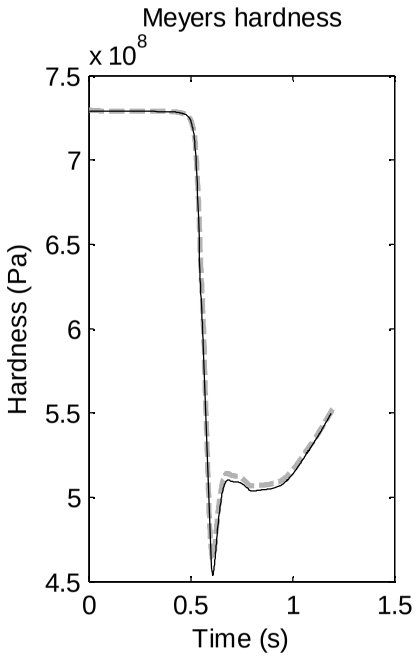

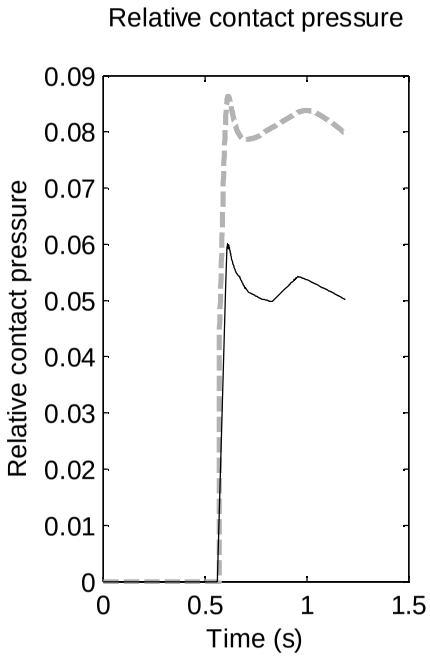

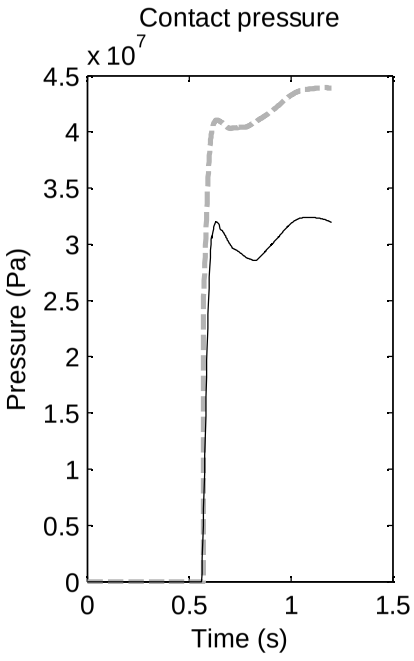

CABRI Na8 scenario, star marks rod burst

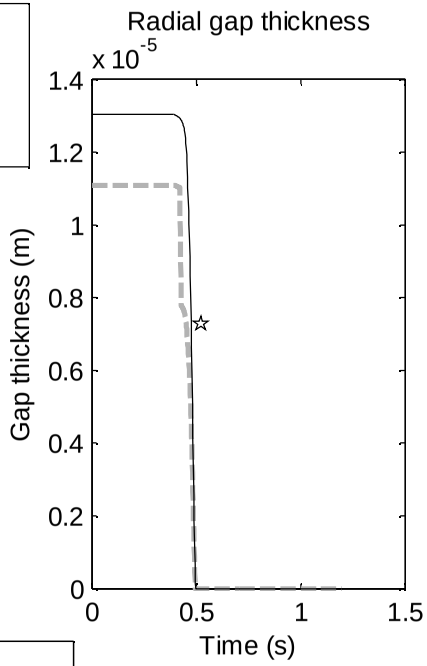

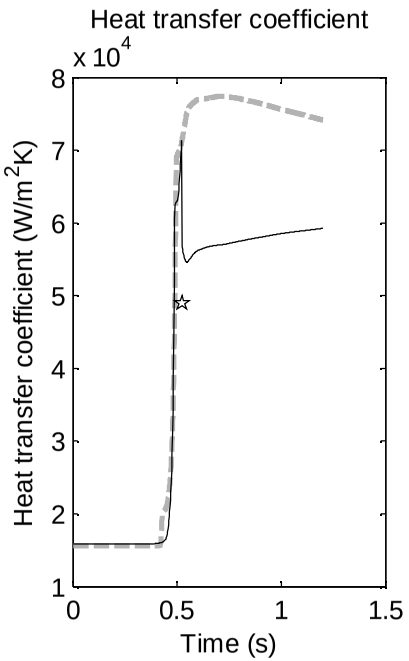

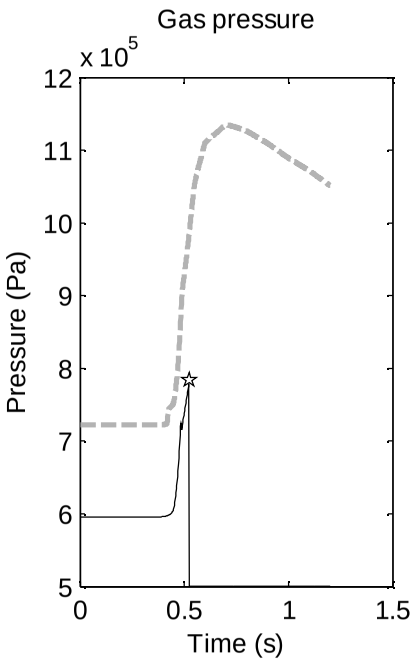

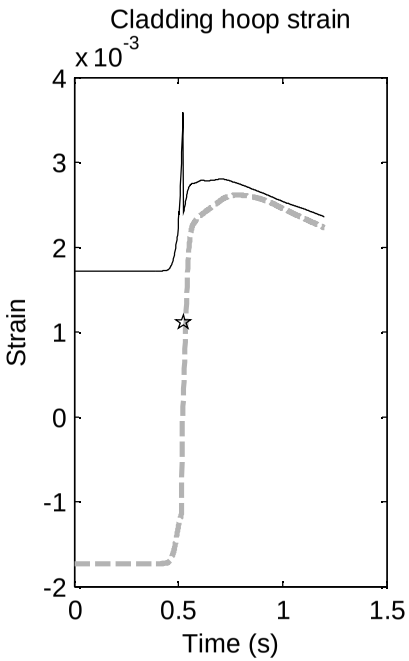

FINIX
FRAPTRAN

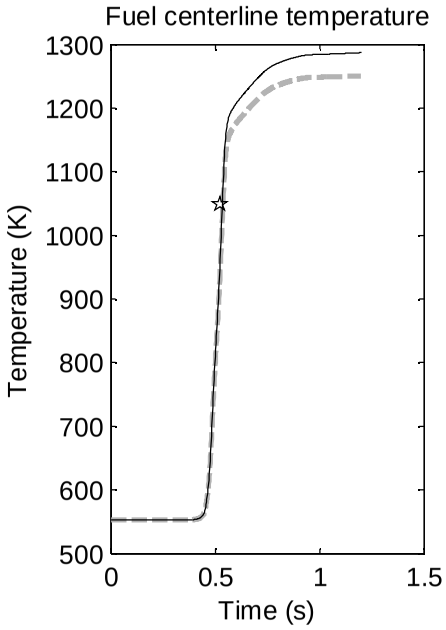

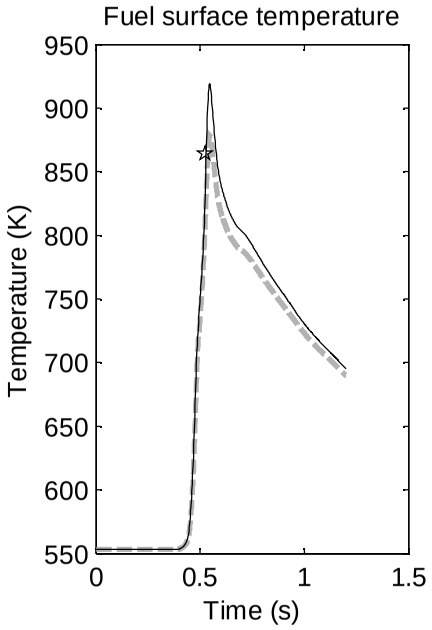

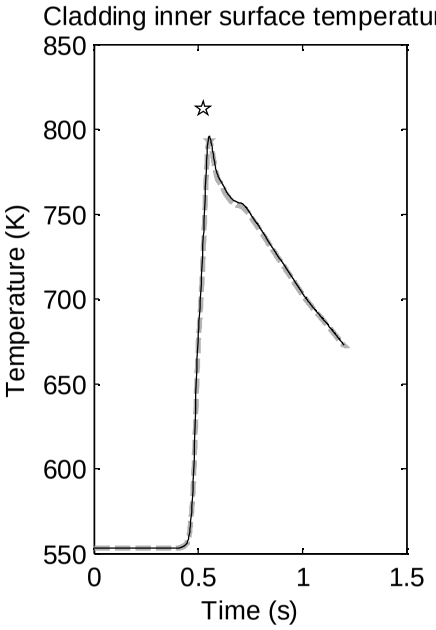

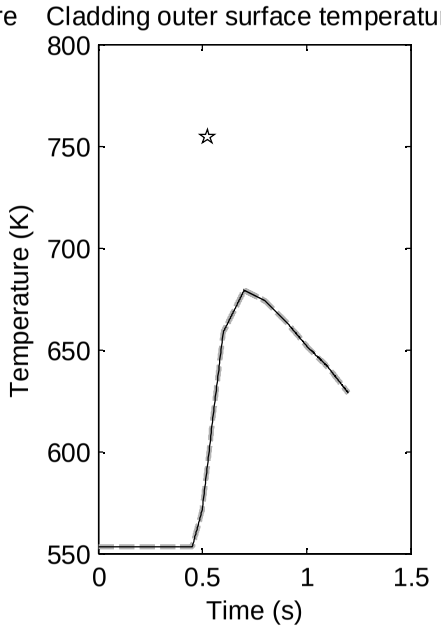

CABRI Na8 scenario, star marks rod burst

FINIX

FRAPTRAN

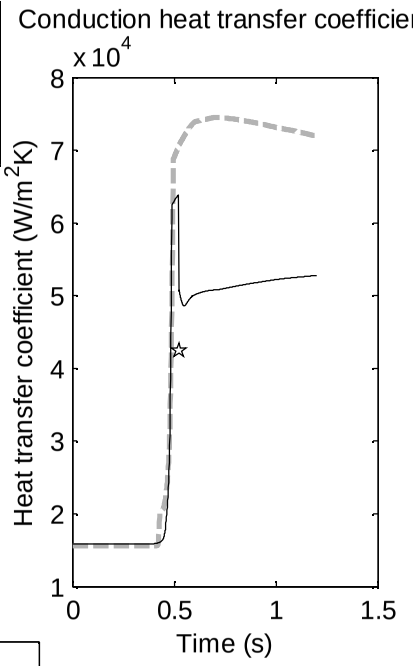

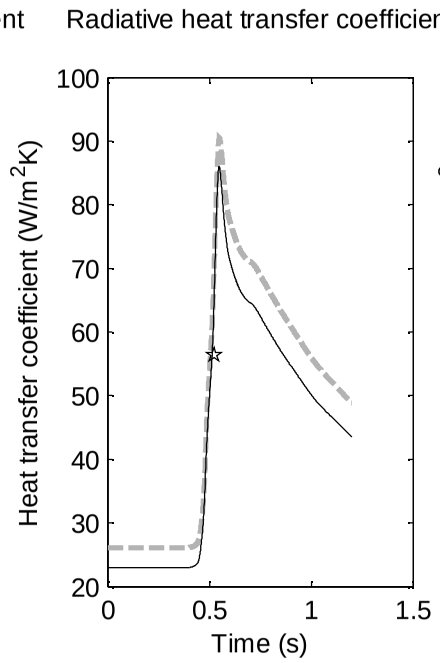

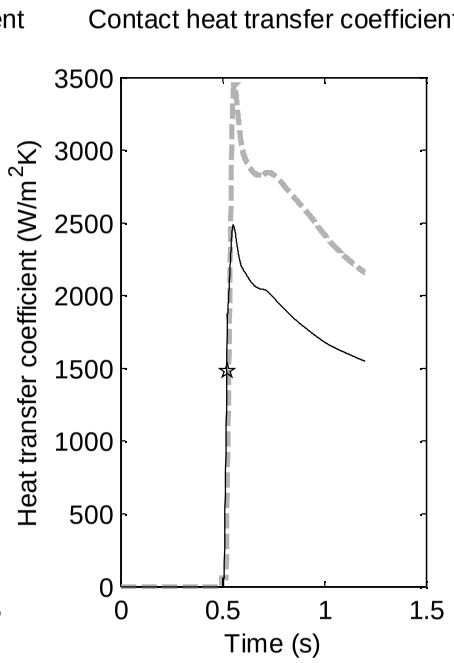

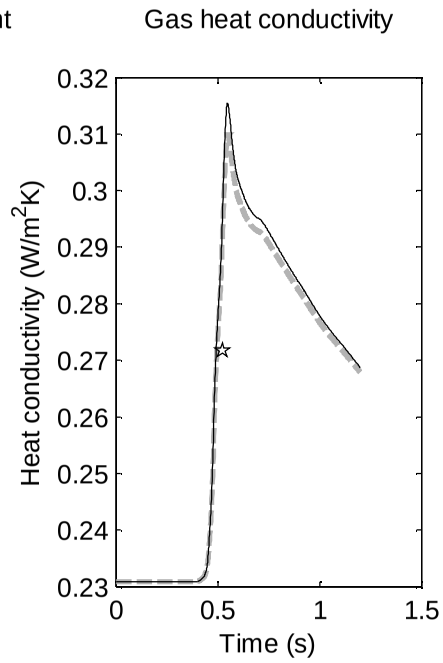

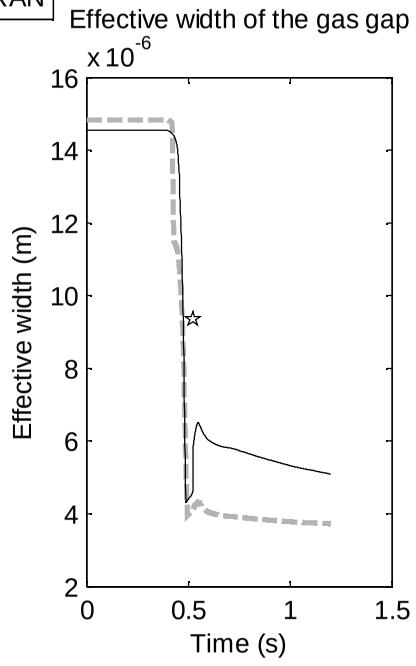

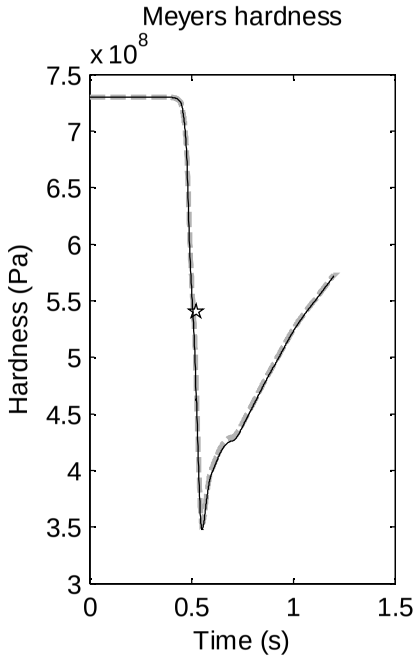

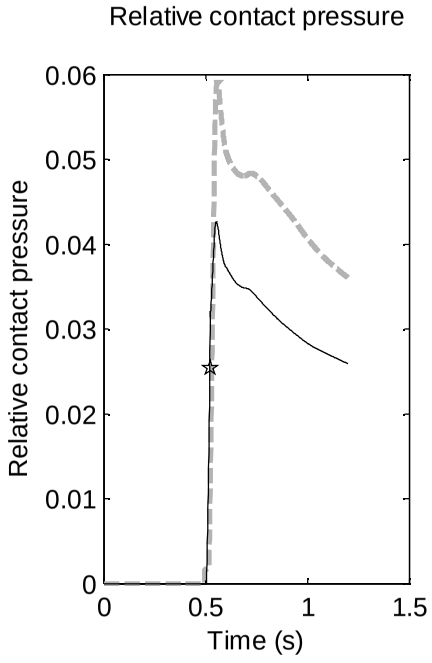

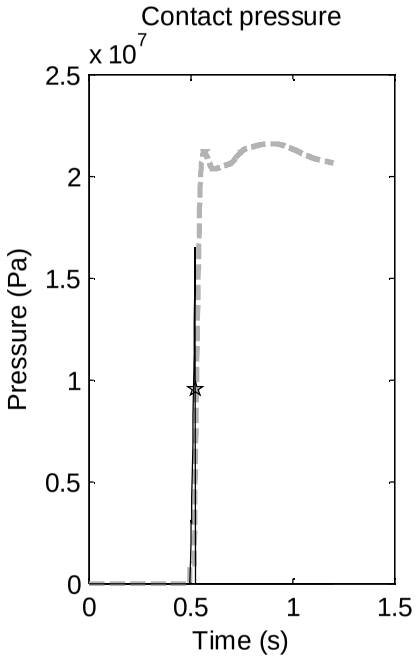

NSRR FK-1
scenario

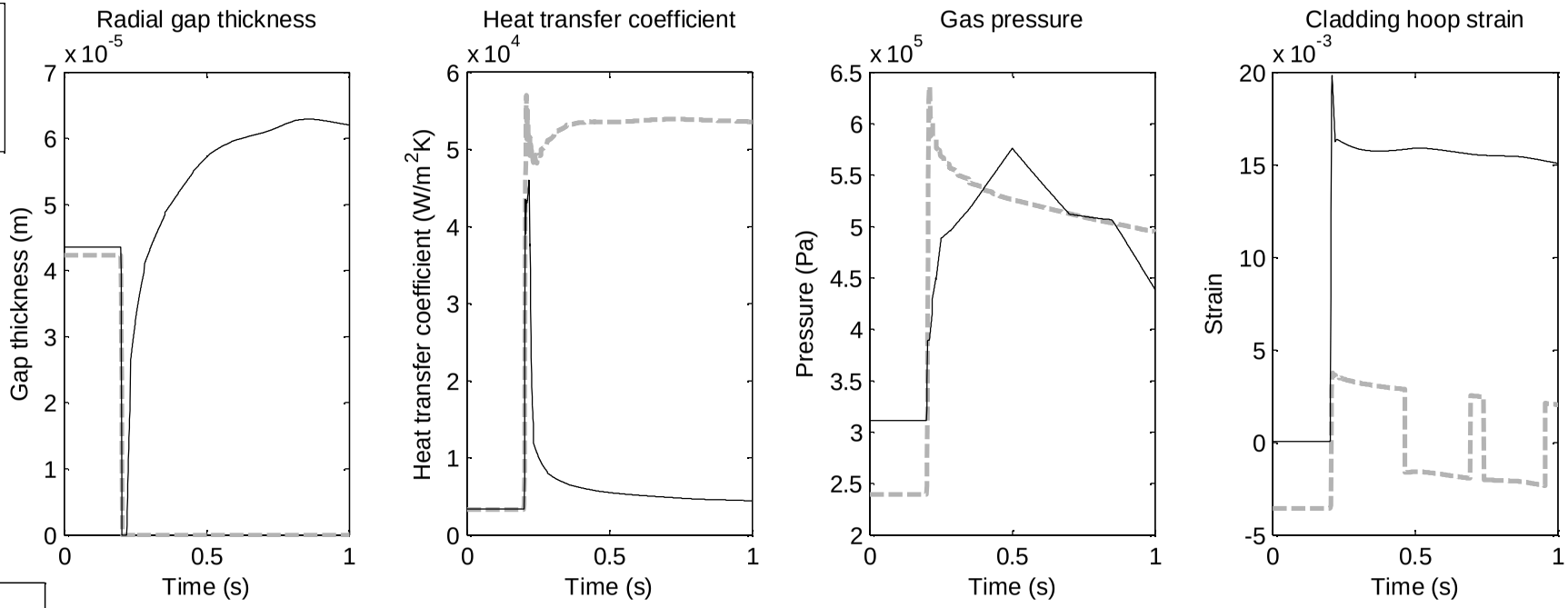

FINIX
FRAPTRAN

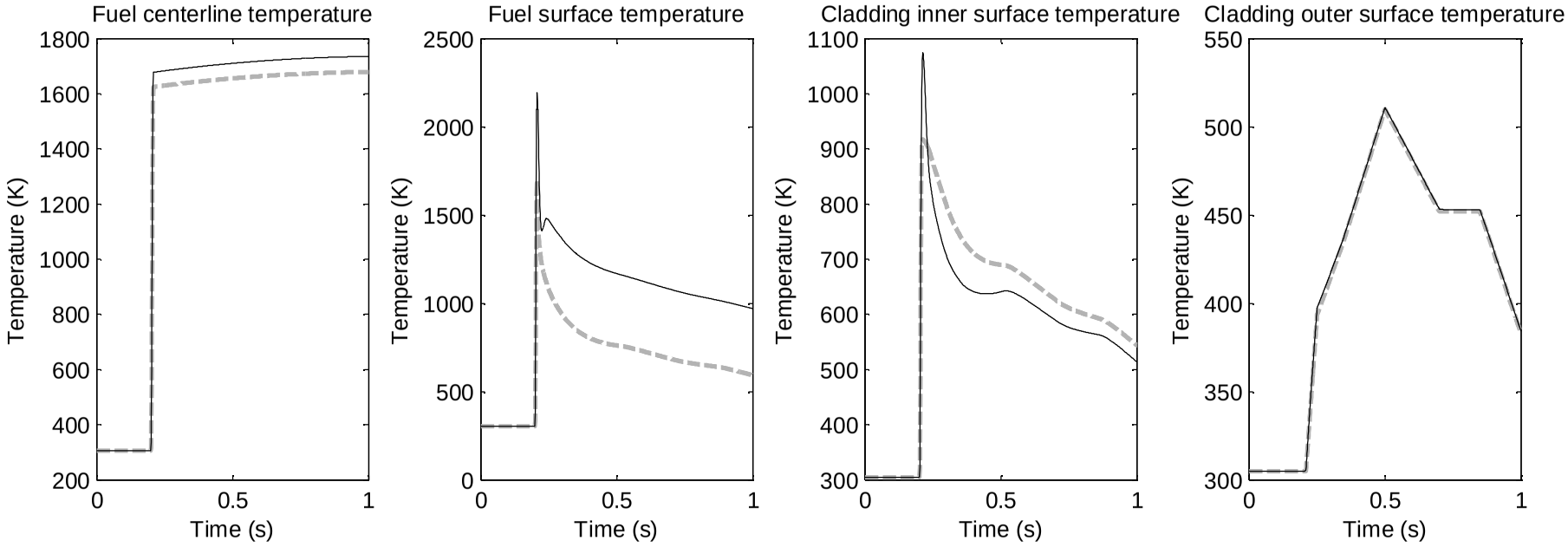

NSRR
FK-1
scenario

FINIX
FRAPTRAN

Conduction heat transfer coefficient

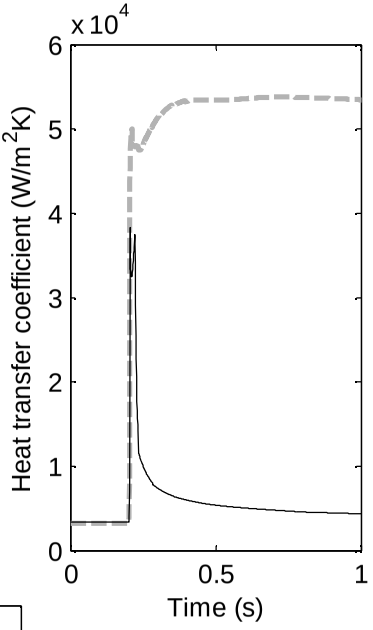

Radiative heat transfer coefficient

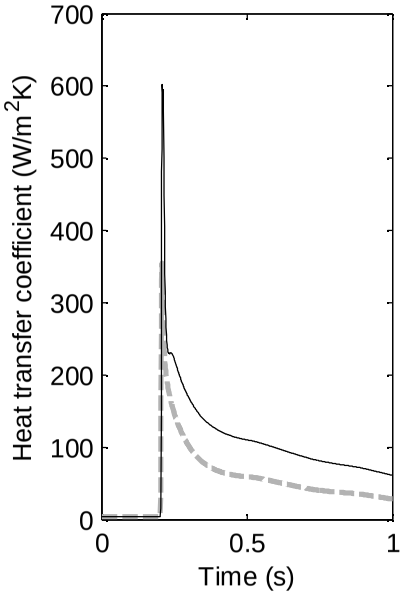

Contact heat transfer coefficient

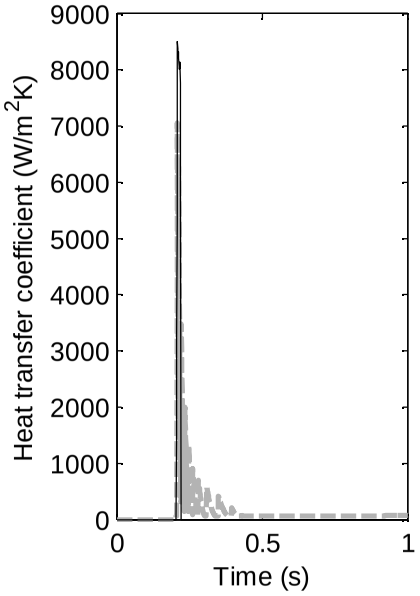

Gas heat conductivity

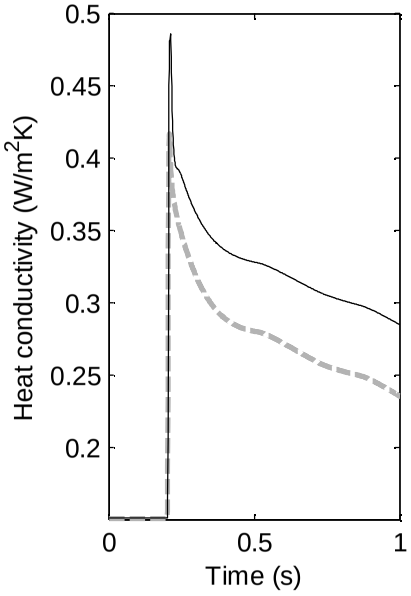

Effective width of the gas gap

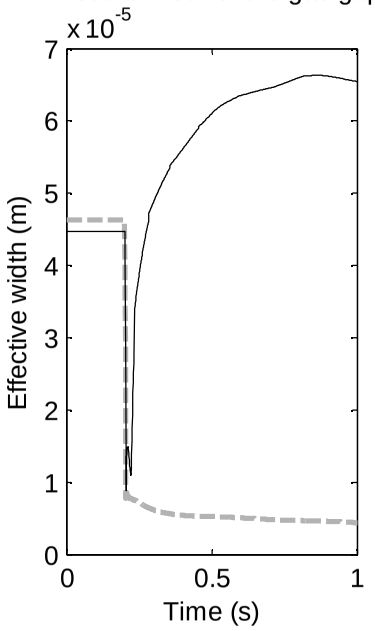

Meyers hardness

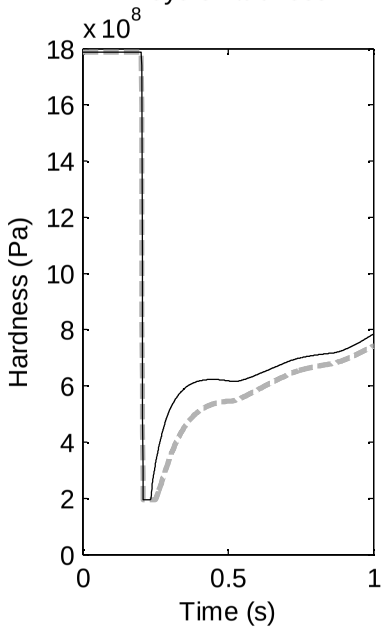

Relative contact pressure

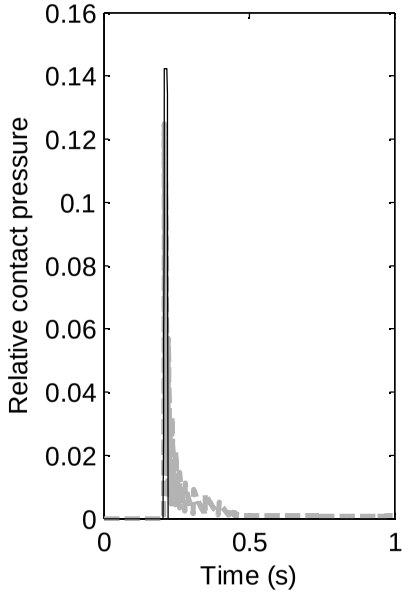

Contact pressure

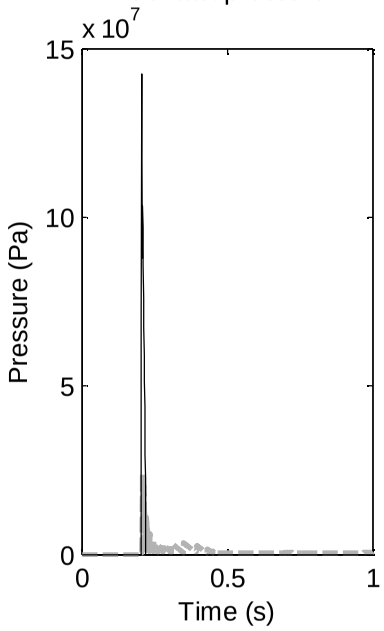

NSRR
HBO-1
scenario

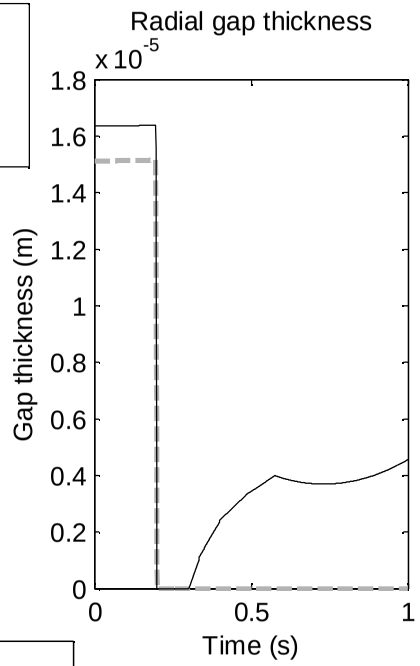

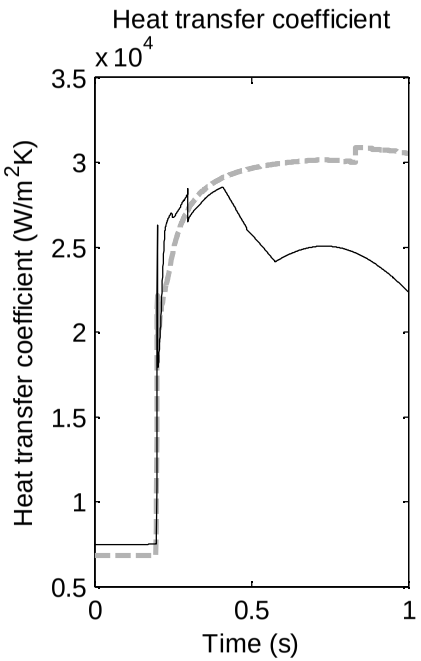

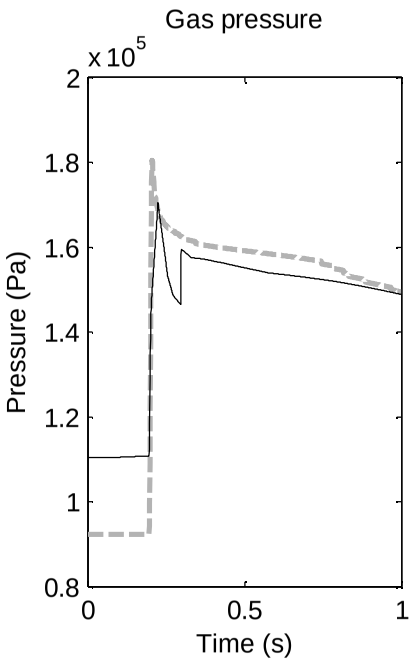

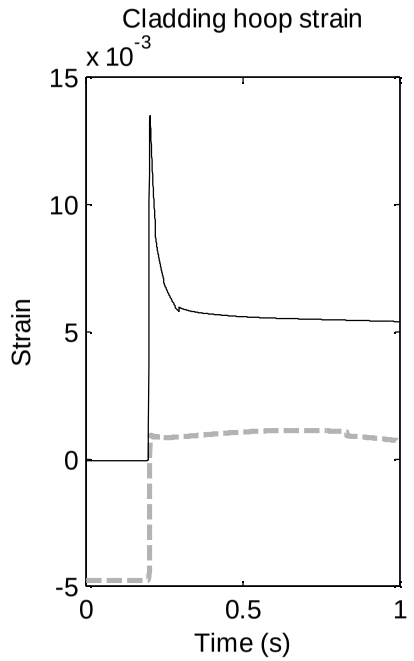

FINIX
FRAPTRAN

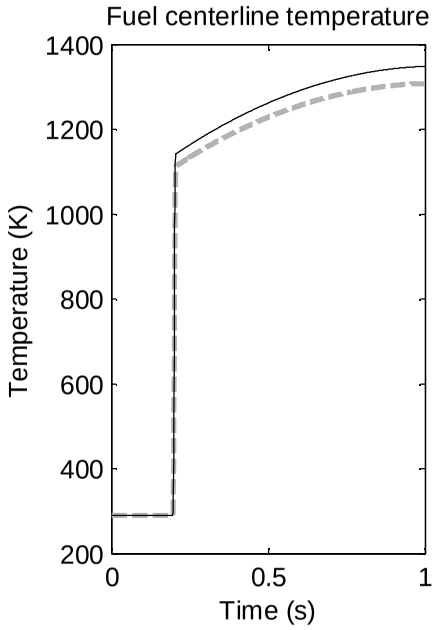

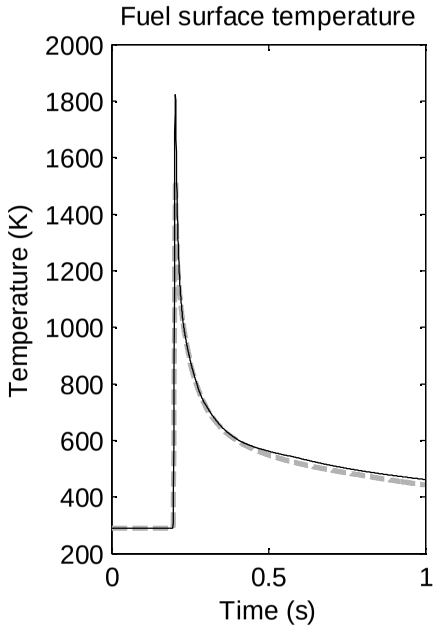

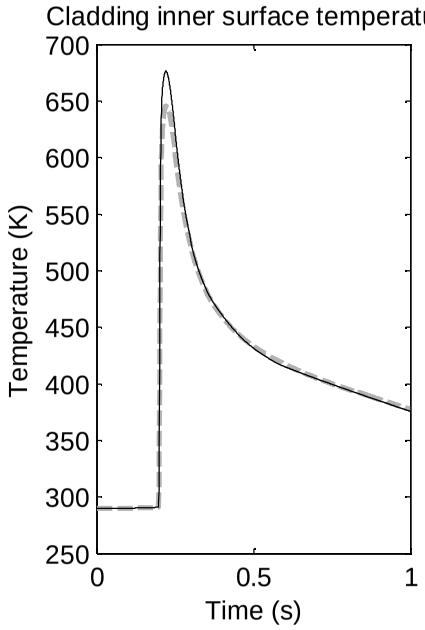

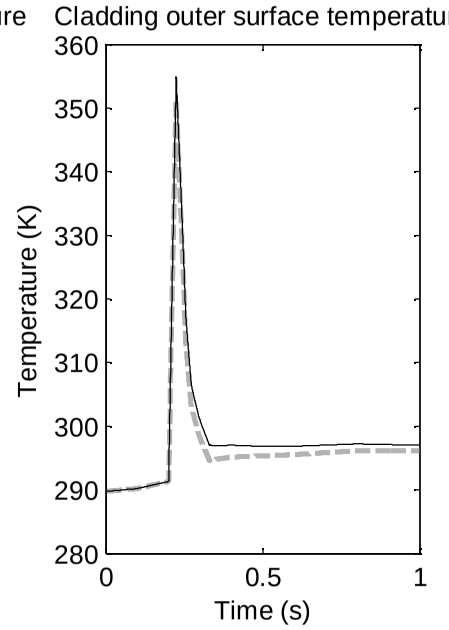

NSRR HBO-1 scenario

FINIX

FRAPTRAN

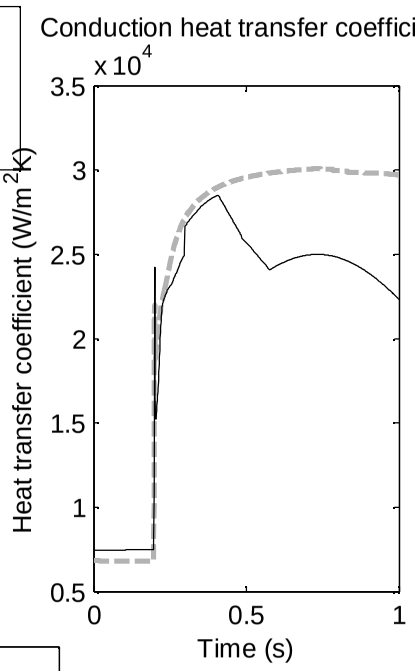

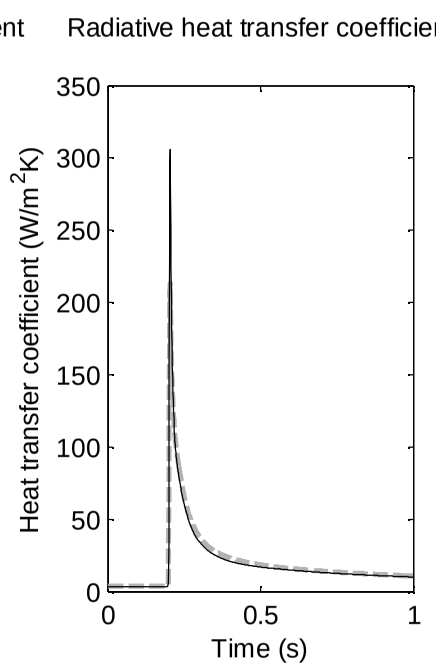

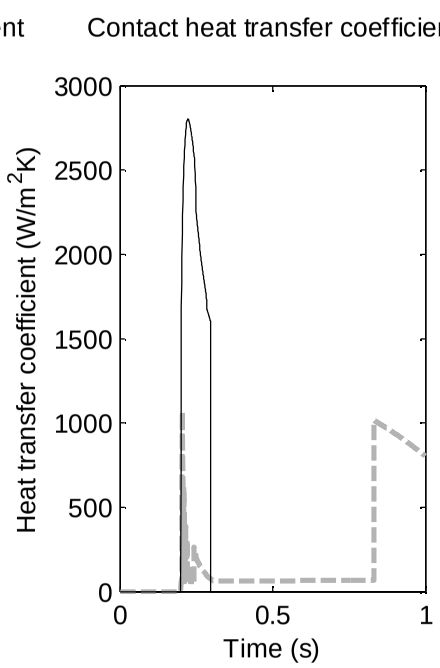

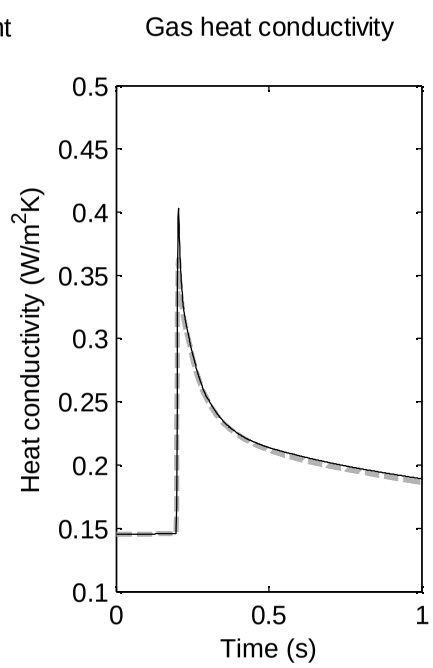

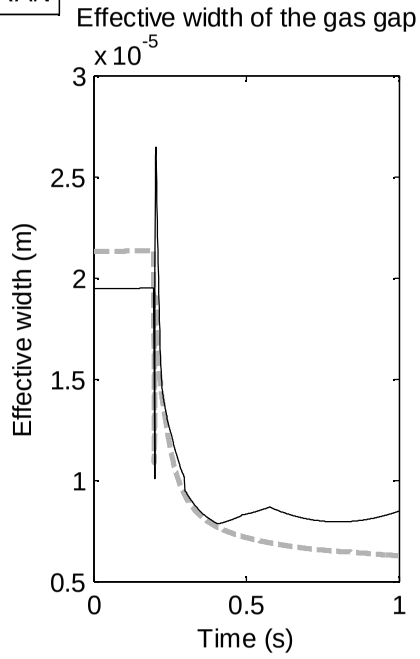

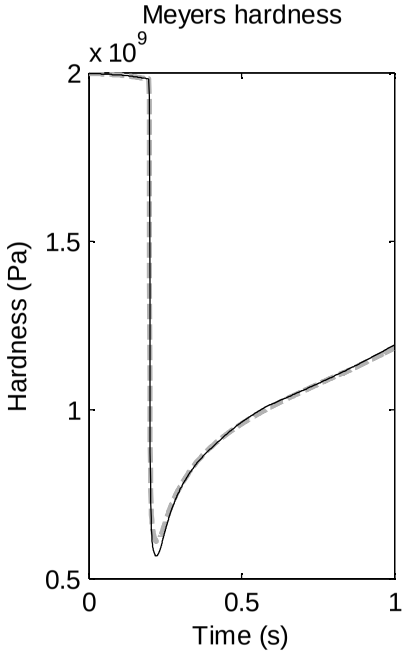

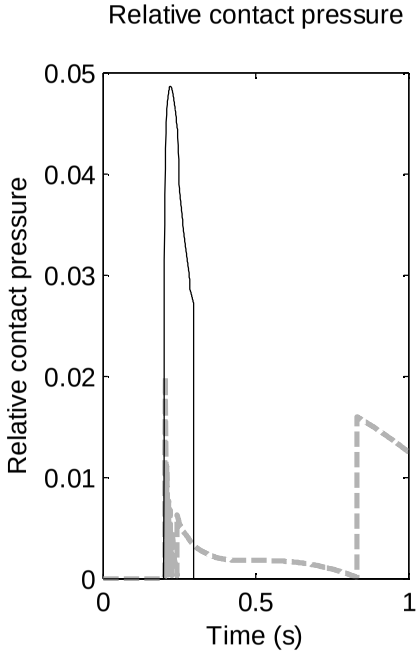

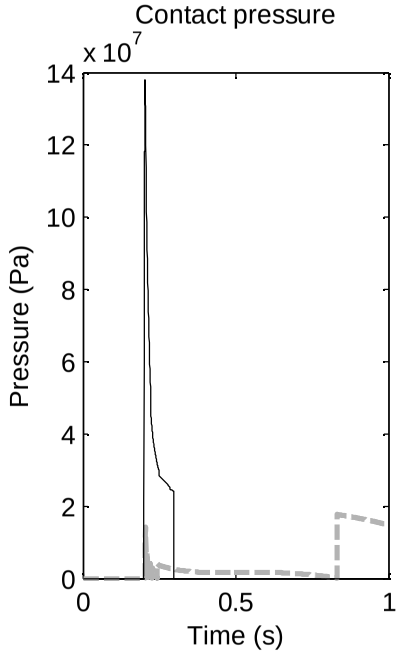

NSRR HBO-5 scenario, star marks rod burst

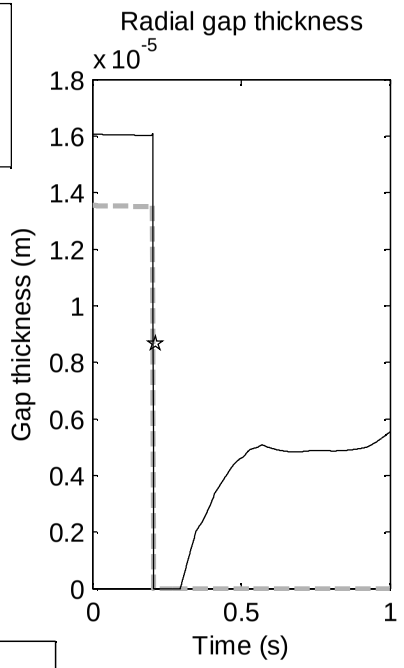

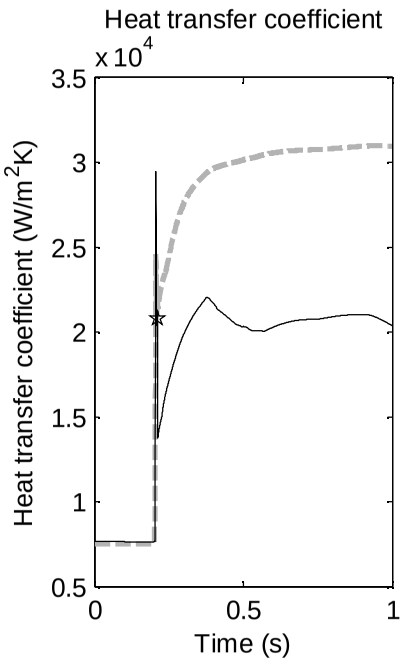

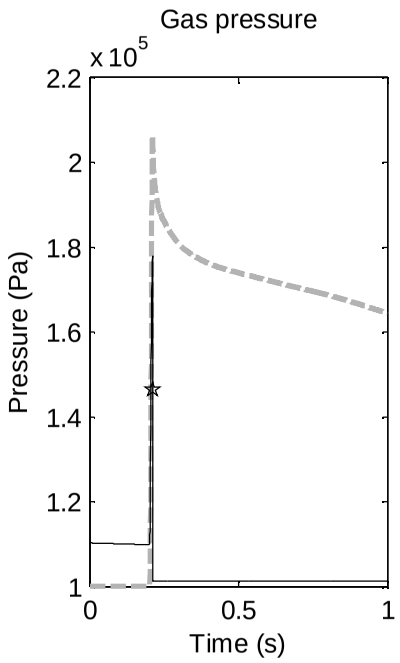

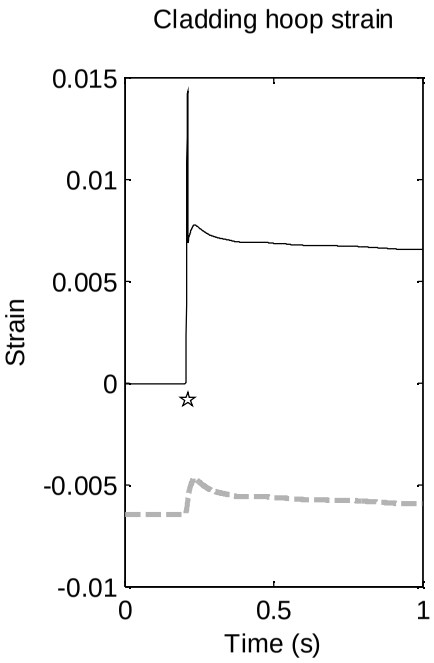

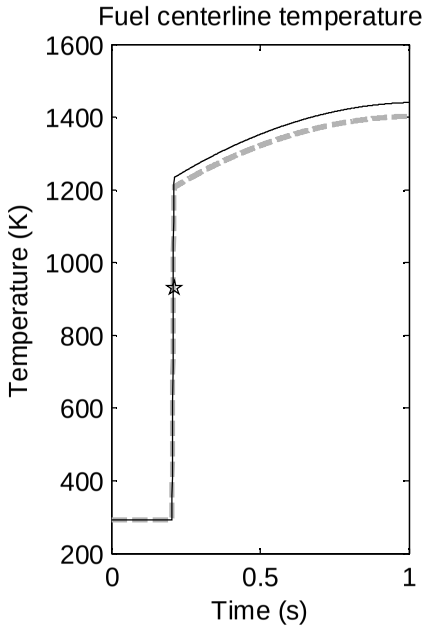

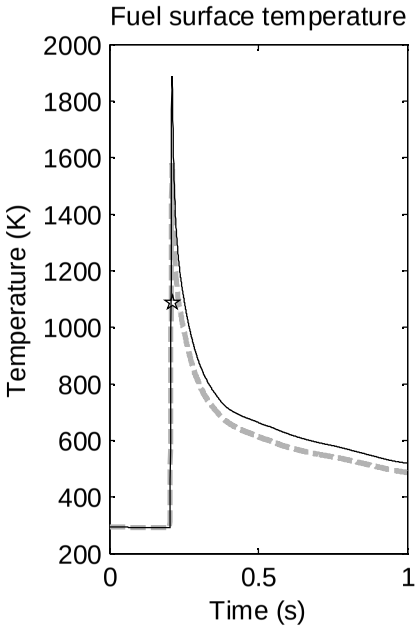

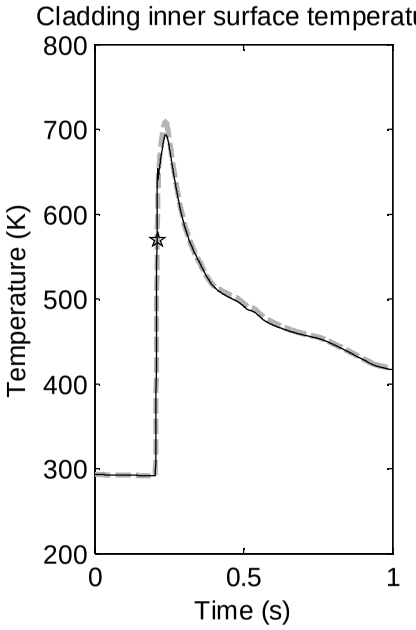

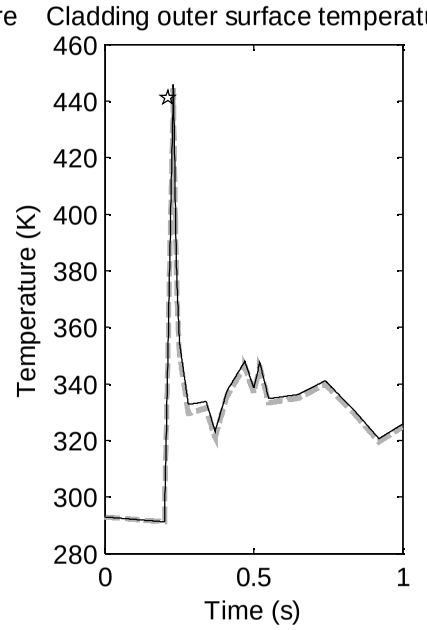

NSRR
HBO-5
scenario,
star
marks
rod
burst

FINIX
FRAPTRAN

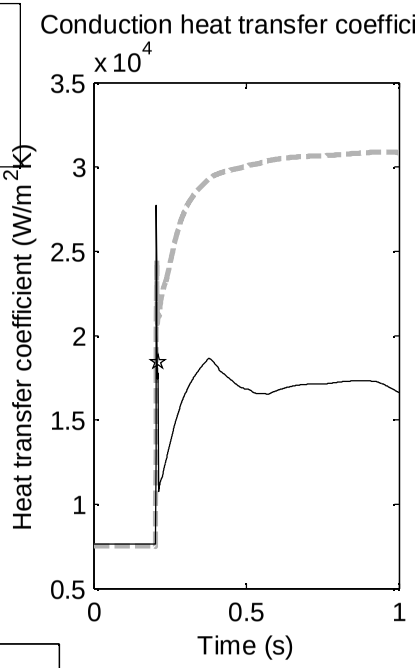

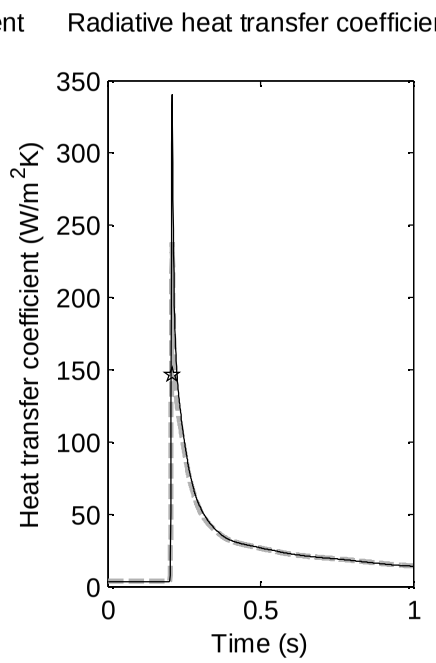

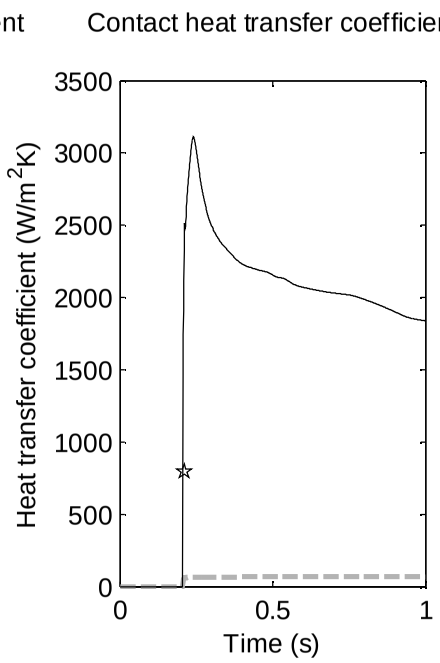

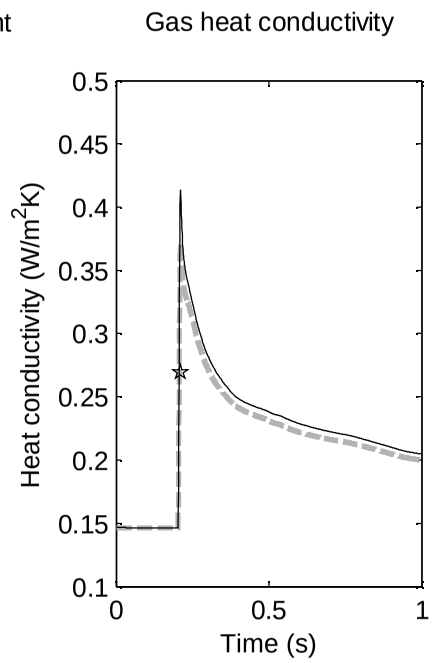

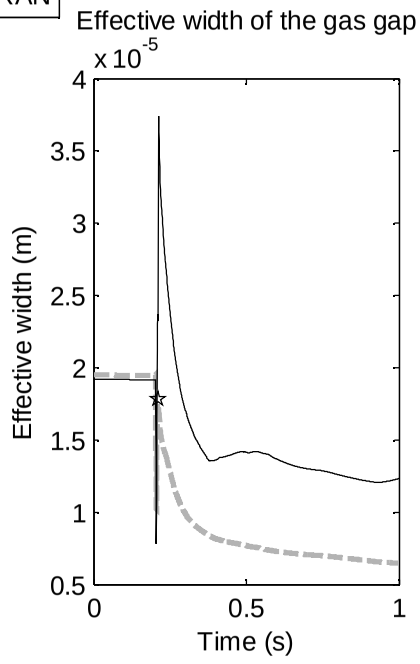

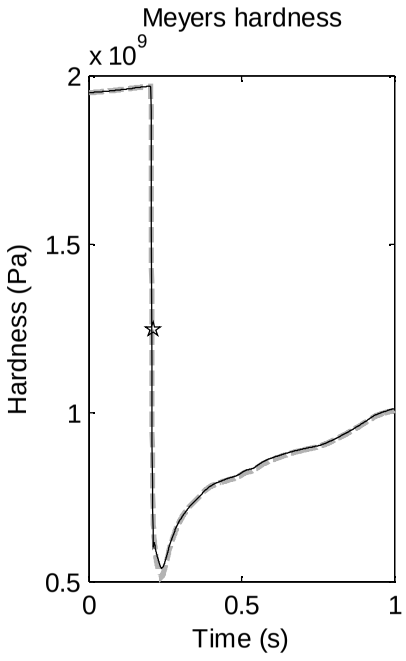

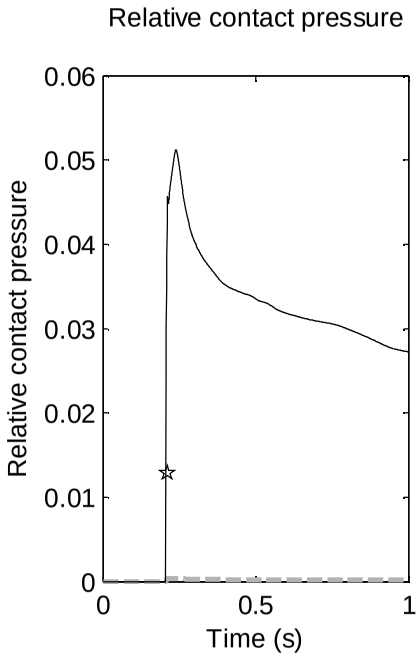

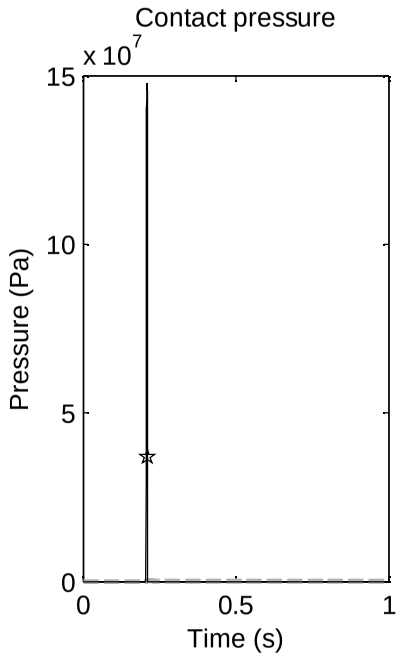

NSRR
HBO-6
scenario

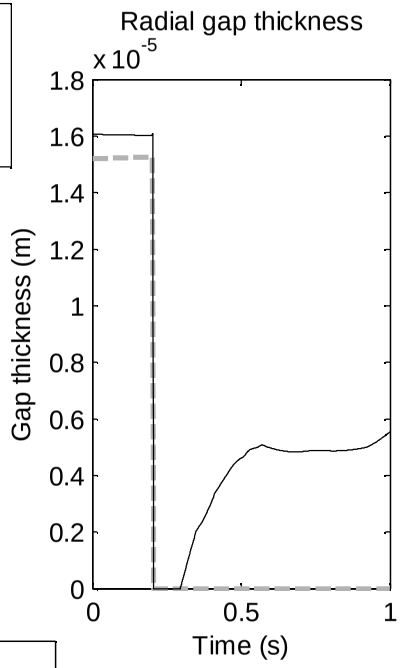

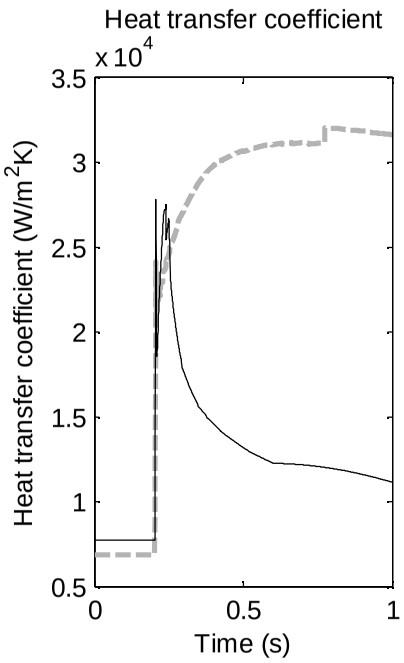

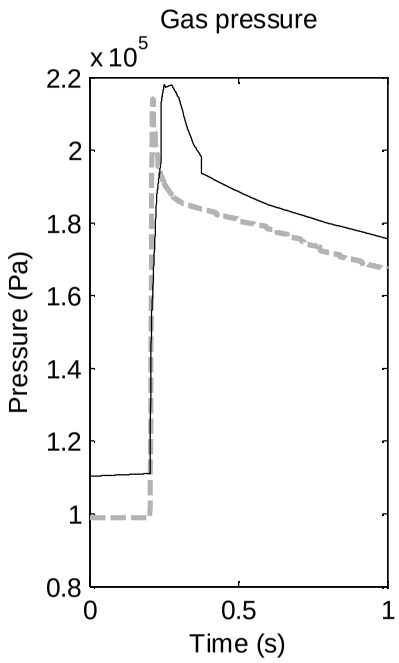

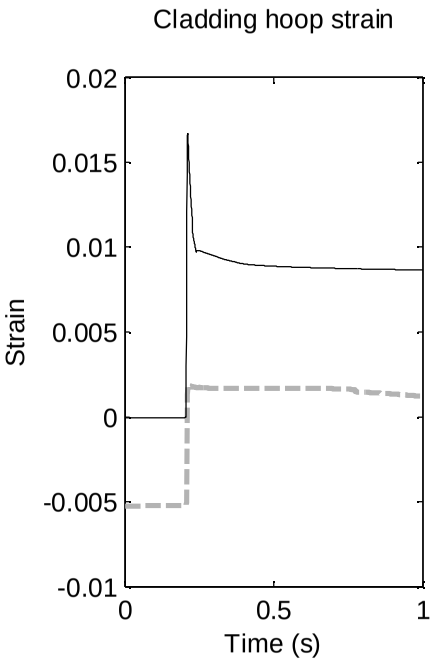

FINIX
FRAPTRAN

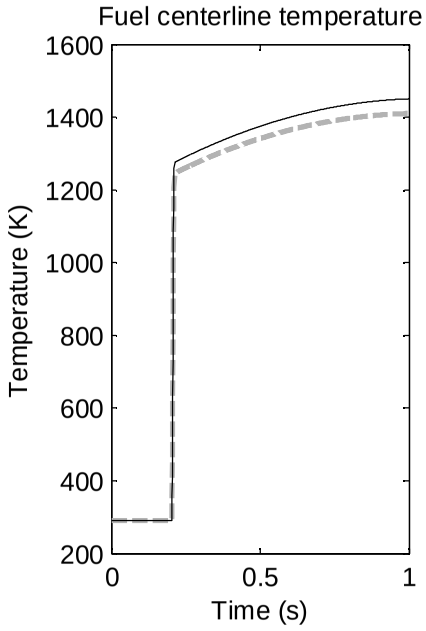

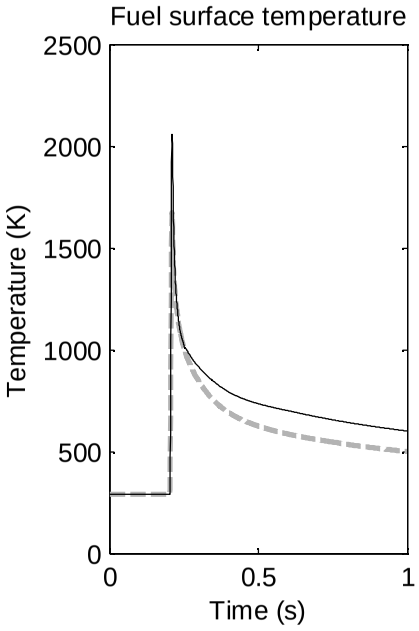

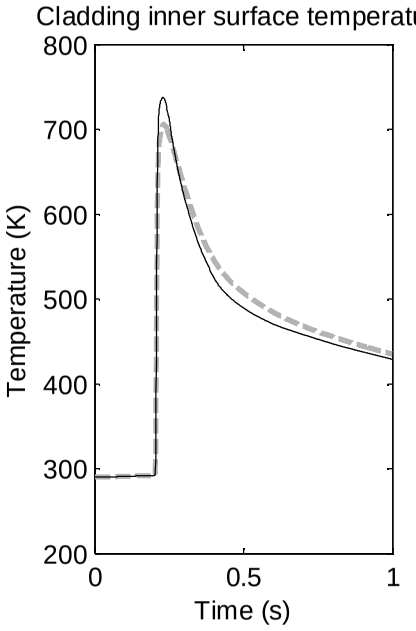

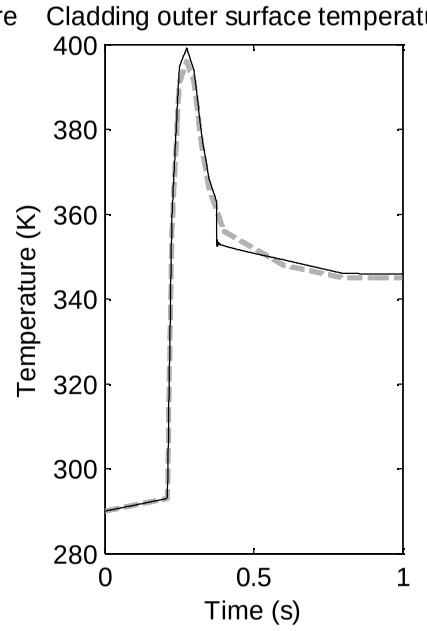

NSRR HBO-6 scenario

FINIX

FRAPTRAN

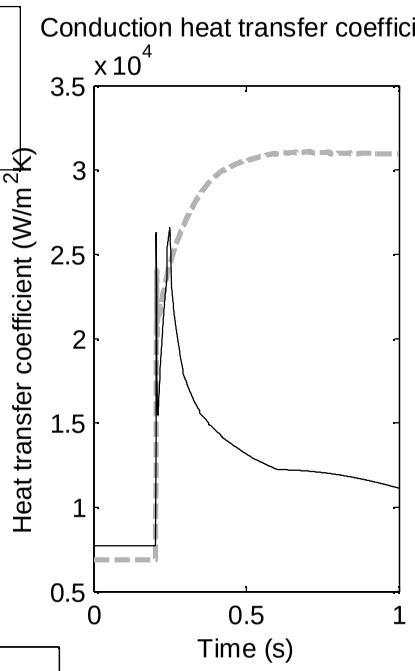

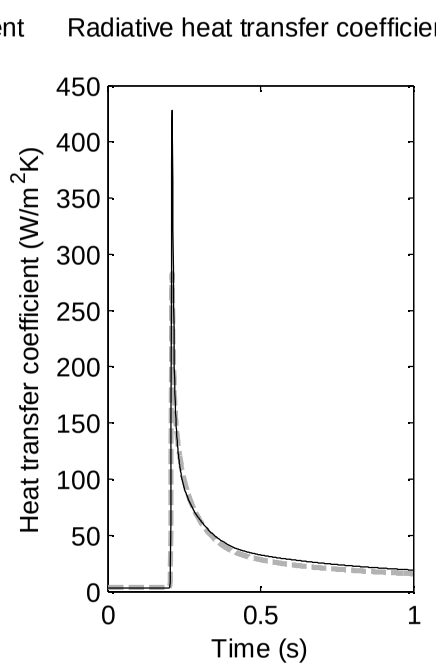

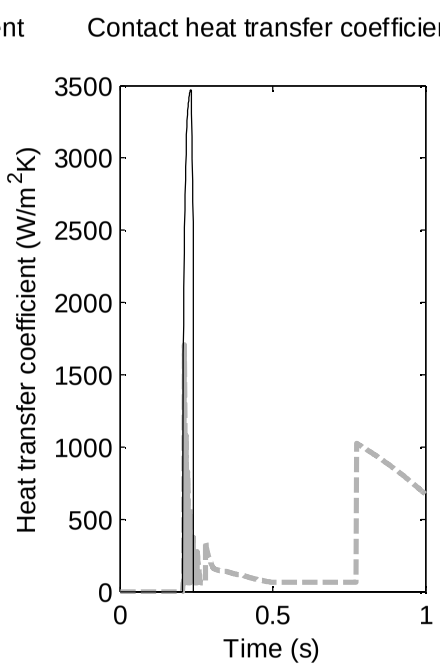

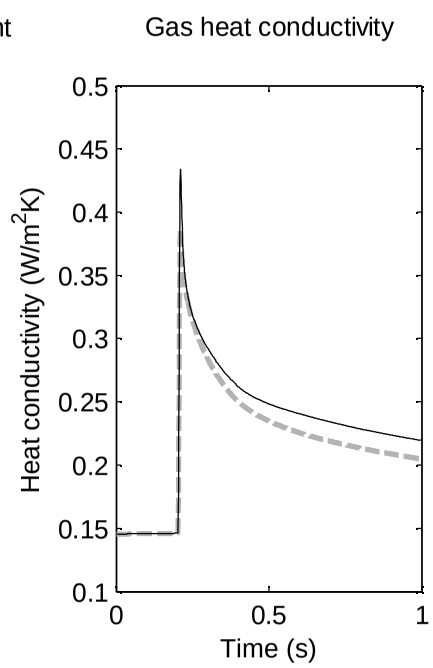

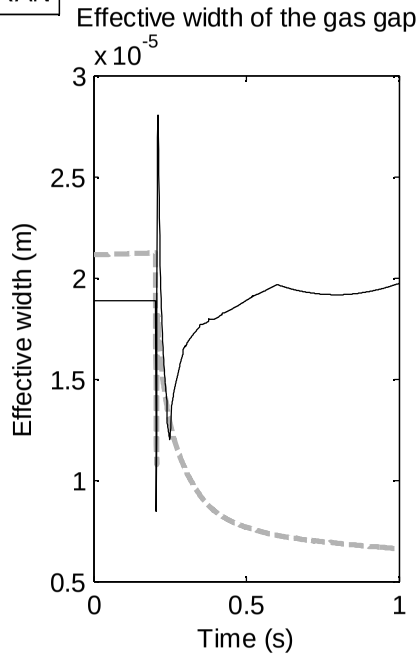

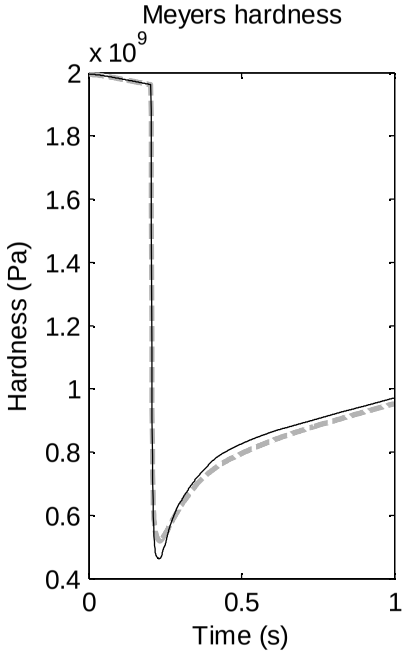

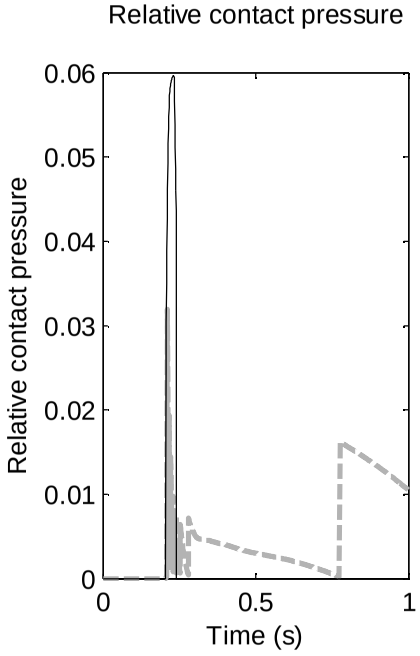

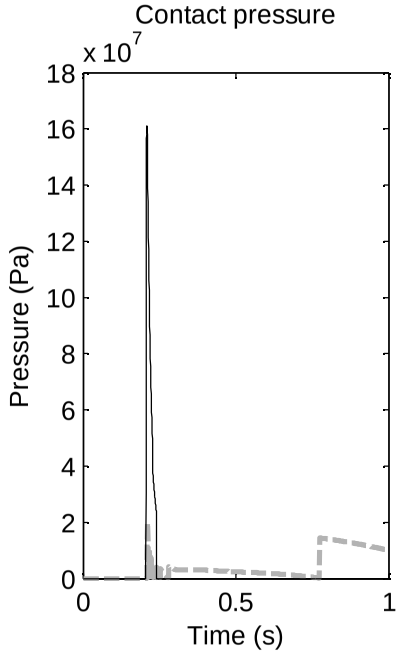

NSRR TS-5 scenario

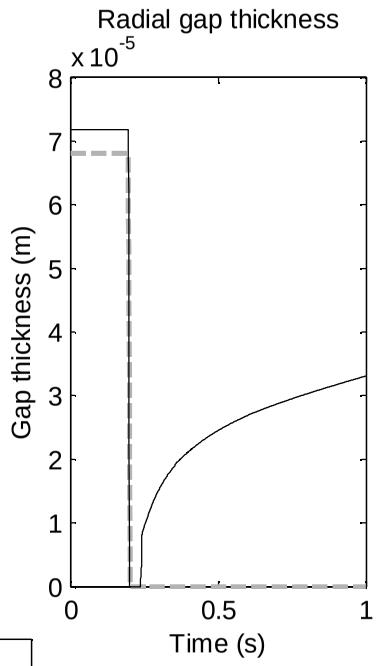

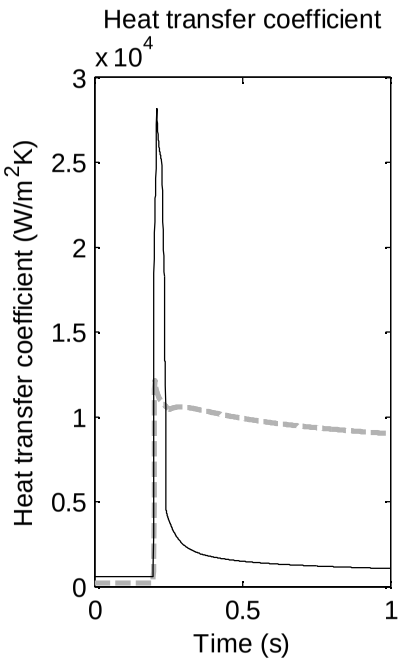

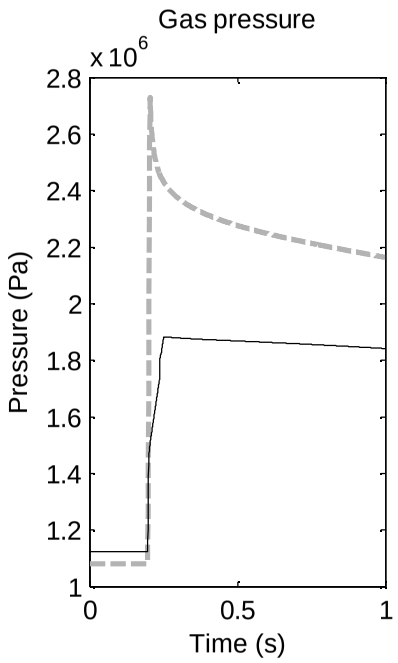

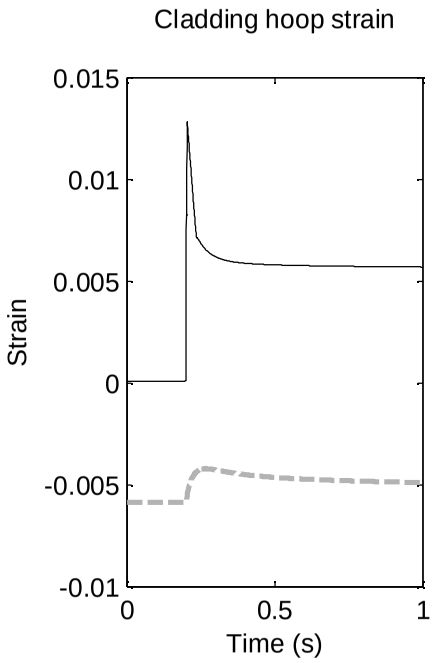

FINIX
FRAPTRAN

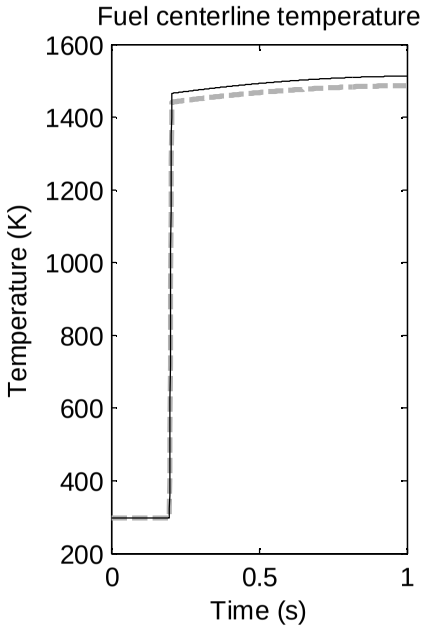

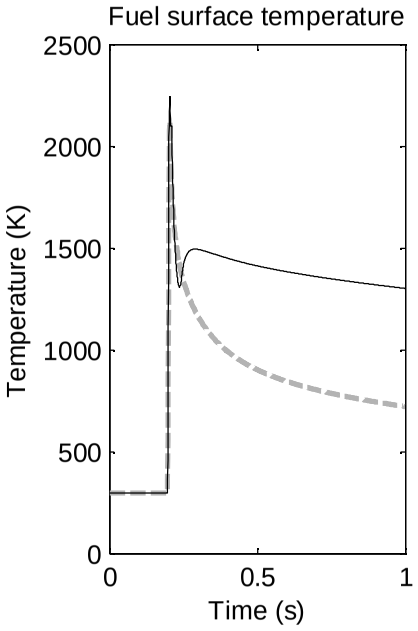

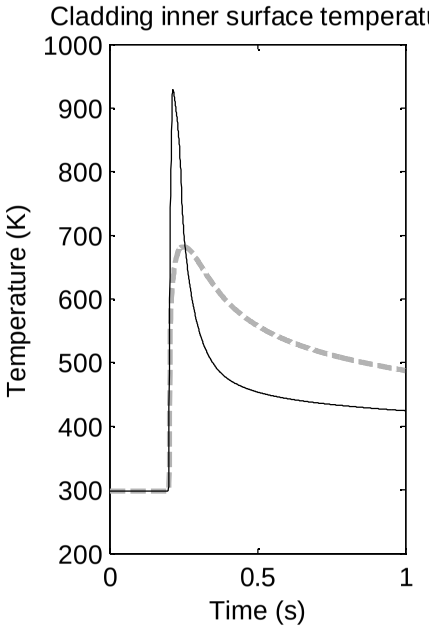

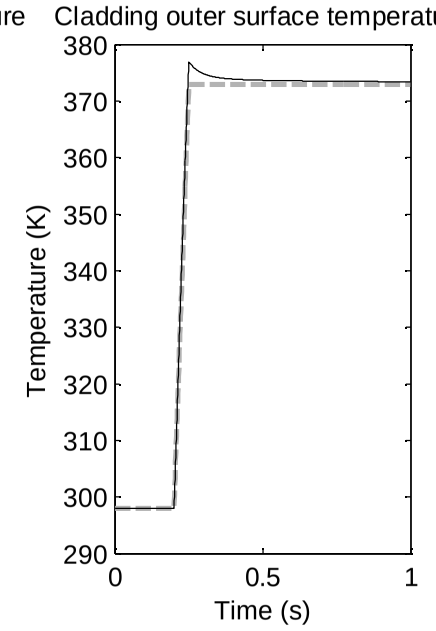

NSRR
TS-5
scenario

FINIX
FRAPTRAN

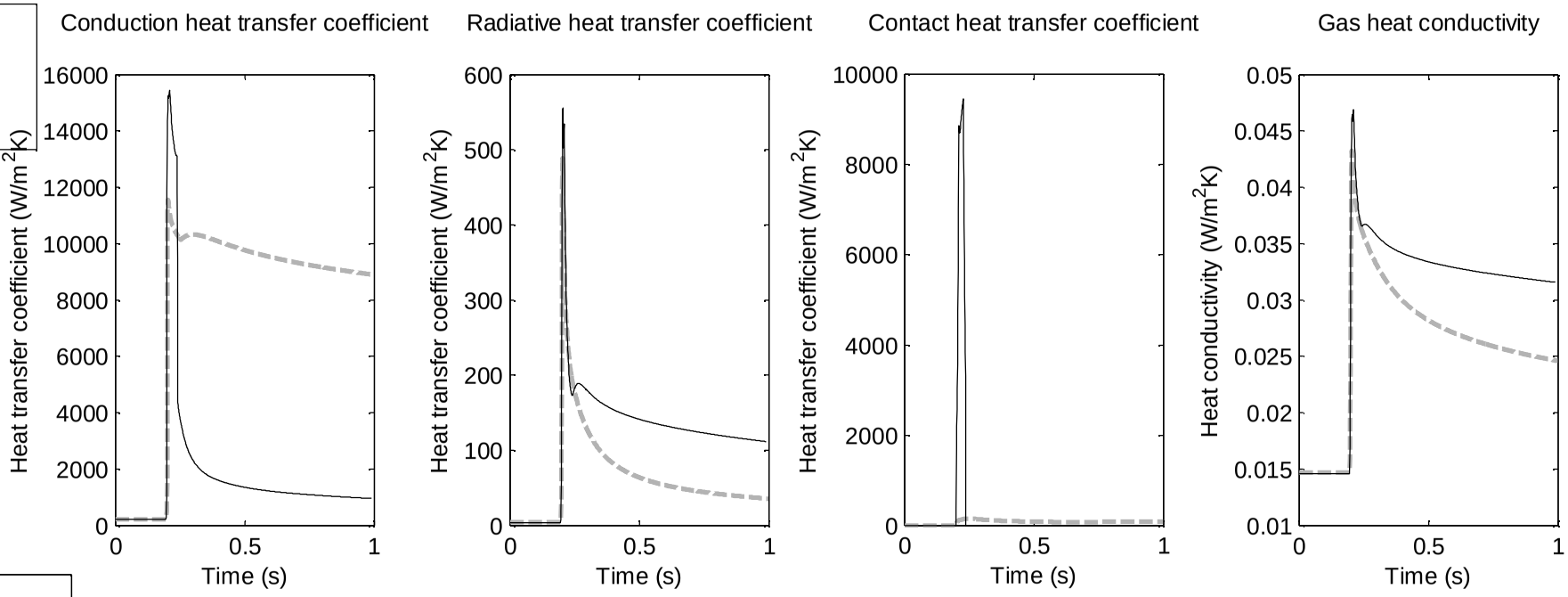

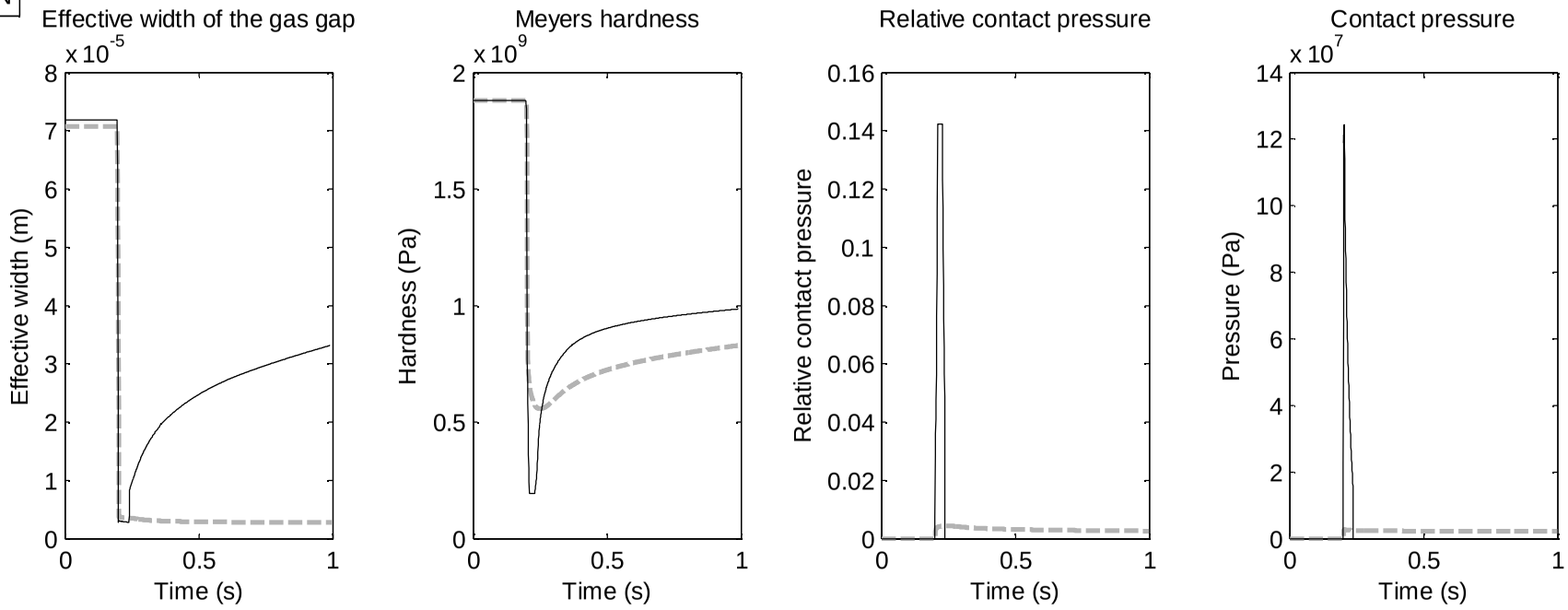

NSRR VA-1 scenario, star marks rod burst

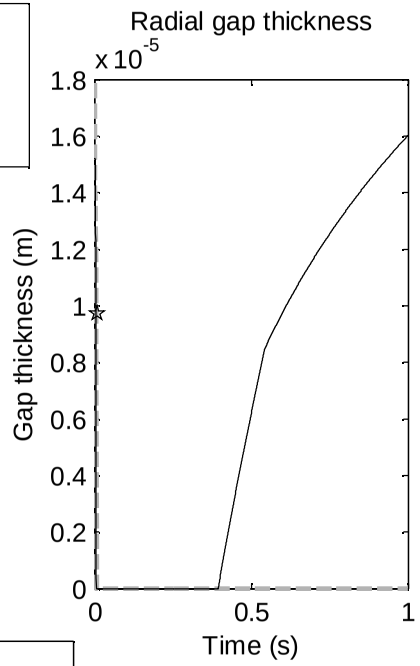

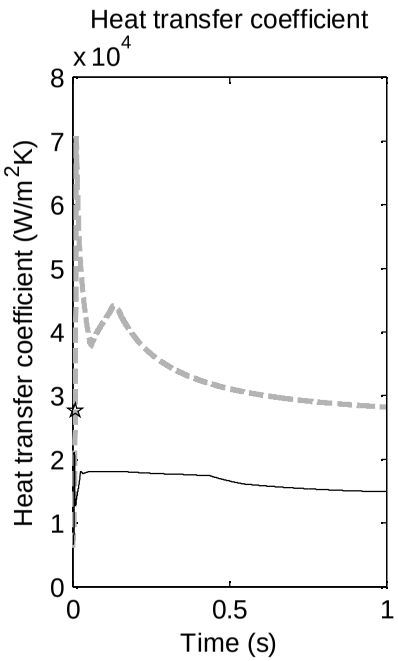

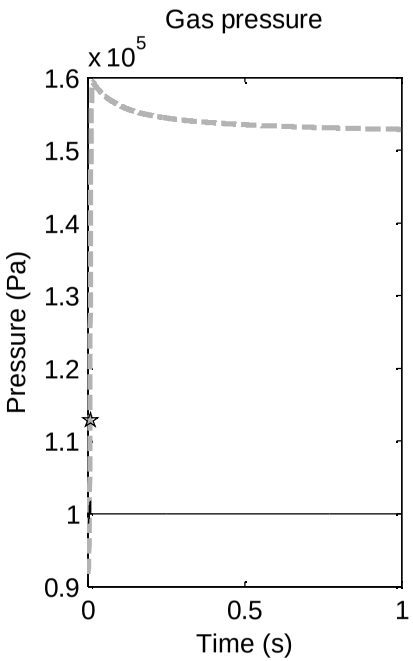

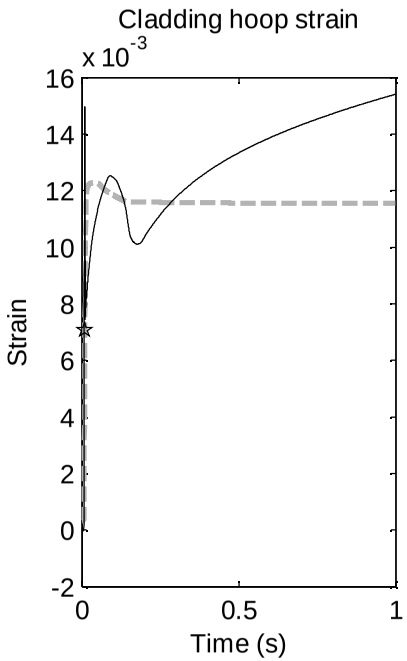

FINIX
FRAPTRAN

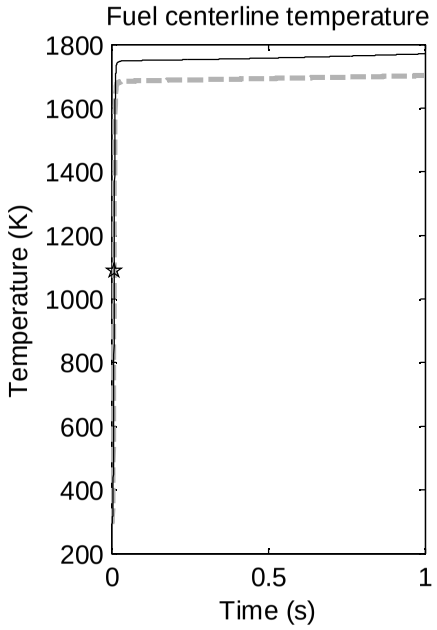

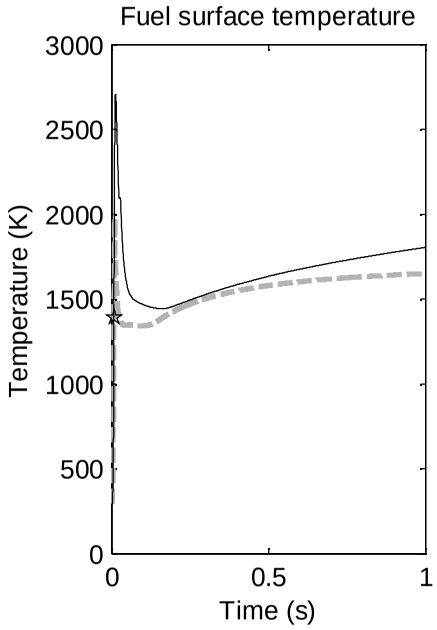

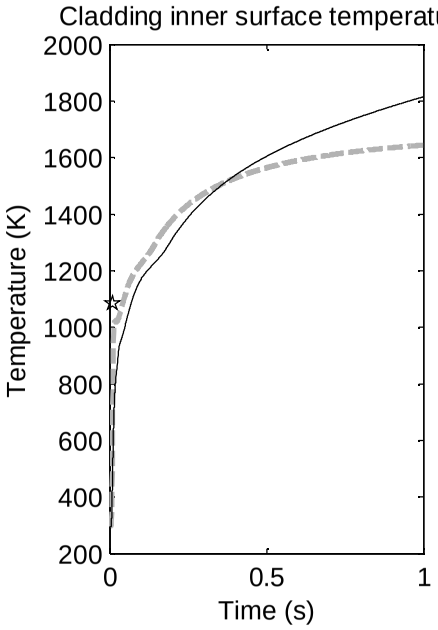

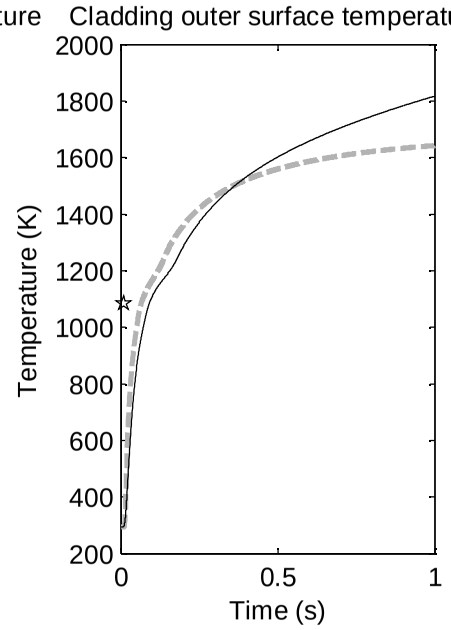

NSRR
VA-1
scenario,
star
marks
rod
burst

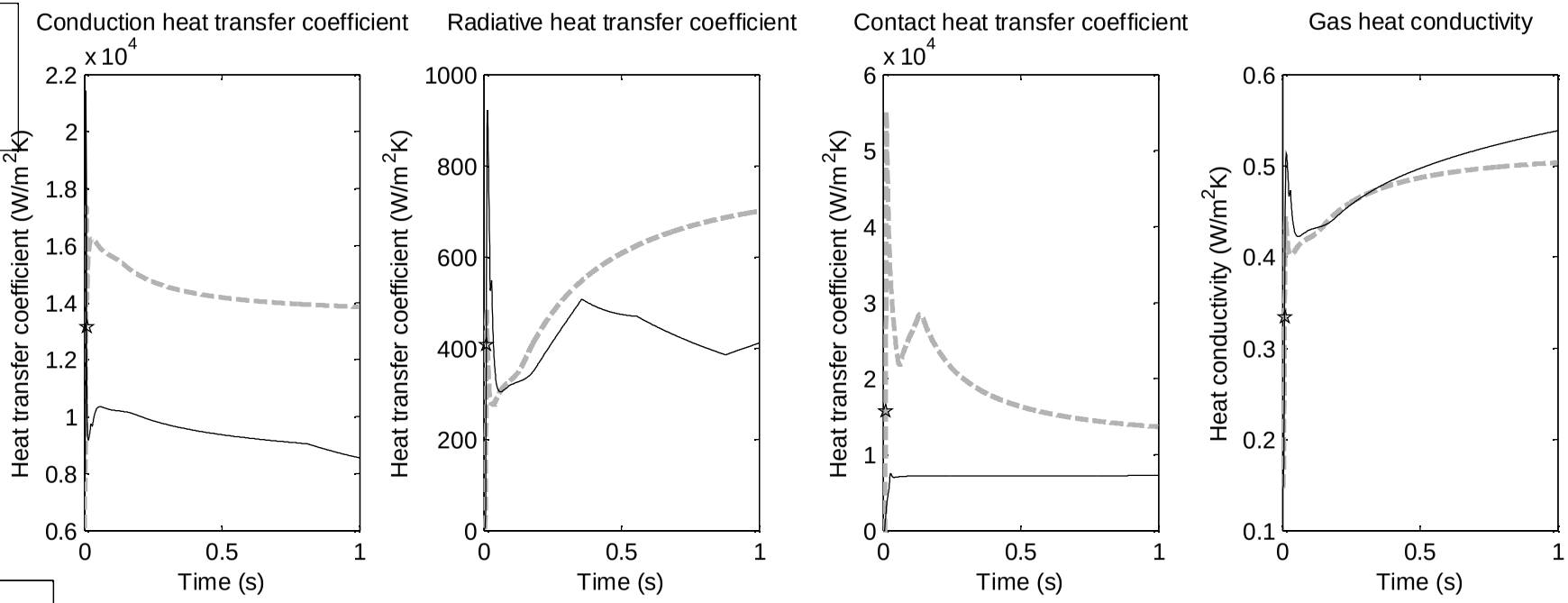

FINIX
FRAPTRAN

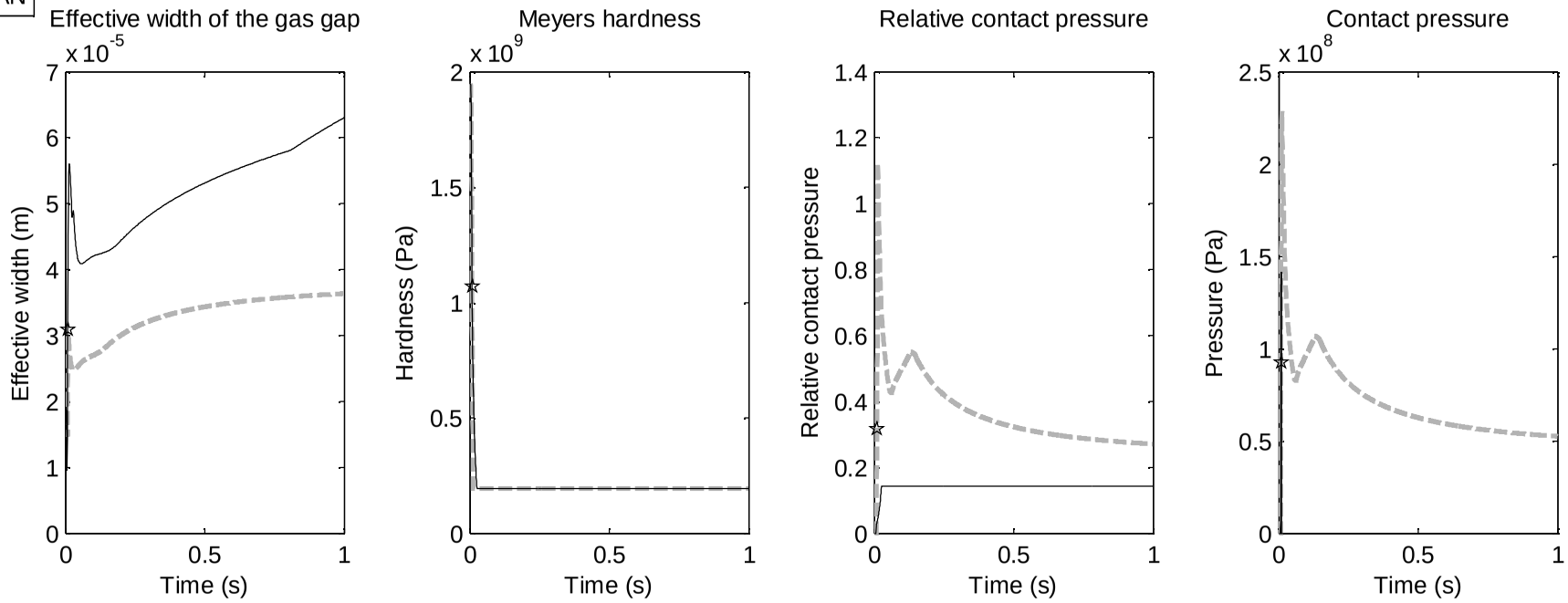

NSRR VA-3
scenario,
star marks
rod burst

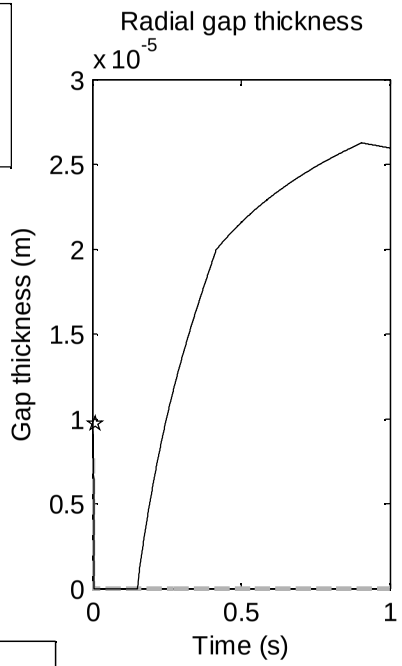

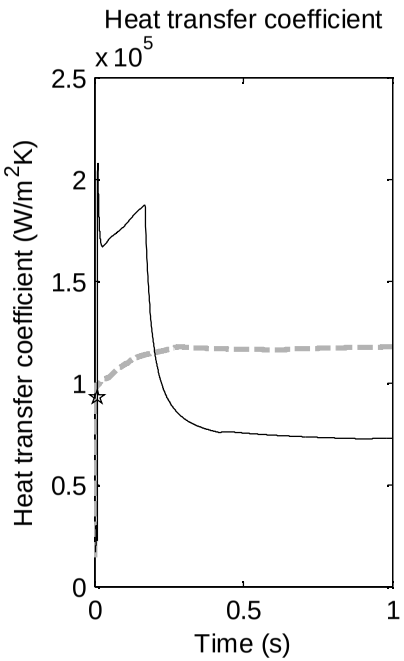

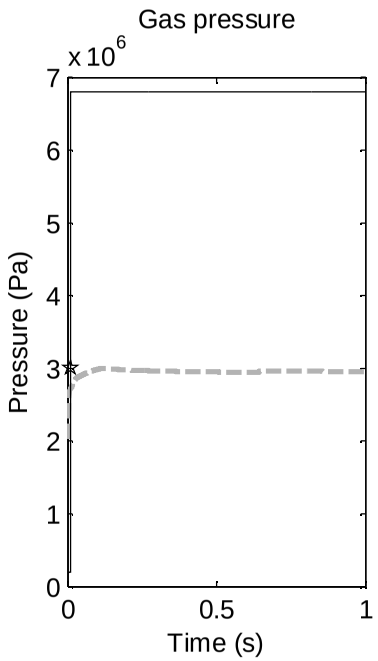

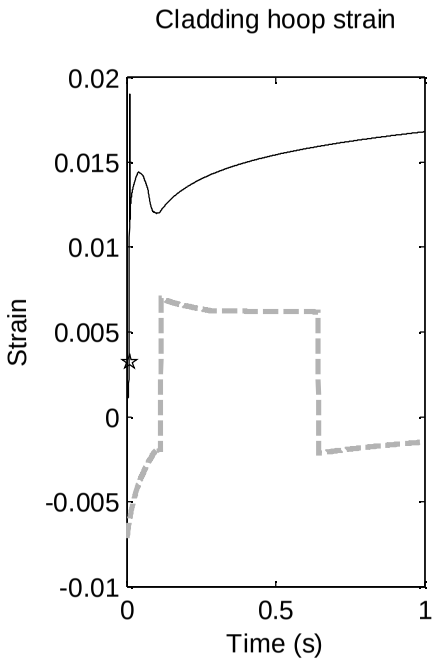

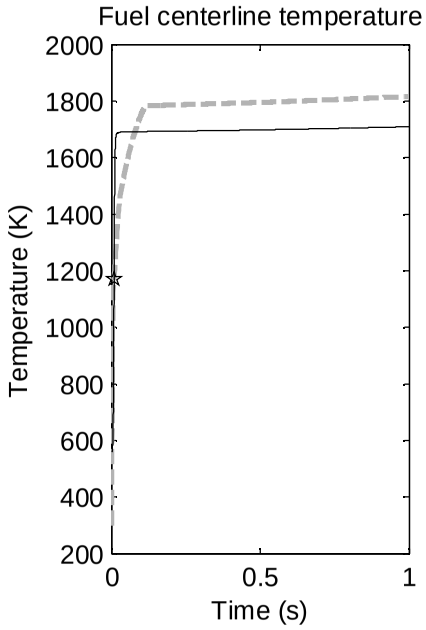

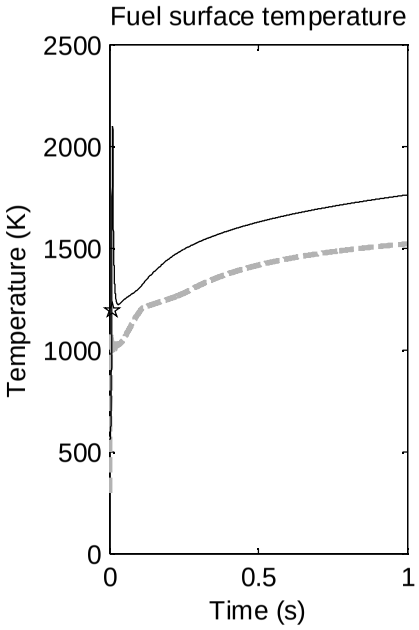

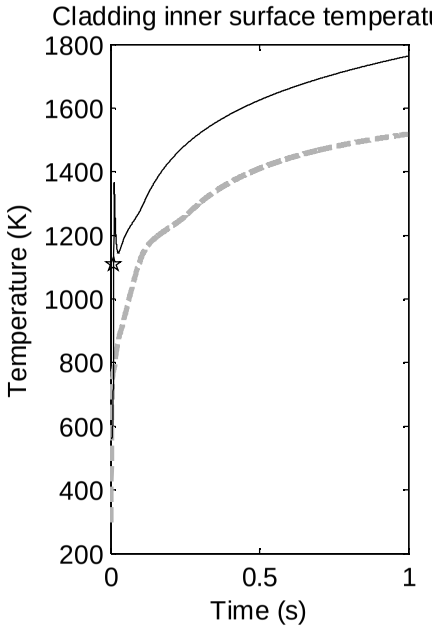

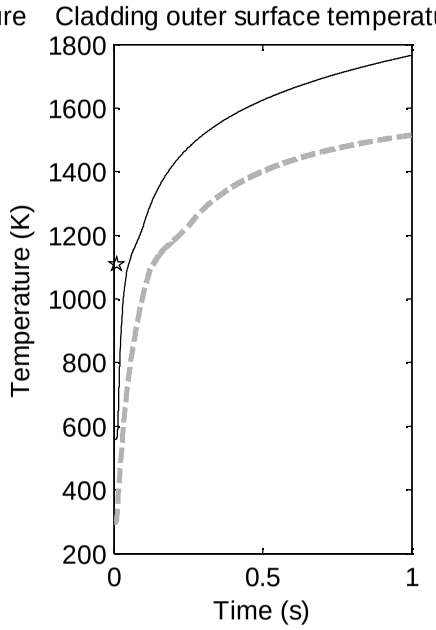

NSRR VA-3 scenario, star marks rod burst

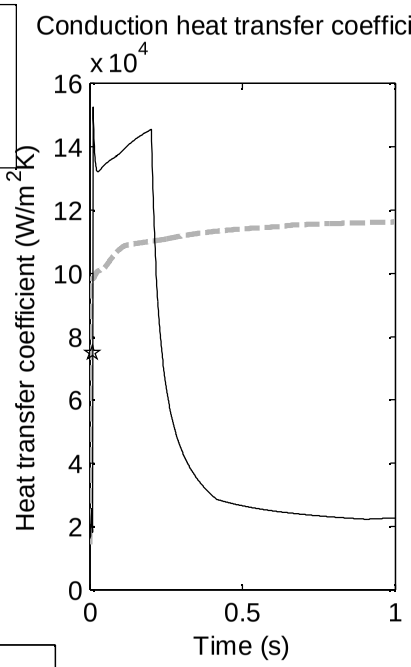

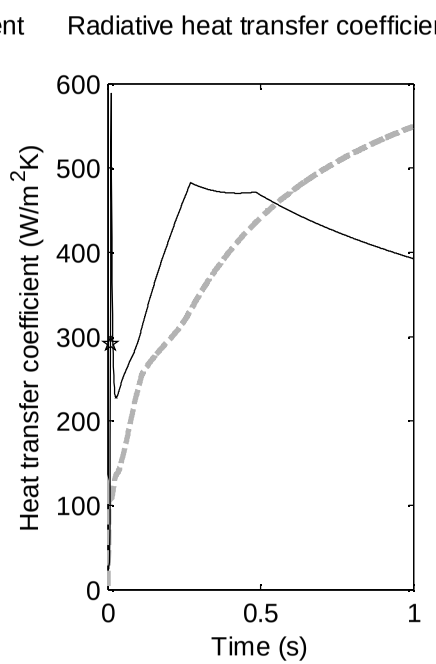

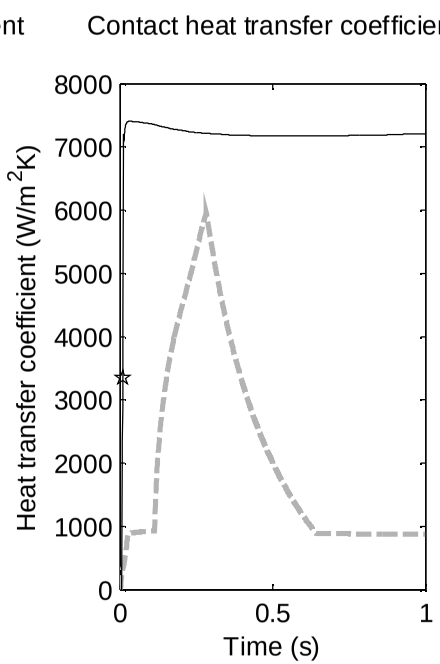

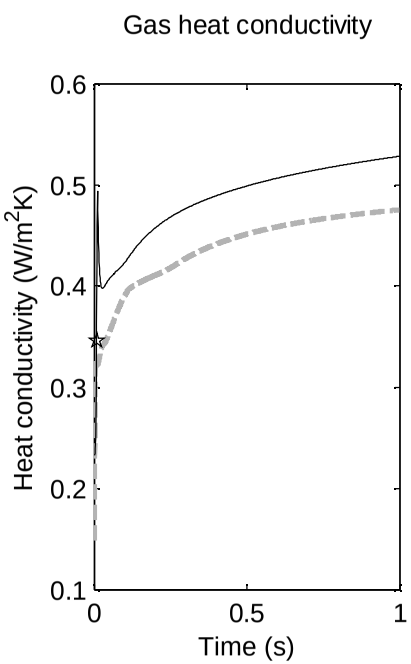

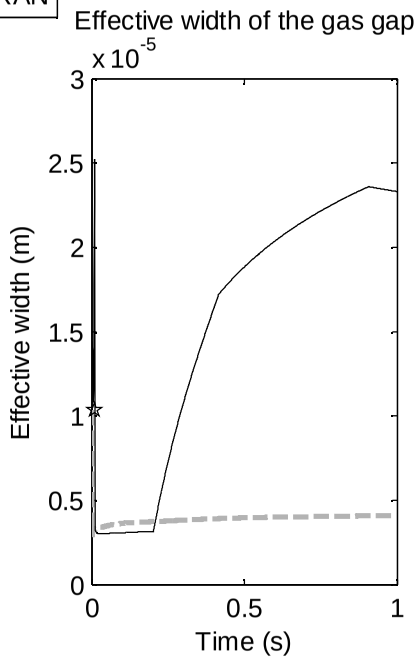

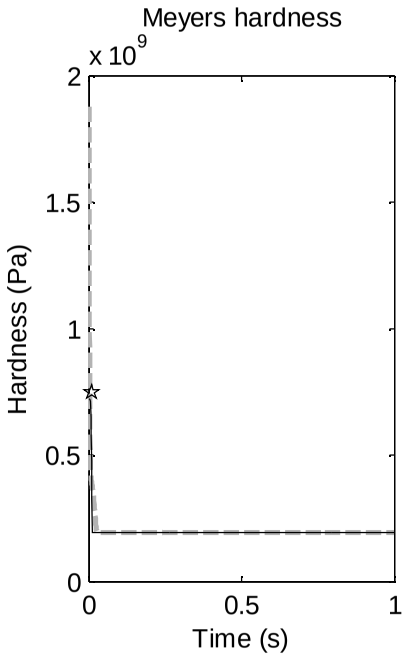

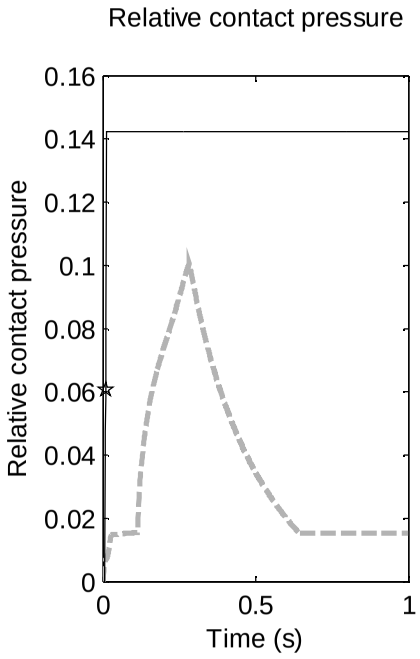

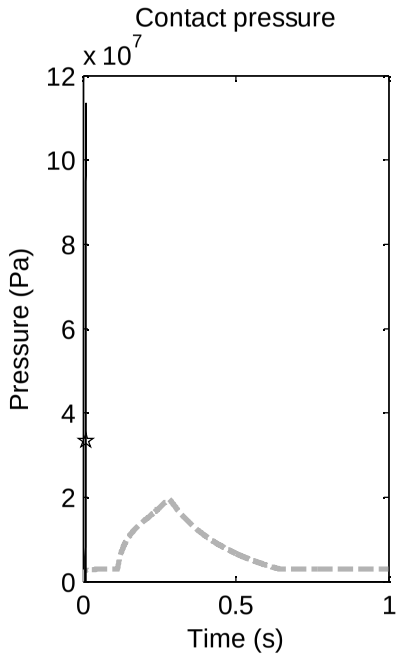

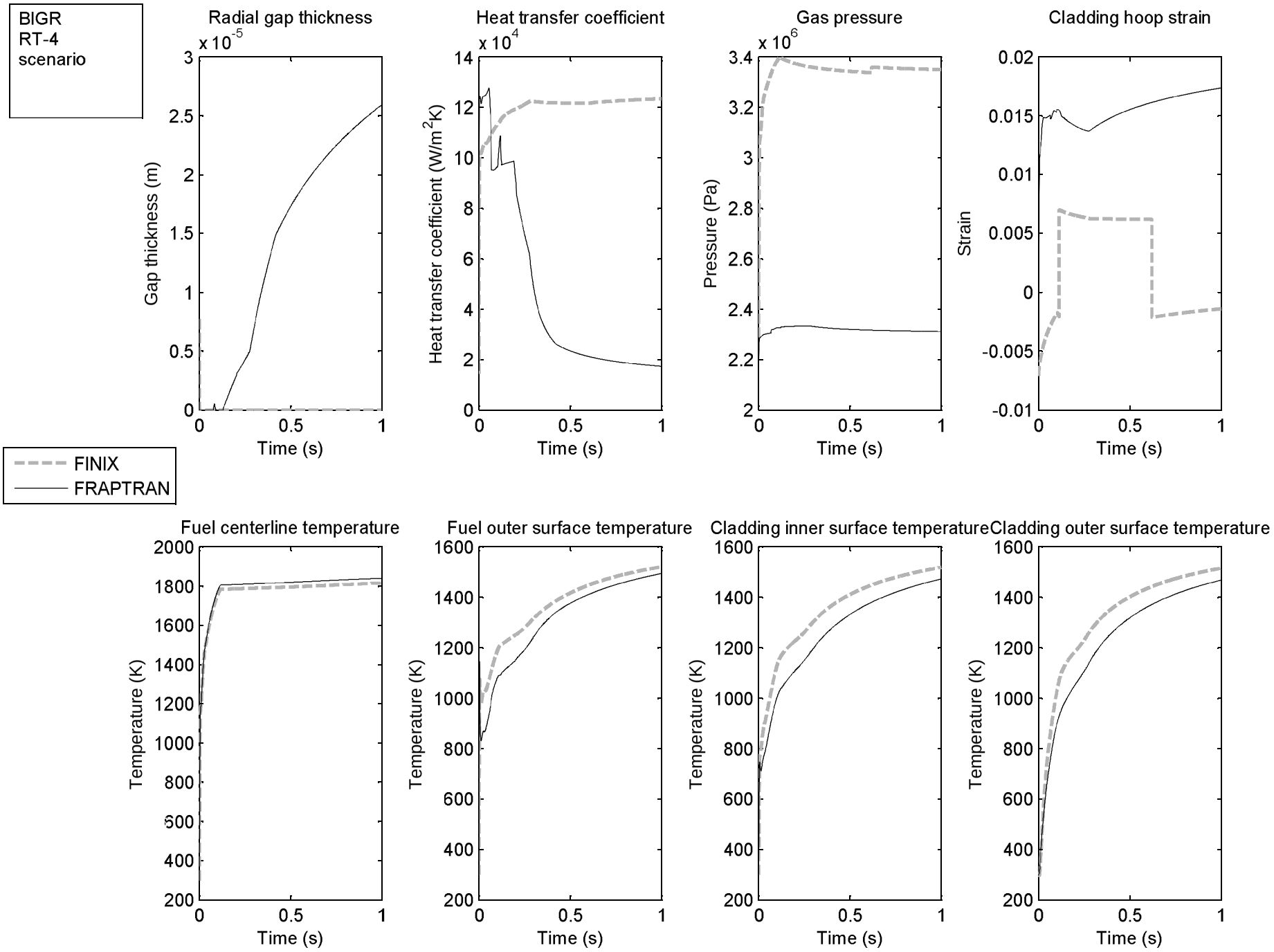
BIGR
RT-4
scenario
Radial gap thickness
x 10^-5
Gap thickness (m)
Time (s)
Heat transfer coefficient
x 10^4
Heat transfer coefficient (W/m^2K)
Time (s)
Gas pressure
x 10^6
Pressure (Pa)
Time (s)
Cladding hoop strain
Strain
Time (s)
FINIX
FRAPTRAN
Fuel centerline temperature
Temperature (K)
Time (s)
Fuel outer surface temperature
Temperature (K)
Time (s)
Cladding inner surface temperature
Temperature (K)
Time (s)
Cladding outer surface temperature
Temperature (K)
Time (s)

BIGR
RT-4
scenario

FINIX
FRAPTRAN

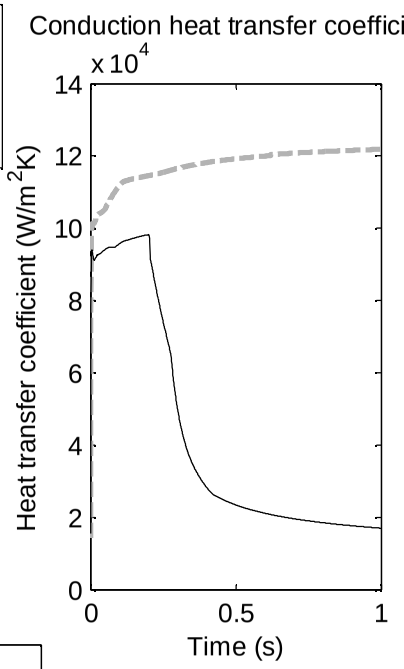

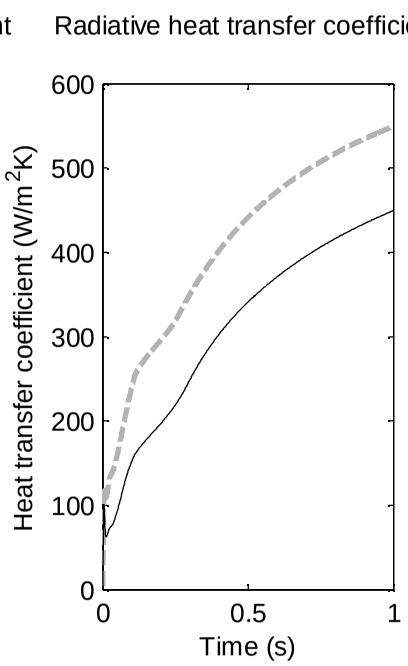

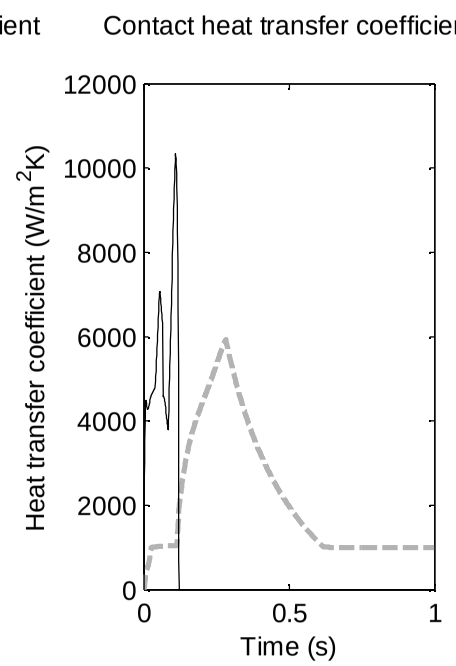

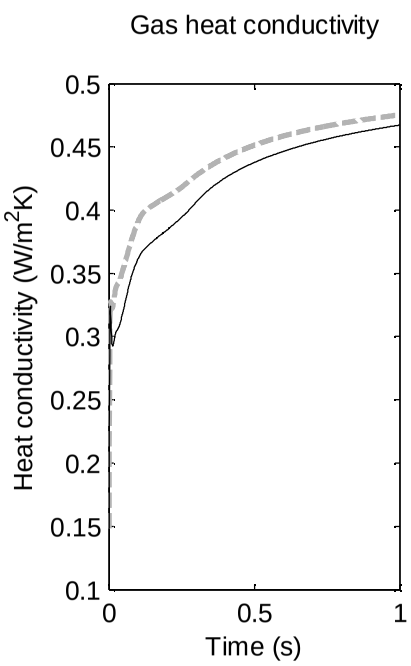

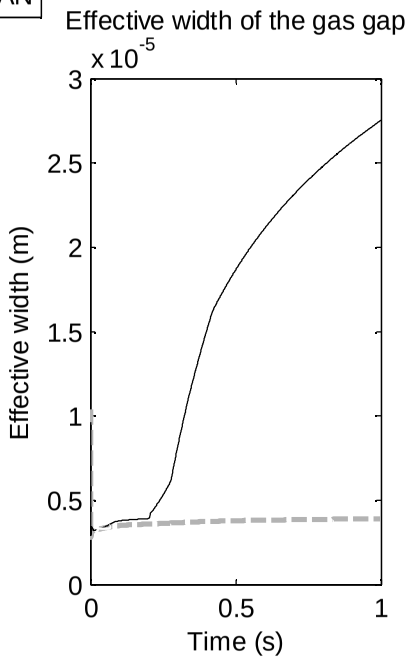

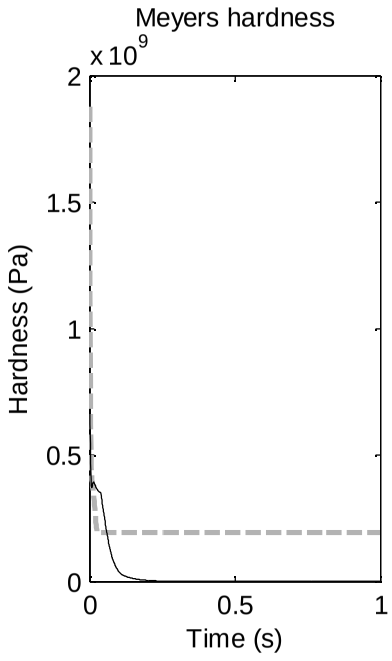

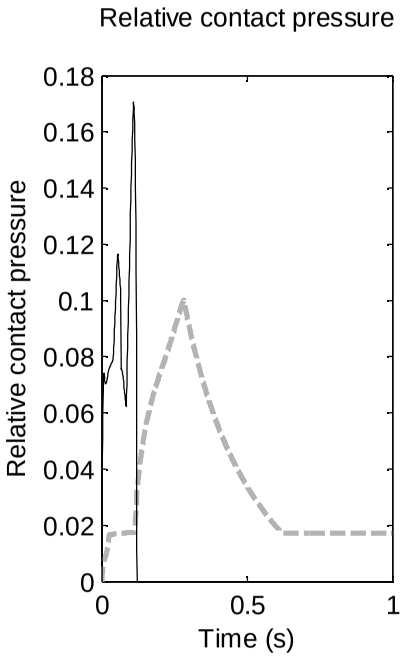

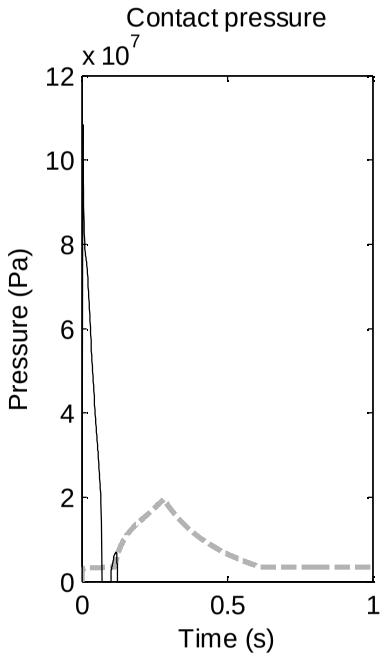

BIGR RT-8 scenario, star marks rod burst

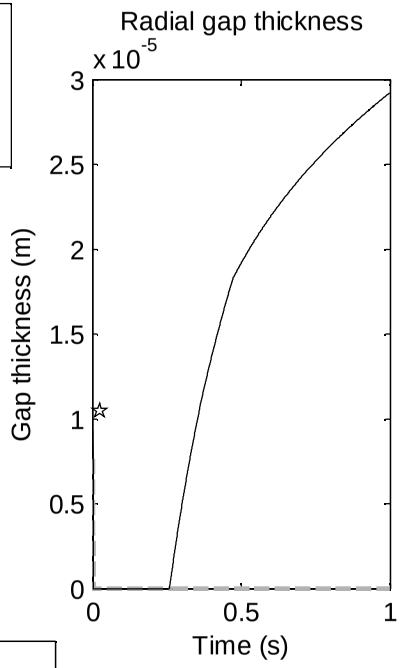

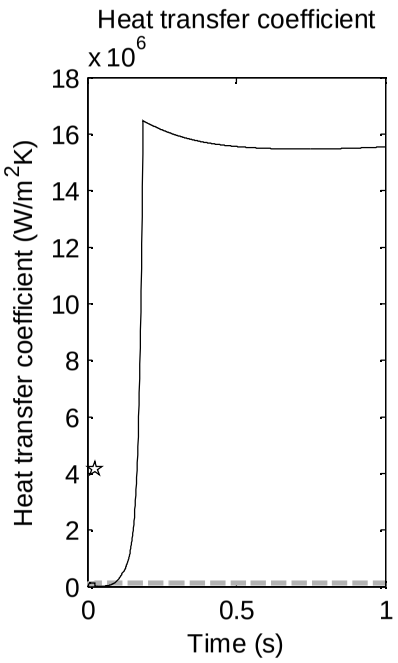

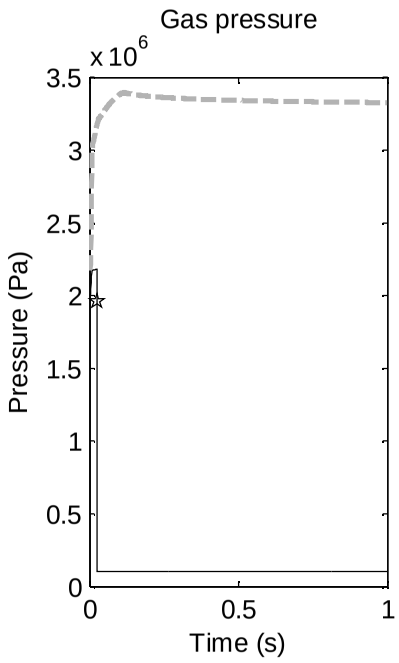

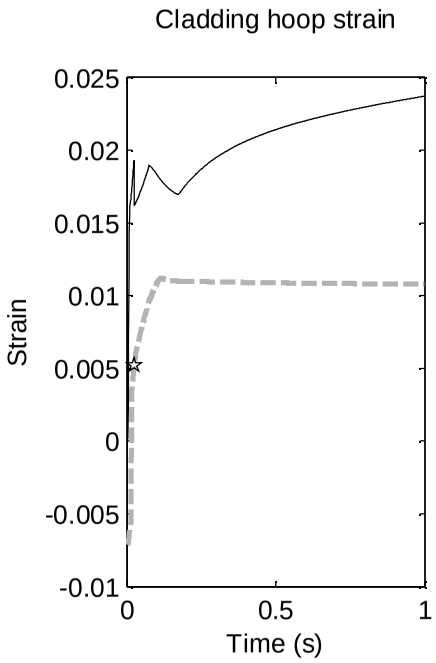

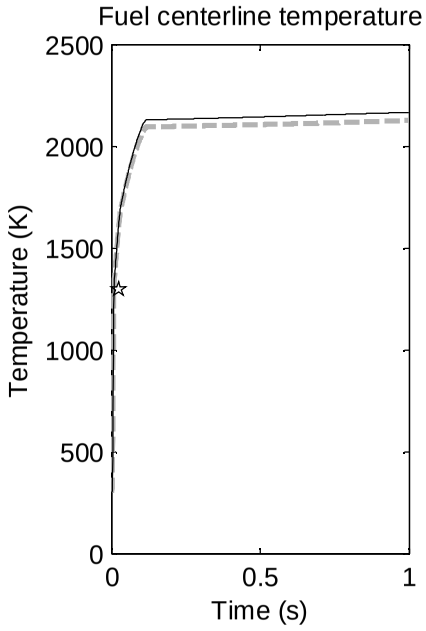

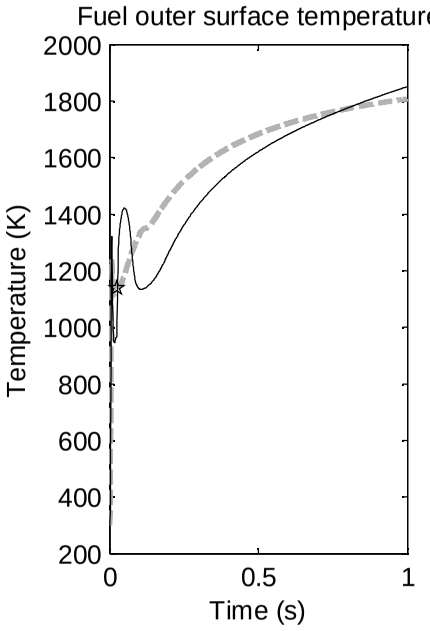

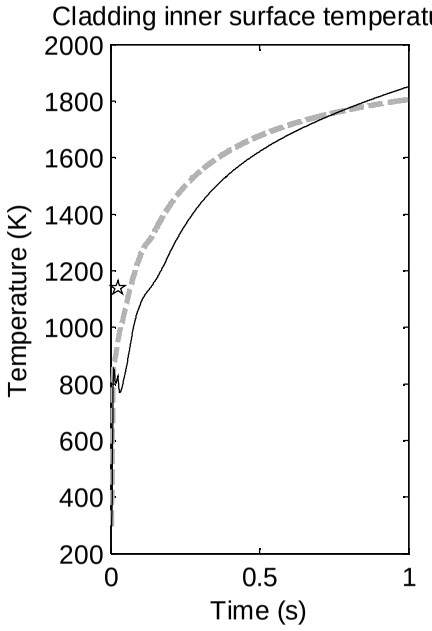

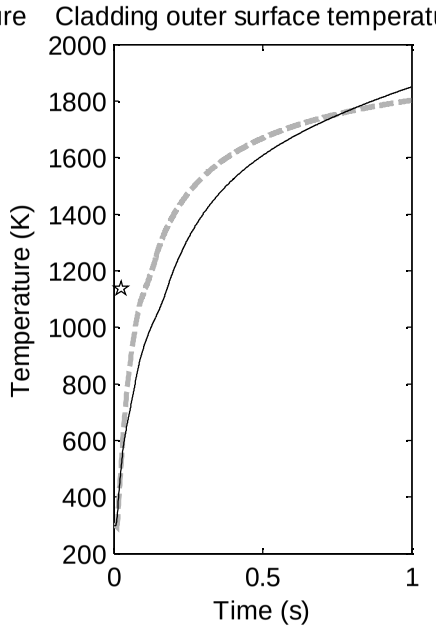

BIGR RT-8 scenario, star marks rod burst

FINIX
FRAPTRAN

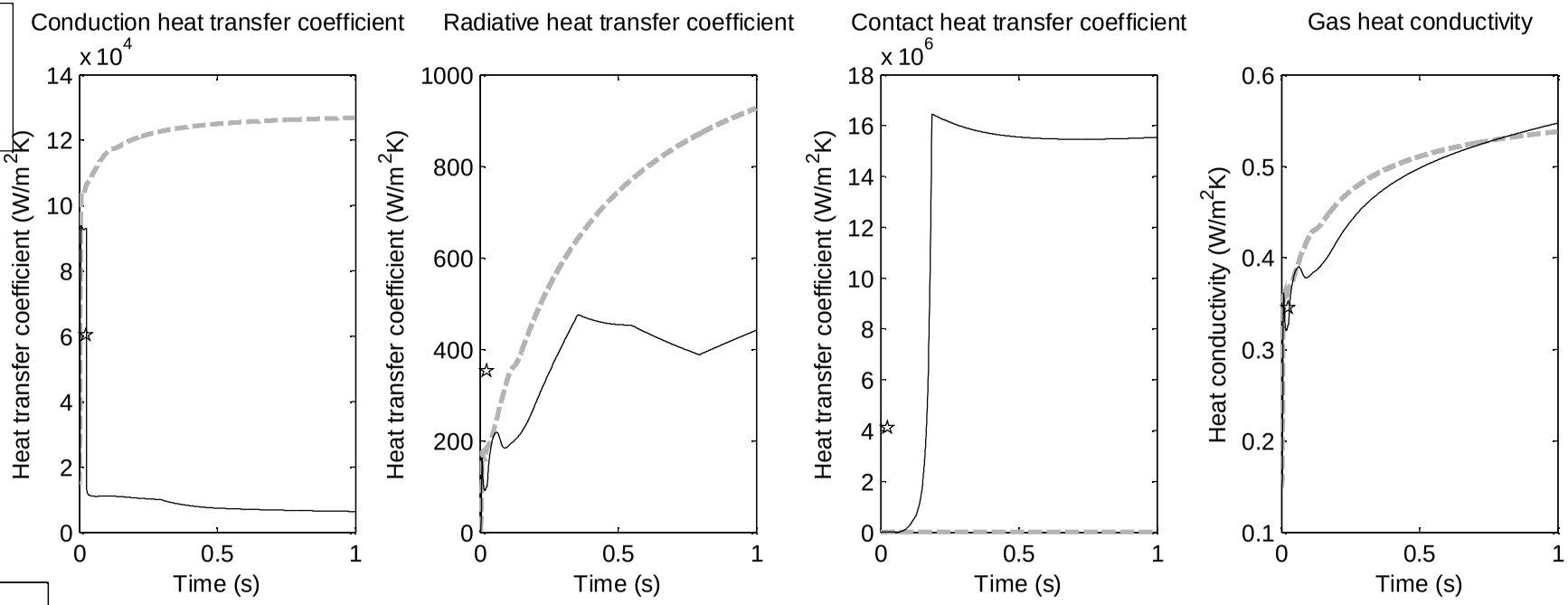

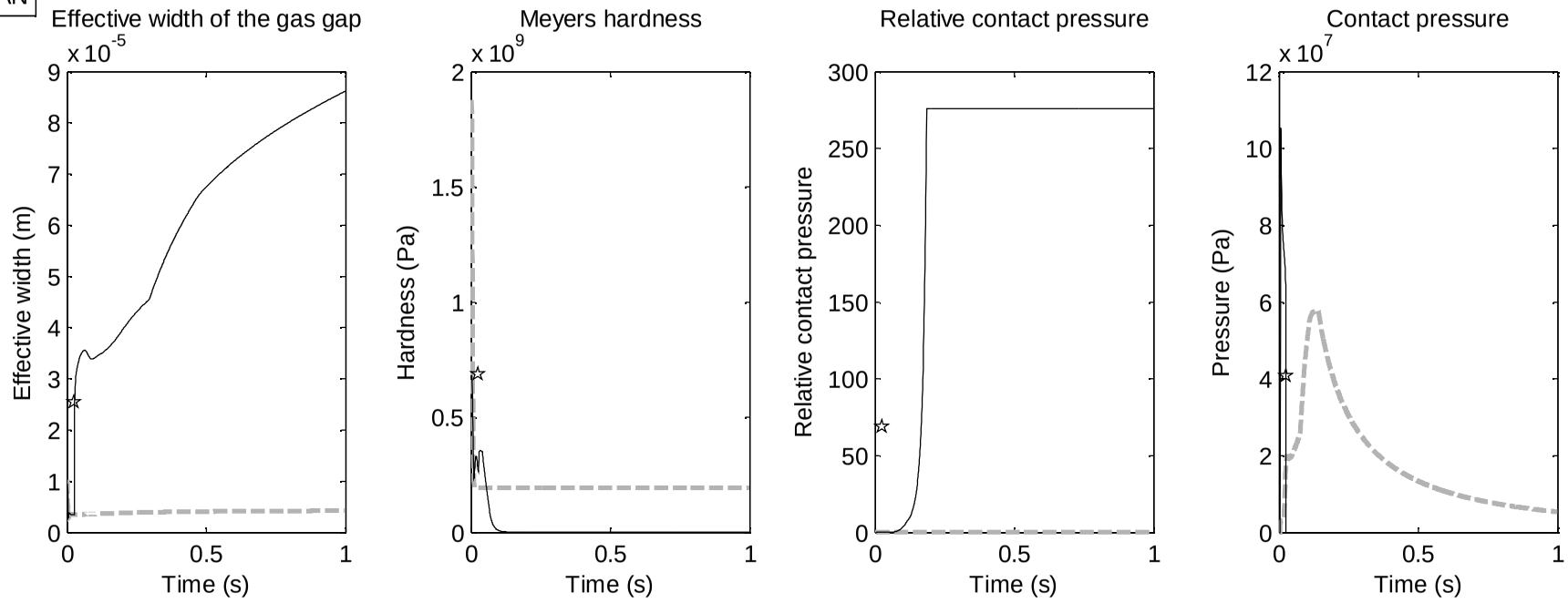

BIGR
RT-10
scenario

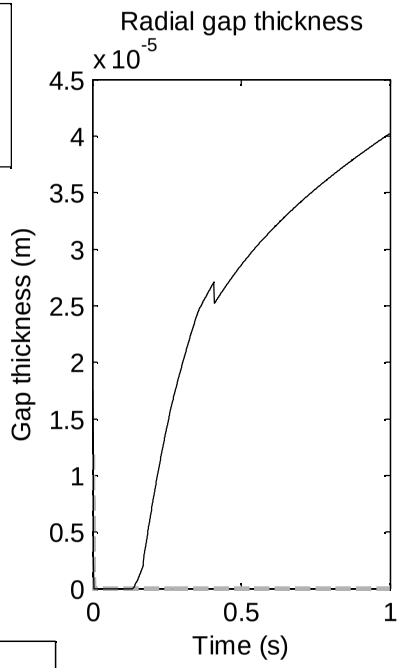

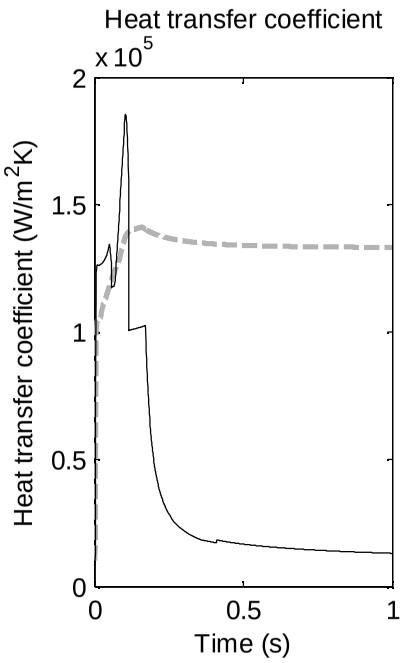

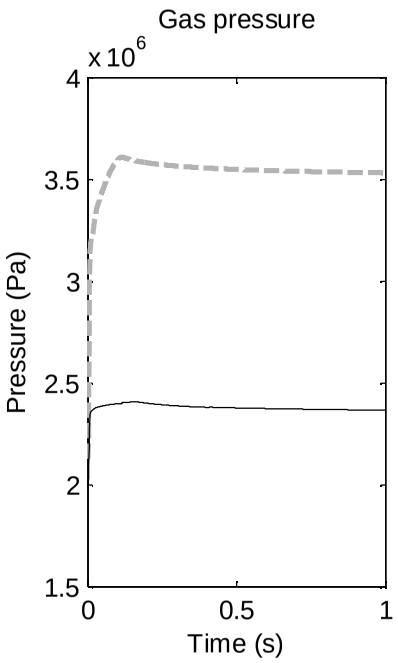

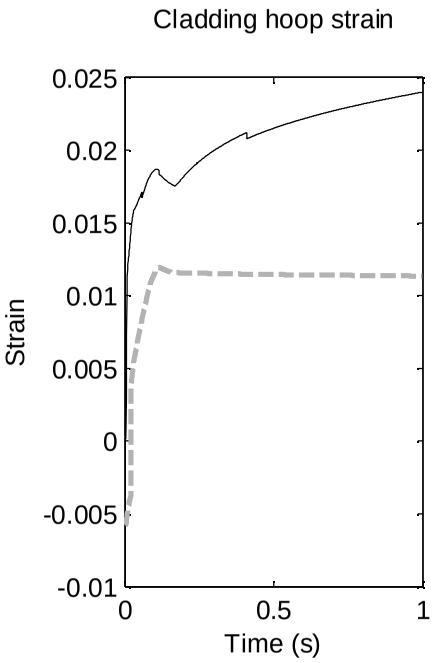

FINIX
FRAPTRAN

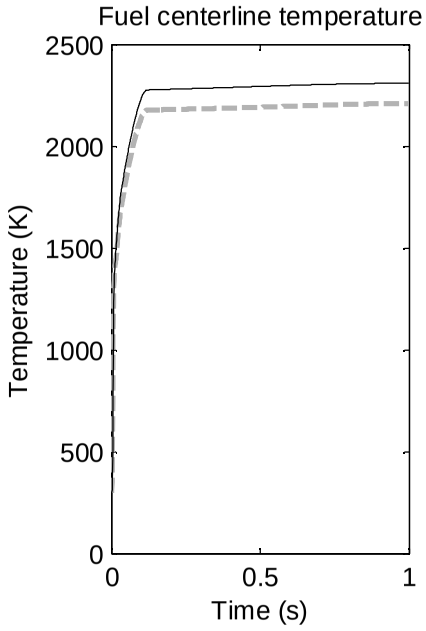

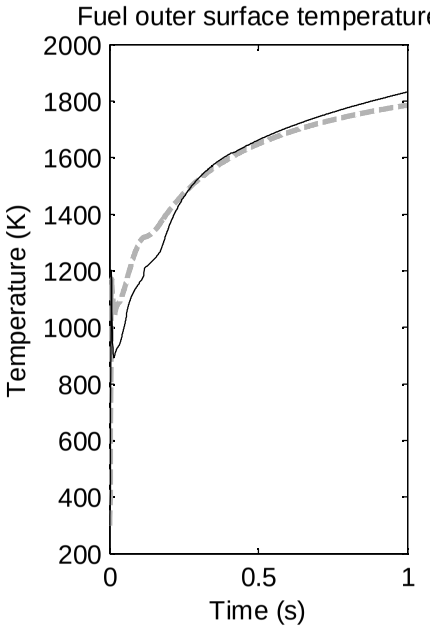

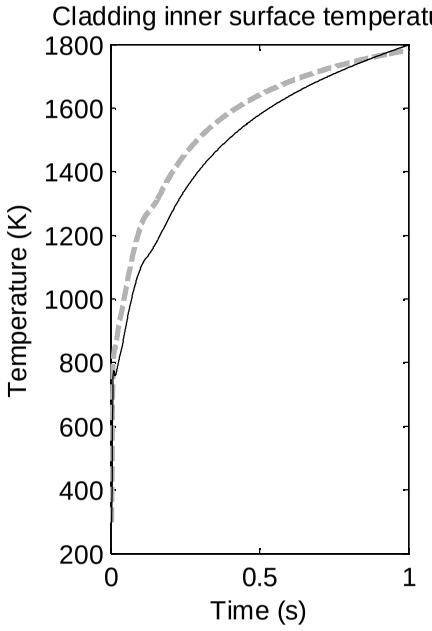

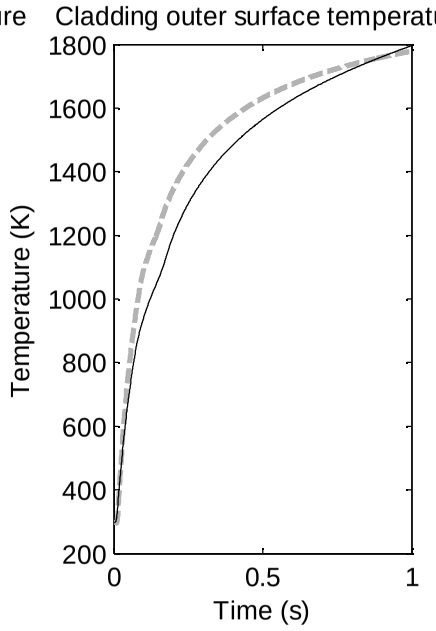

BIGR
RT-10
scenario

FINIX
FRAPTRAN

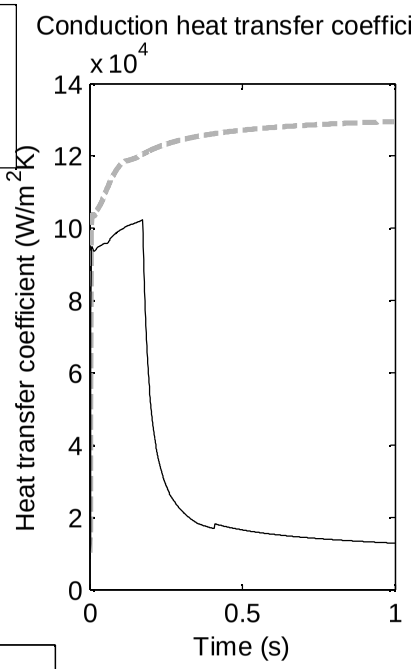

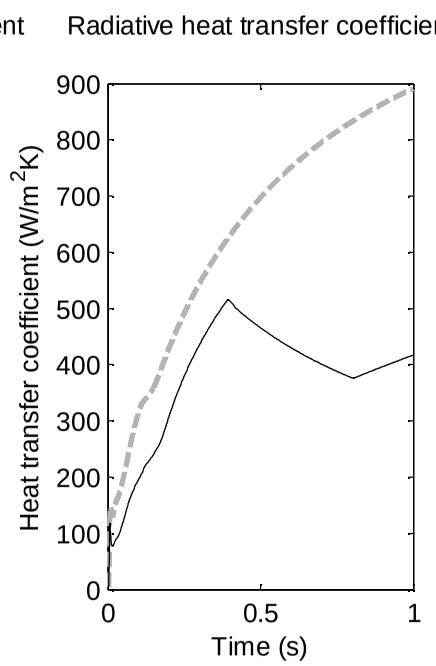

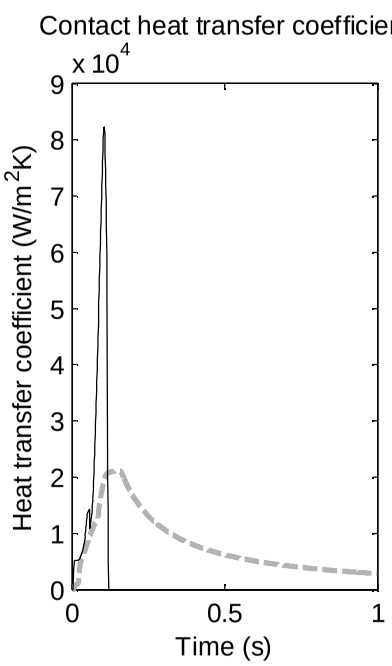

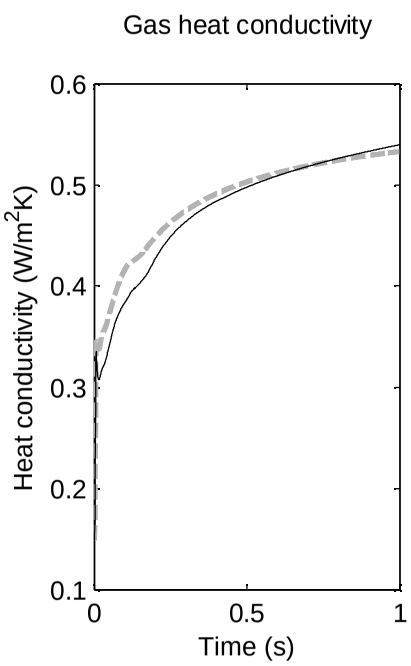

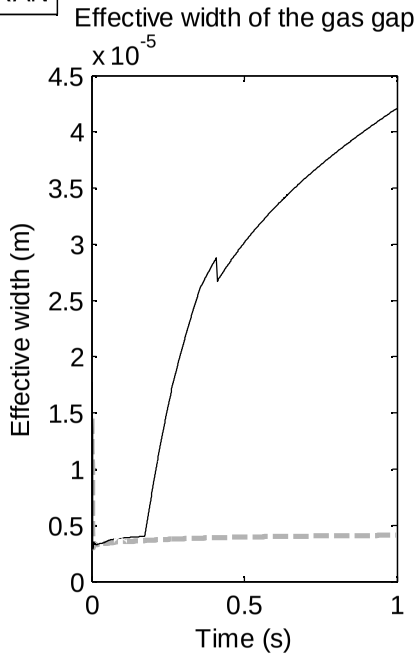

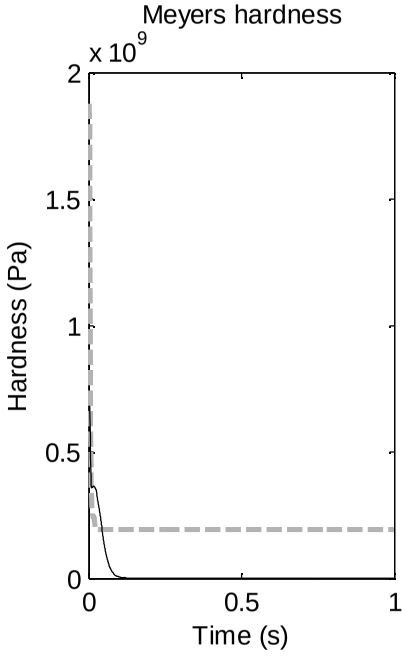

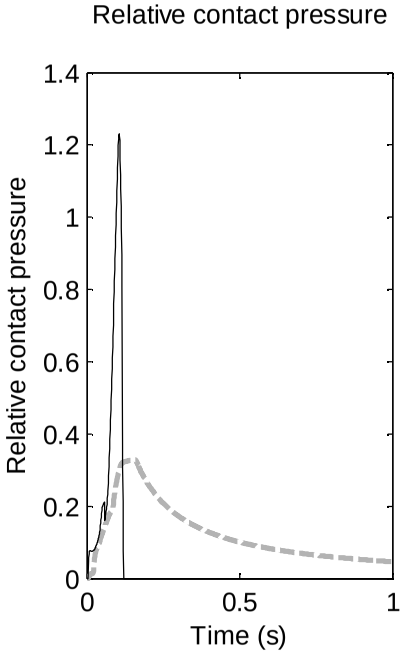

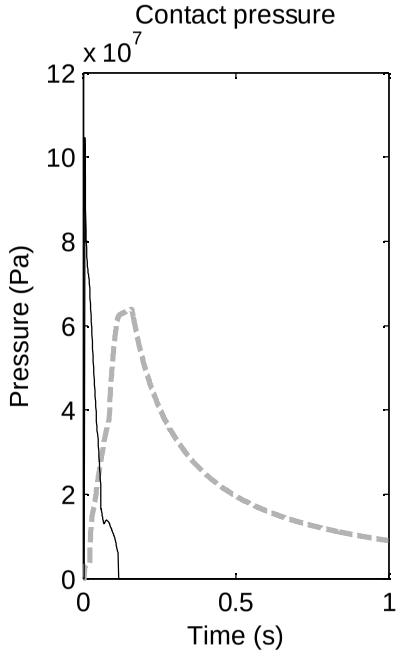

BIGR
RT-12
scenario,
star
marks
rod
burst

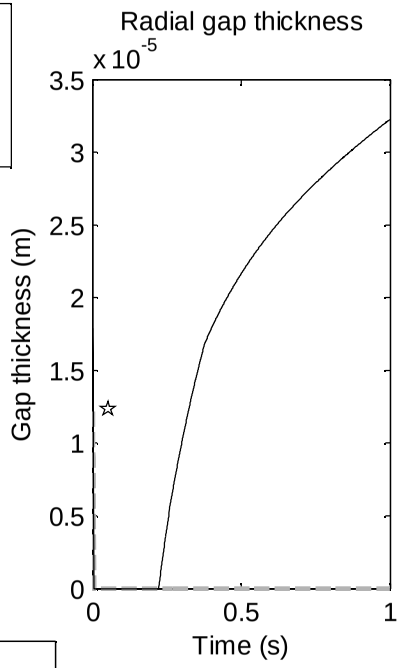

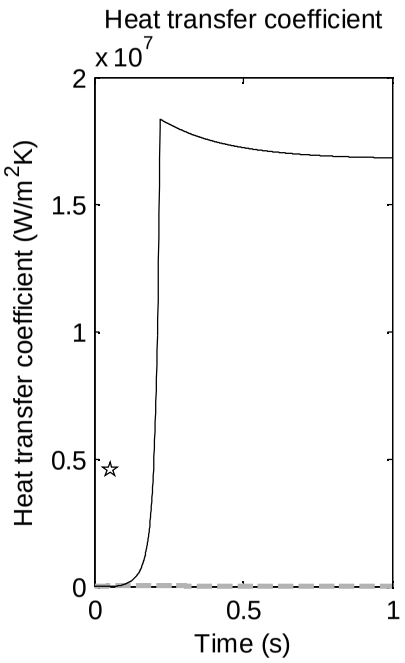

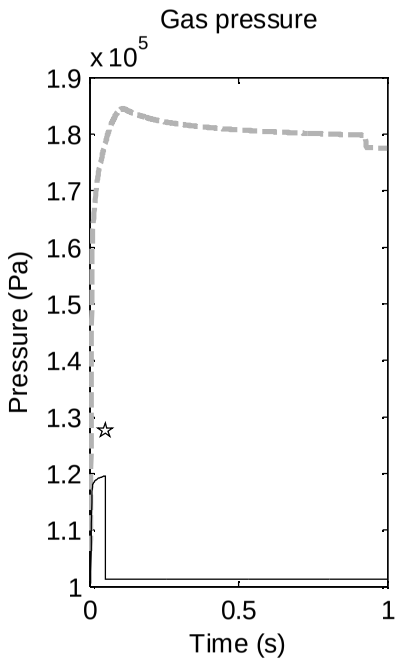

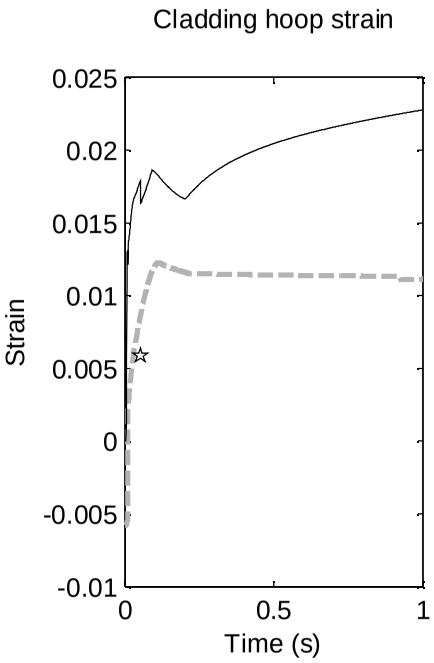

FINIX
FRAPTRAN

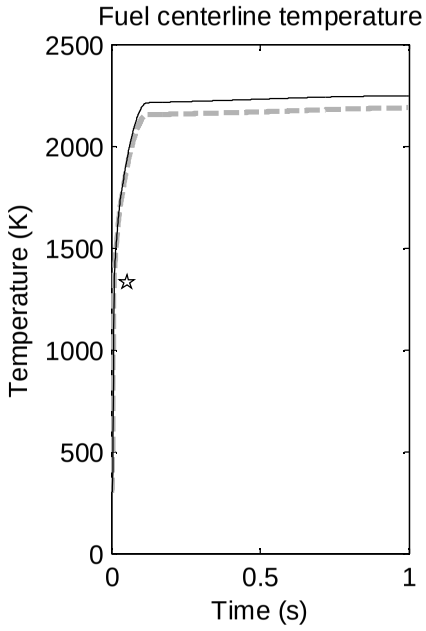

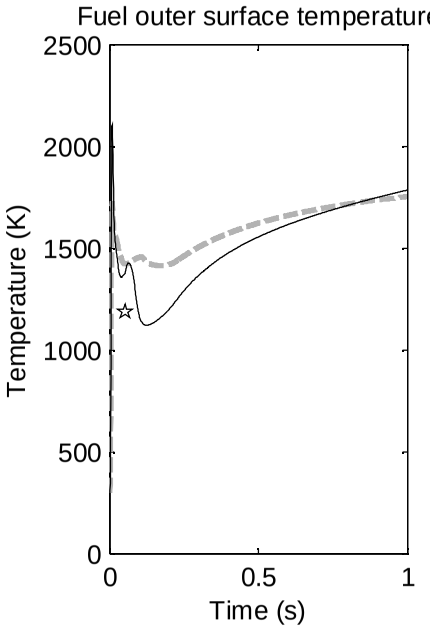

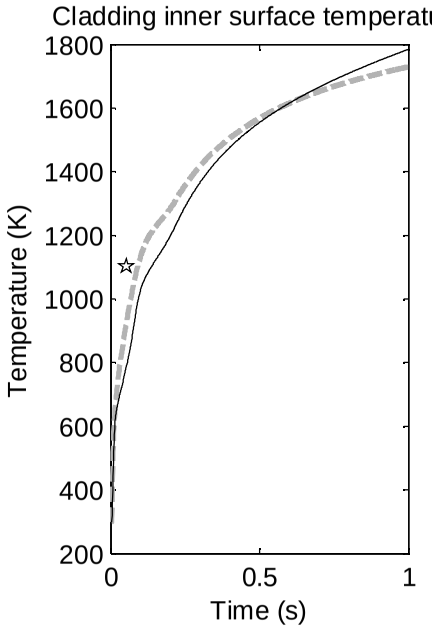

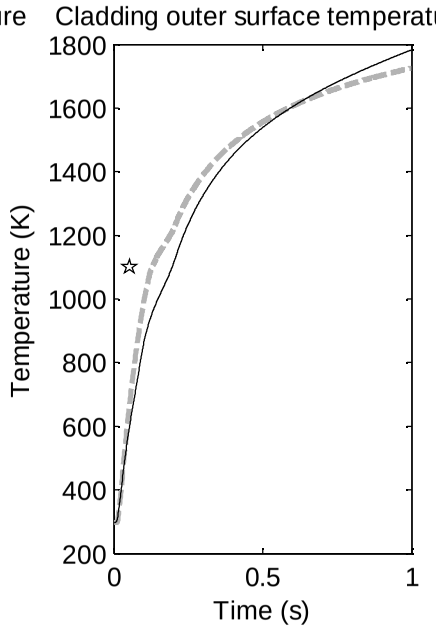

BIGR
RT-12
scenario,
star
marks
rod
burst

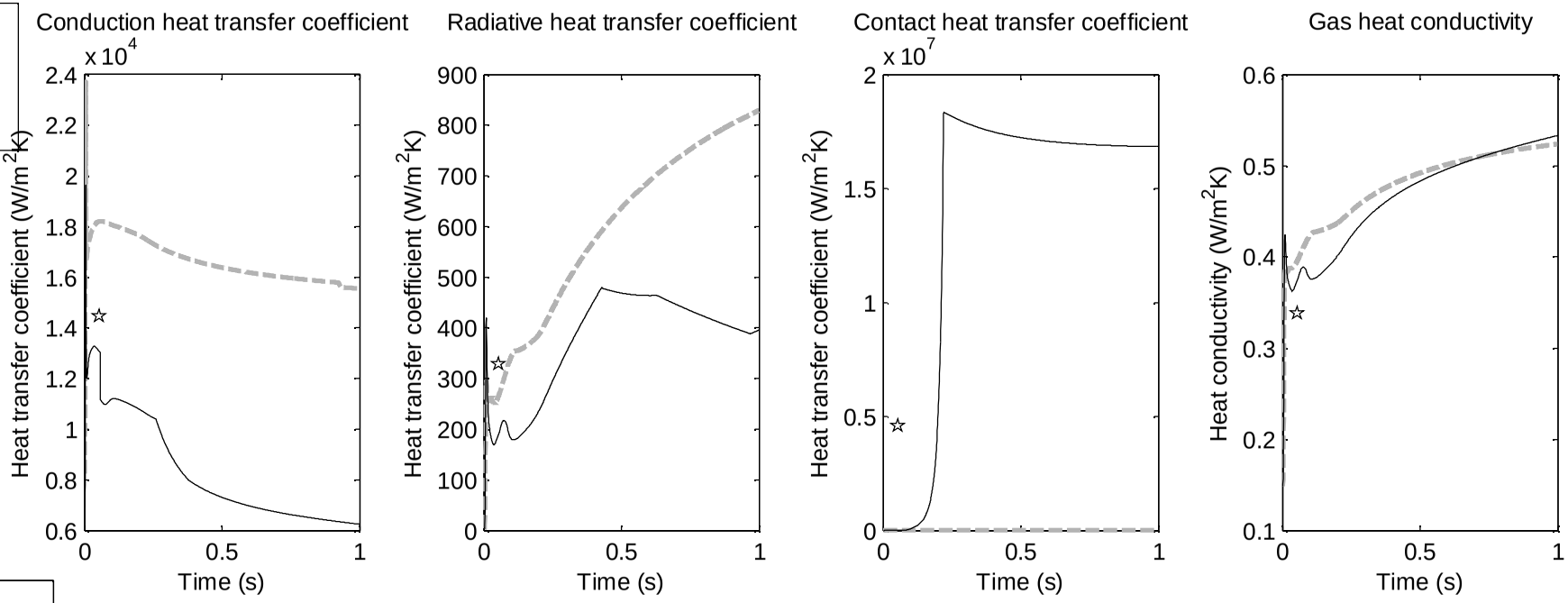

FINIX
FRAPTRAN